Project 3-55(5) Copy No._____

Capacity and Quality of Service of Weaving Zones

FINAL REPORT

Prepared for

NATIONAL COOPERATIVE HIGHWAY RESEARCH PROGRAM
Transportation Research Board
National Research Council

Prepared By

Richard W. Denney, Jr., P.E.
Principal Investigator
Iteris, Inc.

James C. Williams, Ph.D., P.E.
University of Texas at Arlington

November 2005

ACKNOWLEDGEMENTS

The research documented herein was conducted from 1996 through 2000 with the intention of developing a new method for calculating the capacity and quality of service for weaving zones for the 2000 Highway Capacity Manual. In the end, neither time nor budget was sufficient to meet this objective. Yet all research has value even when its ultimate purpose is not achieved. Many contributed to the work reported here. One of the principal authors of portions of the work was Dr. Stephen L. Cohen, who performed the modifications and calibrations of the FRESIM model. Greer Johnson Gillis performed the simulations and reduced much of the data, including summarizing the aerial photography data collected by Skycomp, Inc. Dr. Nagui Rouphail provided insight into alternative capacity models. These contributions are greatly appreciated by the principal authors.

Because this research did not meet its ultimate objective and because insufficient resources were available to complete the work, the authors acknowledge that the work described in this report will not fully satisfy its readers. The authors themselves are not fully satisfied with the work in its incomplete state. Even so, the work revealed valuable insight that changes the way they view capacity in the most common forms of weaving zones.

This report was compiled by the authors listed, even though portions of the writing were taken from previous reports written by others on the research team. Those team members were not involved in the compilation and editing of this final report, and have had no opportunity to review it. Thus, they cannot be held responsible for the contents of this report.

As always, the authors express gratitude to the National Cooperative Highway Research Program, and to the panel members selected to oversee this work, for their support and cooperation.

TABLE OF CONTENTS

FIGURES AND TABLES

PART I. INTRODUCTION

CHAPTER 1. PROBLEM STATEMENT AND RESEARCH APPROACH

Introduction

All discussions of weaving begin with a definition usually quoted from the Highway Capacity Manual, which reads, "Weaving is defined as the crossing of two or more traffic streams traveling in the same general direction along a significant length of highway, without the aid of traffic control devices." Specific capacity considerations must be made in weaving areas because drivers from two upstream roadways must merge into a single roadway, and then diverge into two different downstream roadways. Weaving areas are characterized by frequent lane changes, where vehicles compete for the same pavement.

Weaving areas are categorized by their lane configuration. The Highway Capacity Manual defines Type A weaving zones (Figure 1.1) by two conditions: No non-weaving vehicle must change lanes, and all weaving vehicles must change lanes. Thus, there is a contiguous lane line from the point of the merge gore to the point of the exit gore across which only weaving vehicles must cross. Type A weaves are further divided into Major and Minor sub-categories. Type A Major weaves are intended for freeway-to-freeway applications where there are two or more lanes on all entering and exiting roadways. Type A Minor weaves are also known as ramp weaves, because the entering and exiting roadways contain only a single lane, as with a freeway entrance ramp and an exit ramp connected by an auxiliary lane. If there is no auxiliary lane, it is a simple entrance ramp followed by an exit ramp and not a weaving zone, by definition.

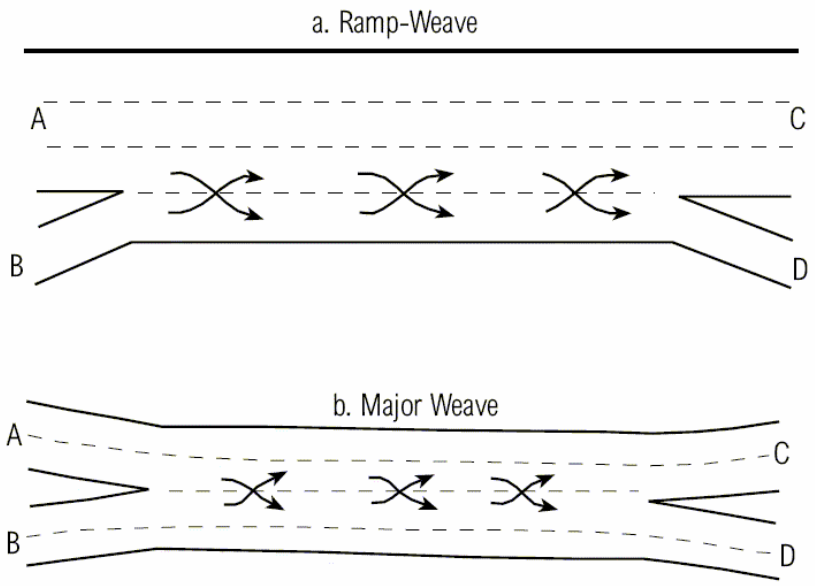

Figure 1.1. Type A Weaving Zones

Type B and C weaves are characterized by having one of the lanes entering from the right roadway leave to the left, or by having one of the lanes entering from the left roadway exit to the right. Thus, not all traffic that weaves must change lanes. In Type B weaves (Figure 1.2), the traffic weaving one way does not have to change lanes, while the traffic weaving the other way only has to change one lane. For this to be true, the diverge gore splits an option lane, allowing the vehicles in that lane to go either way. In Type C weaves (Figure 1.3), the traffic weaving one way does not necessarily have to change lanes, but the traffic weaving the other way has to change two lanes. Thus, a lane entering from the left roadway exits

exclusively to the right, or vice versa. Type B weaves are recognizable by their option lanes, and Type C weaves by their required two lane-change maneuvers.

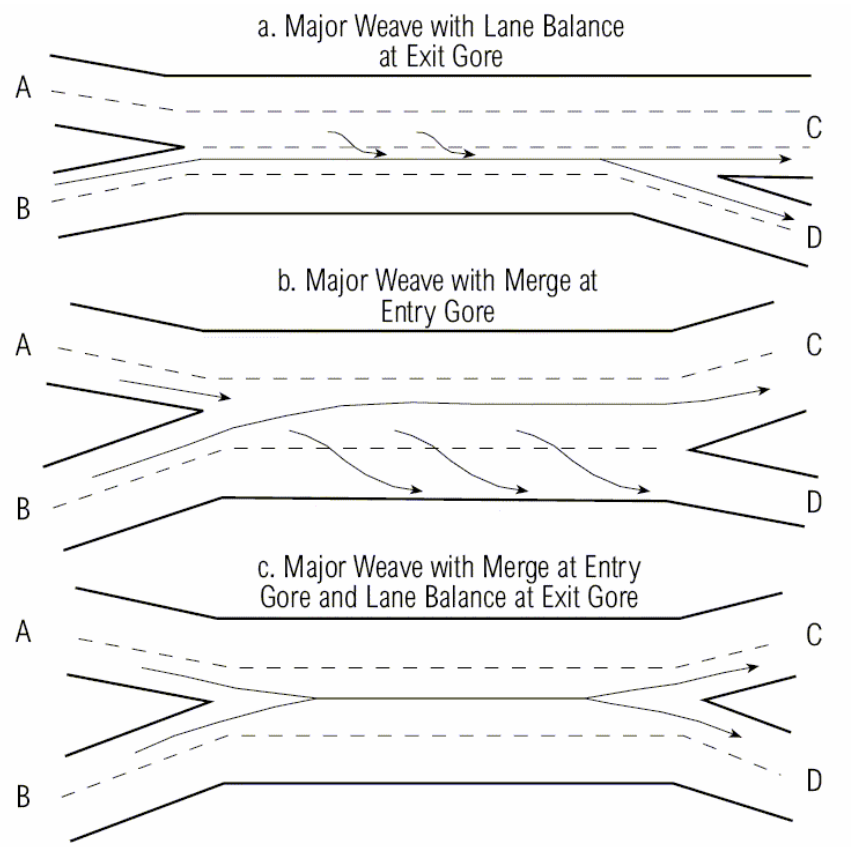

Figure 1.2. Type B Weaving Zones

A final special case of Type C weaves is the two-sided weave, where the weaving traffic enters on a single-lane entrance from one side and exits from a single-lane exit on the other side, crossing at least two lanes in the process, with (as for all Type C weaves) at least two lane changes.

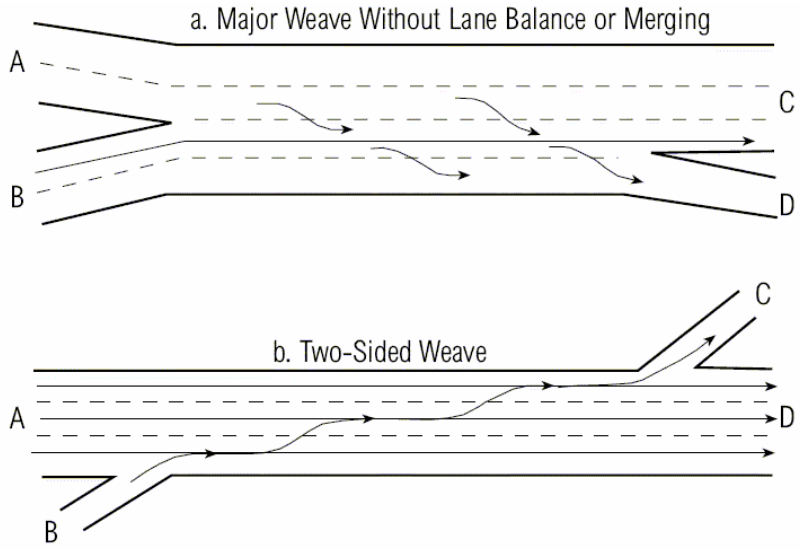

Figure 1.3. Type C Weaving Zones

The traditional weaving analysis method in the Highway Capacity Manual use roadway geometry and traffic volumes as inputs, and provide an estimate of speed as an output. The use of speed for assessing the capacity of weaving areas has proved to be a poor choice. Initial observations suggested that speed might be the result of many factors, only one of which is proximity to capacity. Throughout the typical weaving zone, speed may vary dramatically, and characterizing speed does not consider the motorist's perception of acceptable operation in a weaving zone. These problems have been noted in other areas of highway capacity, and the trend in level of service calculation has been toward using density as a service measure. Density is the result of both speed and flow, and therefore acts as a single measure of congestion.

Speed is a more useful measure of the ability of a weaving zone to handle smooth flow. This research suggests that *at capacity,* weaving zone length has little or no effect beyond a surprisingly short minimum (for Type A weaves at least). Experienced observers, however, will note that the problem with weaving zones that are too short is that they force freely flowing drivers to slow down significantly to complete the maneuver. At low flows, a useful congestion measure is not needed. Much more useful in these situations would be a measure of the performance of the geometry, and speed is a useful measure.

Another problem with existing methods has been that they are difficult to justify or explain to practitioners. They depend on regression analysis to fit complex curves to widely scattered data points, resulting in usually poor correlation and physical dimensions taken to unrealistic fractional powers.

The objective of this research was to develop new methodologies for weaving zone capacity and level of service evaluation, with the intent of correcting the above problems. The project budget was highly limited, and the team therefore proposed and depended on existing data and simulation to provide the comprehensive empirical support needed for all-new methods.

In the end, the resources proved to be insufficient to meet all the goals of this research. New methods were developed for Type A weaving zones, based on a reasonable selection of field studies and extensive simulation. Some new basic concepts were suggested and supported by the work, and some traditional approaches were challenged. Some data were collected for more complicated weaving sections, and extensive simulation was performed there, too. But the project did not have sufficient resources to create new methods based on these analyses.

Report Organization

This report is divided into three sections, the first being the introduction. The research approach and model requirements are detailed in the remainder of this chapter. The second chapter contains an extensive literature review. The development of freeway weaving models used in the various editions of the Highway Capacity Manual is described, beginning with the first edition in 1950. Then other freeway weaving models are detailed, followed by a brief review of research into arterial weaving. In particular, the special case of frontage road weaving is discussed, where the weaving occurs between the exit ramp onto the frontage road and the downstream arterial intersection. The role of simulation in this work is discussed in Chapter 3, along with the calibration and validation of the selected model. The successful completion of this process was a vital element of this work, as much of the modeling is based on the results of the simulation. Thus, the authors have opted to place this chapter in the report introduction. Details of the collection of data used in the calibration and validation are reserved for a subsequent chapter.

The second part summarizes the work on Type A weaves, and consists of four chapters. The researchers developed several potential capacity models, which are described in some detail in this part (Chapter 4). This is followed by a description of the data used in the development of a capacity model and a level of service model for Type A weaves. The research largely relied on two sets of previously-collected data; one collected by JHK for the FHWA, the other collected by the California Department of Transportation. In addition, the researchers collected data at two locations: a ramp weave in Houston (our original pilot study) and a Type A Major weave near BWI Airport in Maryland. The calibration described in Chapter 3 was performed using some of this data.

The development of a final capacity model for Type A weaves is described in Chapter 6, reflecting the collected data and simulation. This format (proposed capacity models, followed by the data description, followed by the model refinement) was used to clearly distinguish considerations in model selection from the needed work in developing a final model. The final chapter of Part 2 describes how the capacity model, which uses flows, is related to the density of the critical lane in the weave, which can be used to identify various levels of service, as are the other elements of freeway capacity in the current Highway Capacity Manual, basic freeway segments and ramp junctions.

The third and final part of this report summarizes the work on Types B and C weaves. The data used for this work was collected in Texas as part of this study. The data collection and reduction are discussed in Chapter 8, and preliminary simulation results for these weaving types are shown and discussed in Chapter 9.

A concluding chapter (Chapter 10) summarizing the main findings of the research, along with suggestions for future work, has been provided.

As mentioned above, project resources did not permit the completion of this work, especially for Types B and C weaves. However, the most developed work herein is for Type A weaves, which represent the vast majority of weaves on US freeways.

User Inputs

Figure 1.4 shows the proposed process for the end user proposed in this research. This process provides a framework defining contributions from this and future research.

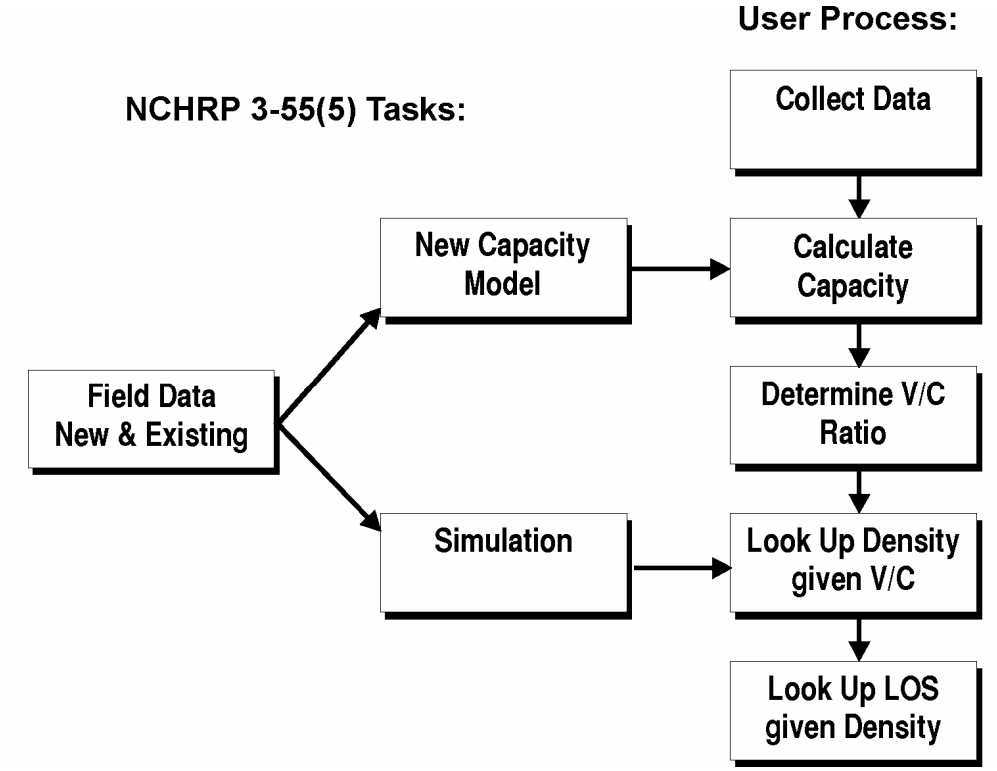

Figure 1.4. Proposed User Process and Required Research Contribution

Rather than determining the performance of the weaving zone, the proposed process starts with calculation of the capacity of the weaving lanes. This approach parallels other chapters of the Highway Capacity Manual.

Once the capacity is calculated, the user will determine the density and speed using relationships that model the relationship of density and speed to saturation. Once the user has determined density, the level of service can be determined using the same procedures in other chapters of the Highway Capacity Manual.

Needed Research Results

Capacity Model

In the process suggested above, the user first determines the capacity of the weaving zone. The capacity model must make use of readily available data or estimates of demand. The capacity model provides only capacity, not a performance measure. This creates an intuitive paradox, because, as will be shown in later chapters, the capacity of a weaving zone depends on the volume of weaving traffic. Thus, the user enters with data that may or may not be at capacity, but if it is not at capacity, the weaving volume will be less than what capacity conditions would allow. Because the capacity is greatly affected by that weaving volume, the changes in weaving volume as demand rises to capacity will change that capacity. Thus, the capacity being modeled is one of many *potential* capacity values.

This paradox is similar for capacity calculations at traffic signals, for example. The capacity of a signalized intersection greatly depends on the amount of green time allocated to each movement, but the

green time to be allocated such that that result is achieved cannot be determined until the capacity conditions exist.

The purpose of calculating capacity is not, however, to determine the actual capacity, unless the conditions are already at that point. The purpose of calculating capacity is to provide a consistent linkage to a model of density. Thus, a model of merely potential capacity is acceptable as long as the model behaves predictably. An essential element of predictable behavior is that it yields saturation ratios between 0 and 1 for all realistic input values. The saturation ratio must also rise monotonically through a range of plausible values. In sub-capacity conditions, these values will not be meaningful except to provide a link to the level-of-service evaluation, which will use saturation as the input. What *is* important, however, is that for a given calculated capacity, a reasonably correct density can be determined.

In the capacity flow regime, the capacity model must be internally consistent. That is, it must be well defined for conditions where the traffic volume in the weaving lanes equals the capacity predicted by the model.

Level of Service Model

Having a reasonably accurate capacity model does not help define level of service at demand levels less than capacity. A clear result reported in the literature is that attempts to model speed have met with little success. The existing equations do not provide good empirical fit to the data available and the change in characteristics from one geographic location to the next overwhelm any attempt to model the distinction between various levels of service.

In this work, the researchers define capacity as that point at which no more cars will be allowed into the weaving zone at the merge point. In the field, this point can be seen when queues *begin* to form upstream from the merge point. The authors favor this definition because it provides a useful way to observe the condition qualitatively in the field.

Other definitions of capacity are possible. One is the point at which some drivers are unable to complete their weaving maneuvers. This definition is very useful, because it defines the point at which the weaving zone is unable to provide its basic service. But the intentions of motorists cannot usually be seen from the outside, and those drivers who are unable to complete their maneuver are never detected. Consequently, this definition is very difficult to observe in the field. It is, however, easy to see in simulation. This point may not be consistent with field observations, because it is highly dependent on the motorist's willingness to forego the desired maneuver to avoid erratic behavior. While simulation will not permit illegal maneuvers, field observations indicate much greater willingness by drivers to perform erratic maneuvers such as driving on shoulders and through gore areas, in addition to forcing entry into a full lane.

This research began with the hope of developing only theoretical models that would provide physical significance and a clearly defined causal mechanism. In the end, this proved only partly successful. The capacity model developed for Type A weaves starts with the capacity of a single lane, and adjusts it upward inversely to weaving activity, and further upward to account for drivers tolerating closer headways as conditions approach capacity. The adjustments are made based on empirical data. After being unable to define a theoretical model for density, the researchers believed that once saturation was determined, density would be obtained by table lookup based on empirical results. In the end, however, the data showed strong correlation between saturation and density, resulting in a simple regression equation for density and speed. None of the results, however, lose physical significance, in that no

physical dimension is manipulated unrealistically, as by, for example, taking speed or distance to a fractional power.

Limited field studies were made of Types B and C weaves, and extensive simulation studies were made. Some of the results are shown for both the field and simulation studies.

Before proceeding with the development of the weaving models, previous work on weaving models is presented in the literature review in the next chapter, and the selection, calibration, and validation of the simulation model is described in the following chapter.

CHAPTER 2. REVIEW OF EXISTING METHODS AND RESEARCH

Weaving areas can be found on all types of highway facilities, ranging from freeways to arterials. The current procedure in the Highway Capacity Manual was developed for weaving areas on freeways, and little has been done for other facility types. This literature review begins with a history of weaving procedures as prescribed in the various editions of the Highway Capacity Manual and related documents. Next, other freeway models are reviewed. Last, overviews of research on non-freeway facilities (frontage roads and arterials) are presented.

Weaving Area Analysis in Past Transportation Research Board Publications

The 1950 edition of the Highway Capacity Manual [Ref. 1] defined weaving as "the act performed by a vehicle moving obliquely from one lane to another, thus crossing the path of other vehicles moving in the same direction." Further, a weaving section was defined as "a length of one-way roadway serving as an elongated intersection of two one-way roads crossing each other at an acute angle in such a manner that the interference between cross traffic is minimized through substitution of weaving for direct crossing of vehicle pathways."

Traffic in the weaving section was divided into weaving and non-weaving flows, and only Type A configurations were considered. The weaving capacity (i.e., the maximum number of weaving vehicles) was then taken to be equivalent to the flow in a single lane (since the number of vehicles crossing the crown line could be no greater than the number that could crowd into a single lane). For very short weaving sections (less than 100 feet), the capacity was 1200 vehicles per hour, with many vehicles stopping before entering the weaving section. A 900-foot weaving section could accommodate about 1500 passenger cars per hour at about 40 mph, and a 450-foot weaving section could accommodate the same number at 30 mph. These flows represent possible capacities for the weaving traffic. The 1950 HCM recommended that additional lanes be added to each side of the weave to fully accommodate the non-weaving traffic.

The design and analysis tools for weaving sections consisted primarily of a single graph relating the length of the weaving section (defined as the distance between the merge and diverge gores), the sum of the weaving flows (up to 3500 vehicles per hour), and the operating speed of the weaving section (see Figure 2.1). A weaving section length of up to 3400 feet is indicated in the figure. An equation was provided to estimate the number of lanes required for the weaving section, which divided the sum of the non-weaving traffic, the larger weaving flow, and three times the smaller weaving flow by the single lane capacity on the approach and exit roadways.

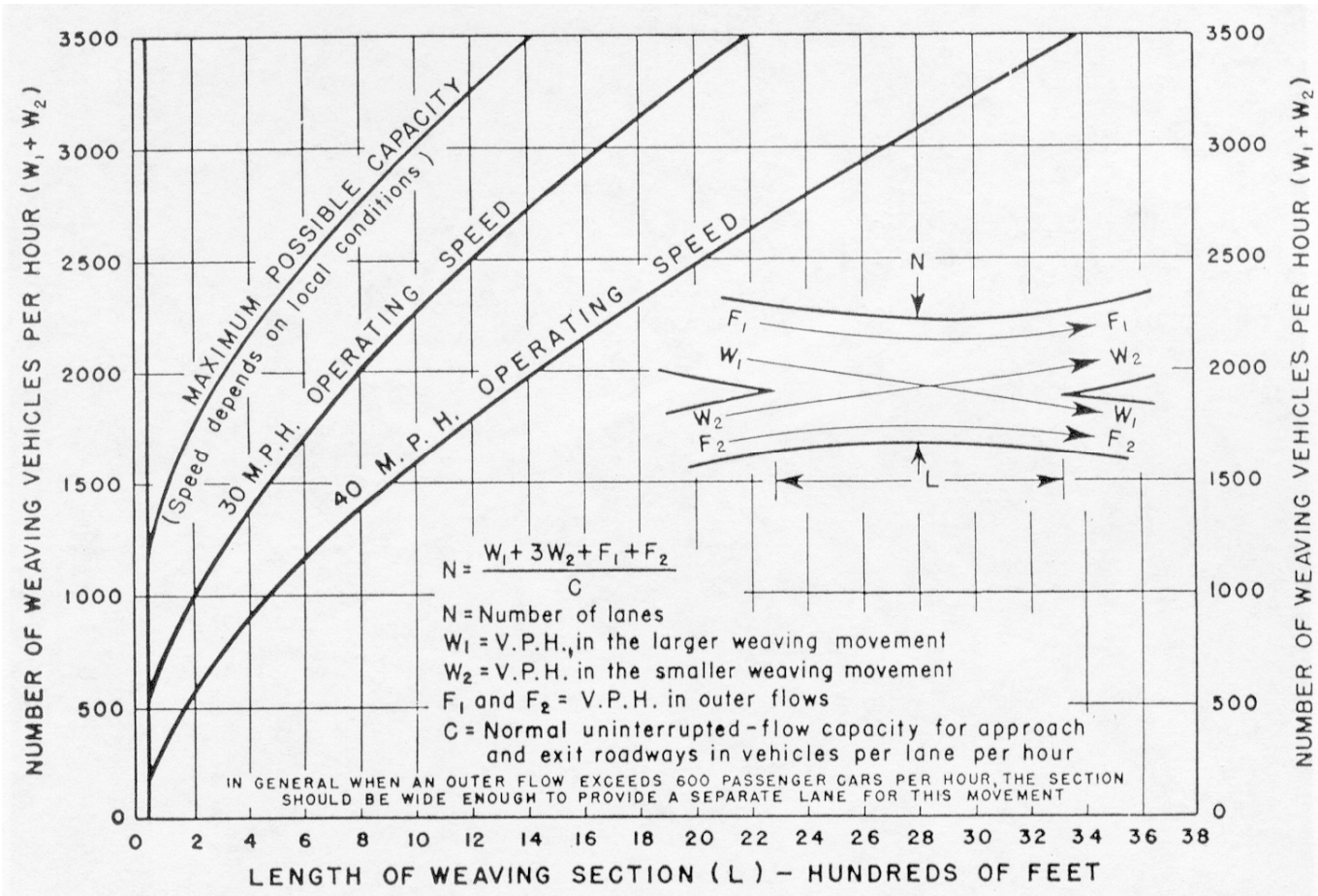

Figure 2.1. Weaving Analysis, 1950 Highway Capacity Manual

$$N = \frac{W_1 + 3W_2 + F_1 + F_2}{C} \tag{2.1}$$

where N = number of lanes

W_1 = larger weaving volume (vph)

W_2 = smaller weaving volume (vph)

F_1, F_2 = non - weaving volumes (vph)

C = normal uninterrupted flow capacity for approach and exit roadways (vphpl)

A footnote further suggested that a non-weaving flow of greater than 600 passenger cars per hour was large enough to justify a separate lane.

The development of the graph and equation was based on data from six sites; four on the roadways surrounding the Pentagon in Arlington, Virginia, and two on the San Francisco Bay Bridge distribution system. The writers also recognized that, at high weaving volumes, some weaving traffic would have to use the lanes adjacent to the lanes on both sides of the crown line, creating a compound weaving section and requiring a longer weaving section. Although, as a practical matter, the 1950 HCM recommended that weaving sections should only be used when the two approach roadways each carried "less than the normal capacity of two lanes of a one-way roadway and the total number of vehicles required to weave

[did] not exceed 1500 per hour." [Ref. 1] This volume restriction applied when the two entering roadways each consisted of a single lane. Additional lanes could be added to accommodate non-weaving flows.

The 1965 edition of the Highway Capacity Manual [Ref. 2] defined a weaving section as "a length of one-way roadway at one end of which two one-way roadways merge and at the other end of which they separate. A multiple weaving section involves more than two entrance and/or exit roadways." The basic design and analysis tools from the 1950 HCM were carried over into the new HCM, but considerably amplified with additional data (33 observations at 27 sites are listed in the appendix, and are selected from the 1963 BPR urban weaving area capacity study). Lane configuration is not specifically considered; all sketches showing lane lines are Type A, but the crown line is defined as a real or imaginary line connecting the merge and diverge gores. The weaving methodology is considered applicable to simple and multiple weaves, as well as one- and two-sided weaving, although the reader is referred to the material in the chapter on ramps when one-sided weaving is formed by an entrance ramp followed by an exit ramp.

The length of the weaving section is revised to begin at a point before the merge gore where the roadways are two feet apart to end at a point after the diverge gore where the roadways are twelve feet apart.

The equation for estimating the required width (number of lanes) was modified from the previous edition by (1) dividing the sum of volumes by a service volume (corresponding to a specific level of service on a basic freeway segment) rather than the single lane capacity and (2) allowing the multiplier of the smaller weaving volume (in the numerator and designated k) vary from one to three rather than defining it as three.

$$N = \frac{V_{W1} + kV_{W2} + V_{O1} + V_{O2}}{SV} \qquad (2.2)$$

where N = number of lanes

V_{W1} = larger weaving volume (vph)

V_{W2} = smaller weaving volume (vph)

V_{O1}, V_{O2} = non-weaving (outer) volumes (vph)

SV = appropriate service volume or capacity on approach and exit roadways (vphpl)

k = weaving influence factor

The concept of quality of flow (distinct from the level of service) was introduced, and five levels were identified, designated as I, II, III, IV, and V. Maximum lane service volume ranged from 2000 passenger cars per hour for level I down to 1600 passenger cars per hour for level V. The quality of flow was related to levels of service, but differed by the type of facility (freeways and multilane rural highways, two-lane rural highways, and urban and suburban arterials).

The graph relating weaving section length to the total weaving volume used the quality of flow rather than operating speed as in the 1950 HCM (see Figure 2.2). However, levels III, IV, and V correspond to speeds of (approximately) 40, 30, and 20 mph, and the lines corresponding to these three levels are very similar to those in the earlier edition. The width calculation sets k equal to 3 for quality of flow levels III,

IV, and V, as in the earlier edition. Smaller values of k, correspond to quality of flow levels I and II, result in longer and narrower weaving sections.

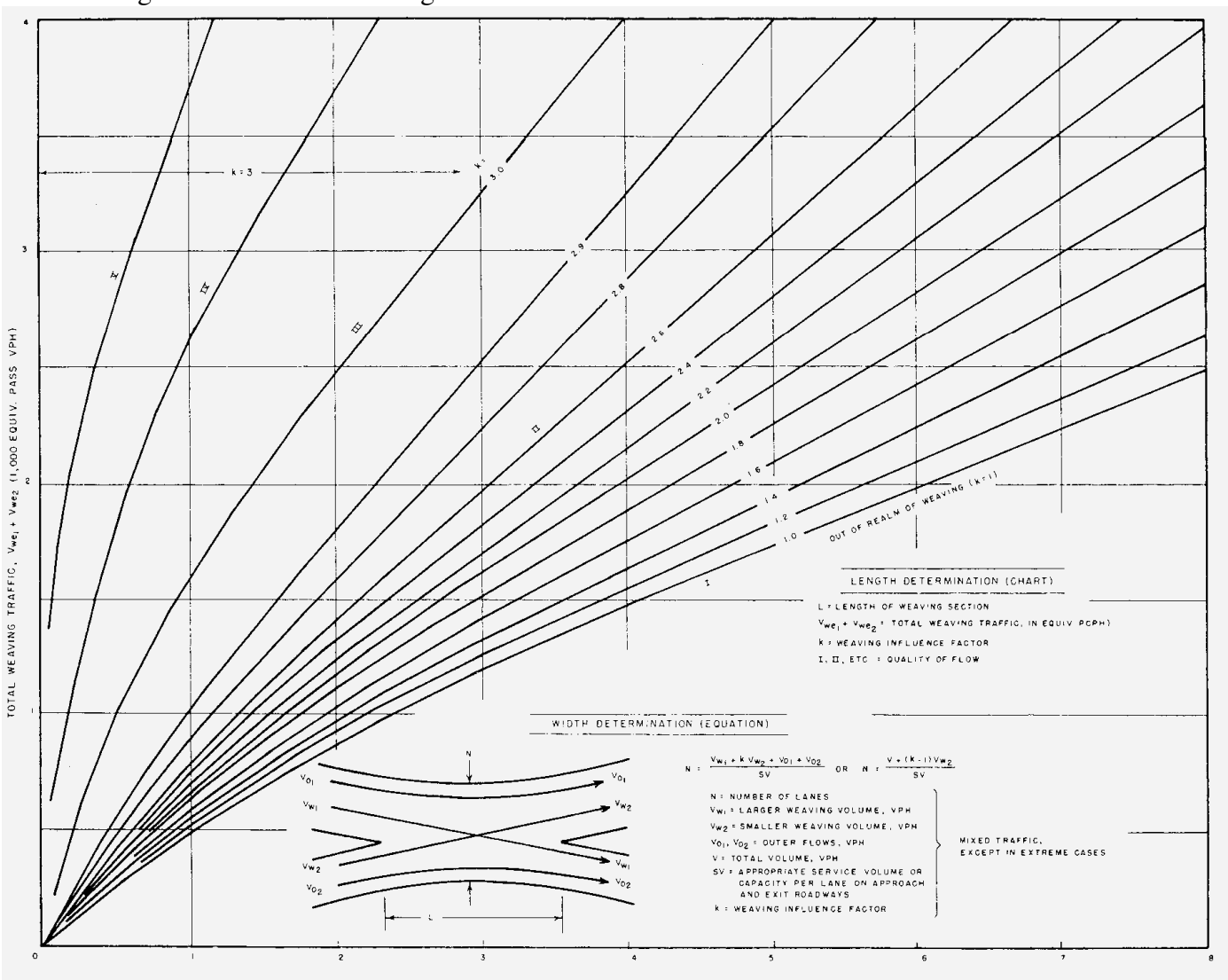

Figure 2.2. Weaving Analysis, 1965 Highway Capacity Manual

Multiple weave sections were analyzed in a very similar manner, but first required that the weaving maneuvers be distributed between the individual sections. Where the weaving could take place over more than one section, it was proportionally distributed over the entire length of the affected portion.

Guidelines were also provided for weaving on non-freeway facilities, where increased friction (such as driveways, parking, pedestrians, and traffic signals) reduces the efficiency of the weave. The use of an appropriate service volume would increase the required width, and use of a higher quality of flow level would increase the required length. For example, if quality of flow level V is expected where there are frictional elements, the length could be selected using level IV.

The third edition of the Highway Capacity Manual [Ref. 3] was initially published in 1985 and reflected the extensive research on weaving areas conducted since the release of the 1965 HCM. Weaving was defined as "the crossing of two or more traffic streams traveling in the same general direction along a significant length of highway, without the aid of traffic control devices. Weaving areas are formed when a merge area is closely followed by a diverge area, or when an on-ramp is closely followed by an off-

ramp and the two are joined by an auxiliary lane." Weaving areas are defined in terms of three principal geometric characteristics: weaving length (defined as in the 1965 HCM), lane configuration (relative placement and number of entry and exit lanes, generalized to three types), and width (number of lanes).

The two major components of the weaving analysis procedure were a model to predict the speed of weaving and non-weaving vehicles for a given weaving length, width and volume conditions, and a model to determine if the weaving traffic in a particular weaving area is constrained by its geometry. The speed estimation equation (eqn. 2.3) was developed through regression techniques on over 207 observations, with different regression constants for twelve categories (weaving and non-weaving traffic, configuration, and unconstrained and constrained operation) [Ref. 4]. The same equation was used for weaving and non-weaving speeds, with unconstrained operation initially assumed [Ref. 3].

$$S_w \text{ or } S_{nw} = 15 + \frac{50}{1 + a(1+VR)^b (v/N)^c / L^d} \qquad (2.3)$$

where S_w = average running speed for weaving traffic (mph)
S_{nw} = average running speed for non - weaving traffic (mph)
VR = volume ratio (fraction of traffic weaving)
v = total flow in weaving area (passenger cars per hour)
N = number of lanes in the weaving area
L = length of weaving area (feet)
a, b, c, d = regression constants, see Table 2.1 in the Ref. 3

Traffic was deemed constrained if the estimated proportion of the width used by the weaving traffic exceeded a specified maximum for each configuration [Ref. 3].

$$\begin{aligned} &\text{Type A}: \quad N_w = 2.19N\ VR^{0.571} L_H^{\ 0.234} / S_w^{\ 0.438} \\ &\text{Type B}: \quad N_w = N\left[0.085 + 0.703VR + (234.8/L) - 0.018(S_{nw} - S_s)\right] \qquad (2.4) \\ &\text{Type C}: \quad N_w = N\left[0.761 - 0.011L_H - 0.005(S_{nw} - S_w) + 0.047VR\right] \end{aligned}$$

where N_w = number of lanes required for weaving
N = number of lanes in the weaving area
VR = volume ratio (weaving volume to total volume)
L = weaving length (feet)
L_H = weaving length (stations)
S_w, S_{nw} = weaving and non - weaving speeds, mph

If N_w exceeded specified maximums (1.4, 3.5, or 3.0 lanes for Types A, B, or C, respectively), the weaving section was considered constrained, and the speeds were re-estimated appropriately. Finally, levels of service for weaving and non-weaving flows were directly related to the predicted speeds.

While this procedure represented a major improvement, particularly with the explicit consideration of the lane configuration, which has a major effect on the number of required lane changes in the weaving area, its use is awkward in design. Both the model for speed estimation and the test for constrained operation require an assumption of the weaving area's length, width, and configuration, thus requiring a trial-and-error approach in design. When the revised edition of the 1985 HCM was released in 1994 [Ref. 5], the weaving area chapter was unchanged.

The procedure for the analysis of weaving areas in the 1985 (and 1994) HCM is a synthesis of three different procedures developed in the 1970s and 1980s [Ref. 4]. The first was developed at the Polytechnic Institute of New York (PINY) [Ref. 6] using the 1963 BPR data and additional data collected as part of the study, and introduced the use of lane configuration as a major determinant of operating quality. The procedure was later revised largely to simplify its use [Refs. 7,8].

The second procedure was developed by Leisch [Ref. 9], and was designed to be used with the 1965 HCM or with Leisch's reformatting and expansion of the 1965 HCM [Ref. 10]. Although the same data was used to develop both procedures (PINY and Leisch), they yielded substantially different results in many cases [Ref. 4]. In an effort to get input from practicing engineers, both procedures were published in TRB's Circular 212: Interim Materials on Highway Capacity [Ref. 11].

Inconclusive results from users of Circular 212 led the FHWA to sponsor additional research, conducted by JHK and Associates [Ref. 12]. This study developed the speed estimation equations, but discarded the concepts of lane configuration and constrained operation. In order to develop the procedure eventually adopted in the 1985 HCM, the basic form of the speed estimation equations was retained, the concepts of lane configuration and constrained vs. unconstrained operation were reintroduced, and the equations recalibrated [Ref. 4].

Other Analytical Weaving Methodologies for Freeways

Fazio's Lane Shift Model

Fazio offered the lane shift concept as a refinement to the estimation of weaving and non-weaving speeds [Ref. 13]. Rather than estimating different model parameters for each configuration, the number of lane changes performed by the weaving traffic was directly incorporated into the speed model. Based on field measurements, the fraction of weaving vehicles entering the weaving section in each lane was found, with the number of lane changes for any one vehicle depending on how many lanes away from the crown line the vehicle entered the weaving section. Incorporation of the lane shift variable in the speed estimation equations improved their predictive ability over the JHK and 1985 HCM models. Type A weaves only were used in this work; however, the use of lane shifts should be applicable to any configuration. Fazio also found that, when evaluating the 1985 HCM procedure, nearly half of the 67 cases in this study did not meet the model's specified constraints, indicating the degree to which the model is limited in its application.

Fazio also developed a model to estimate speeds in each lane of a weaving area [Ref. 14]. The model was developed for a Type A weave with single lane entrance and exit ramps and a three lane freeway (resulting in a four lane segment between the ramps: three freeway lanes plus an auxiliary lane). The lane number was directly incorporated into the model as a multiplicative factor (lane 1 was the auxiliary lane, lane 4 the left lane). He found that average speeds increased the further the lane was from the crown line, and that the prediction of average weaving area speed outperformed the 1985 HCM speed estimation model. (The average weaving area speed in Fazio's model was found by weighting the lane speeds by

volume; for the 1985 HCM model, the estimated weaving and non-weaving were weighted by volume.) Fazio also found that the average speed of the weaving section is directly related to its length. He also noted that only 28 observations from three sites were used in model development and that the model itself is extremely configuration dependent.

California Weaving Model

Cassidy, Skabardonis, and May [Ref. 15] evaluated the weaving zone analysis and procedures found in the 1965 and 1985 (1994) HCM and those originally developed during developmental work for the 1985 HCM by PINY, Leisch, and JHK, using 143 15-minute observations at eight sites in California. These sites represented a range of design characteristics and configurations. Initial comparisons showed that all methods typically predicted operating speeds slower than observed speeds, although they were quite variable. The JHK and 1985 HCM models were recalibrated for the California data, resulting in R^2 values of less than 0.10 for the JHK model and less than 0.30 and 0.45 for Type B and Type C weaving areas respectively with the 1985 HCM model. The reestimated parameters of both models were quite different from the original parameters, particularly for the JHK model.

Cassidy, et al., developed several models using linear regression analysis, aggregating the data in a variety of ways. Most models had low R^2 values. Unsatisfactory results were also found through cross-validation analysis and classification and regression tree (CART) analysis. They found that the basic freeway segment analysis (Chapter 3 of 1985 HCM) more reliably predicted average speeds than the weaving analysis methods from the 1985 HCM.

Speed-flow scatter plots were assembled using five-minute observations from the eight sites, and, for non-weaving speeds, speed appeared to be insensitive to flows up to a v/c of 0.8, similar to results found for basic freeway segments. The speed-flow scatter plot for weaving speeds showed a high degree of scatter, and separate plots by configuration did little to decrease this variation. These results, in combination with those mentioned above, led the authors to conclude that "average travel speed is not an ideal measure of effectiveness for weaving sections." However, Cassidy, et al., found that density-flow scatter plots showed much less variation. Regression models for density prediction (as a function of the flow) resulted in R^2 values of nearly 0.90.

Continuing this work, Cassidy and May [Refs. 16,17] suggest that a more microscopic approach, i.e., modelling operational performance on a lane-by-lane basis, can more reliably describe the interactions between weaving and non-weaving traffic. The proposed procedure predicts the lane distributions of the four traffic streams through a weaving area (the two weaving streams, freeway-to-ramp and ramp-to-freeway; and the two non-weaving streams, freeway-to-freeway and ramp-to-ramp). The procedure was developed for major weaves (where at least three of the entering and exiting roadways have at least two lanes) and used data collected from nine sites in California. The development of the procedure for a variety of configurations is reported in Ref. 18; a single Type B weave is used in Ref. 16 and consists of a four-lane freeway with a single-lane entrance ramp resulting in a five-lane weaving area. The diverge is a five-lane to a four-two lane split, and the weaving area is 1460 feet long. Thus, freeway-to-ramp flows were not required to change lanes, but ramp-to-freeway flows had to change lanes at least once. Spatial distribution data (flows and lane changes) were collected only in the two lanes directly involved in the weave (lanes 1 and 2).

The fractions of freeway-to-ramp flows in lanes 1 and 2 were observed throughout the weave area. The majority of lane changes occurred within the first 500 feet of the weave. Their analysis suggested that the weaving flow rate (the sum of the two weaving flows) was the most significant factor affecting the spatial

distribution of the lane changes. Three regimes were identified: weaving flows of less than 2000 pcph, 2000 to 2300 pcph, and greater than 2300 pcph. Higher weaving flows resulted in larger proportions of the freeway-to-ramp flow changing lanes earlier in the weave.

The lane changing characteristics of the ramp-to-freeway flows were similar to the freeway-to-ramp flows; however, the variance of the spatial distribution of the lane changes was much higher. At this site, the freeway-to-ramp flow was the larger weaving volume and had a larger number of gaps into which the vehicles could weave. On the other hand, the ramp-to-freeway flow had a smaller number of gaps to weave into, resulting in a higher variance.

The fraction of freeway-to-freeway flow in lane 2 showed little change over the length of the weave. Some ramp-to-ramp traffic drifted into lane 2 (both lanes 1 and 2 could exit), but both of the non-weaving flows did not appear to be influenced by variations in the traffic flow conditions.

The proposed weaving procedure predicted spatial distributions for each of the four traffic streams through graphs representing empirical and simulated data. The INTRAS model (predecessor to FRESIM) was calibrated and used for this purpose. A set of graphs was required for each configuration, with a separate graph for each of the four traffic streams in each of the three weaving flow regimes. Since the non-weaving flows (and occasionally one of the weaving flows) tended to not be sensitive to the magnitude of the weaving flows, this resulted in six to eight graphs for each configuration. Multiple weaving zone lengths were accommodated on single graphs for each flow.

The user would then determine the fraction of each of the four traffic streams at various points within the weave. Multiplying by the measured or expected flows, lane volumes at any point within the weave could be estimated. Two major limitations were indicated: extreme traffic flow conditions may fall beyond the data set used in model development and not all weaving configurations are considered. The number of lanes in the weaving area was not found to be significant with respect to the lane changing behavior of the weaving traffic, although the sites used all had five or six lanes. Finally, the pre- or post-positioning of traffic in specific lanes due to downstream or upstream ramps was not considered due to understandable data collection considerations.

The authors recognized that weaving area capacity is not a specific value, but varies with volume of weaving traffic. They define capacity as (1) the maximum flow of vehicles that can travel at any point in a single lane and (2) the maximum rate of lane changing that can occur between two adjacent lanes over any 250-foot segment. Simulation modeling indicated a capacity of 2200 pcphpl at any point within the weaving area, and 1100 to 1200 lane changes per hour within any 250-foot segment of the weaving area.

Average density within a small segment of a weaving section was selected as the measure of level of service. As indicated earlier [Ref. 15], average flow is a reliable predictor of density. Thus, once the flow in a lane was estimated using the graphs, density could also be estimated. Density at capacity was estimated to be 46 pcpm, and level of service boundaries were found by dividing the density at capacity evenly.

Ostrom, Leiman, and May [Ref. 19] presented the FREWEV model, which is a weaving area analysis model and is an implementation of the point flow by movement method, which was discussed above. The point flow by movement method estimates the fraction of vehicles in each of the weaving lanes for each of the four weaving and non-weaving flows. Total lane flow at each point is then found by summing over all four flows. Ostrom, et al., also discussed the total point flow method, which estimates point flows in each lane simultaneously for all four weaving and non-weaving flows. The point flow by movement

method appears to work best for major weaves, while the total point flow method appears to work better for ramp weaves [Ref. 20].

The Level D method was developed by Caltrans [Ref. 21] for the analysis of ramp weave sections, and is appropriate only for high or near capacity traffic flow levels. Like the point flow by movements and total point flow methods discussed above, the Level D method predicts the distribution of traffic in the two right lanes (the auxiliary lane plus the right through lane) of the weaving section. The total point flow method was found to be somewhat superior in prediction of the lane flows by Windover and May [Ref. 20] largely due to inaccuracies in predicting the fraction of through freeway traffic in the right through lane. Windover and May describe the improvements to this estimation, and its inclusion (with the total point flow method) in the FRELANE program. FRELANE is a computer model designed to analyze isolated freeway sections, including weaving areas [Ref. 20].

Other Freeway Weaving Studies

Harkey and Robertson [Ref. 22] applied the 1985 HCM weaving methodology to two curved freeway segments in North Carolina. They noted that the geometry affected the traffic operation in the weaving areas, but did not quantify it. The authors were satisfied with the results of the HCM method; however, their recommended solution included an internal merge.

Pietrzyk and Perez [Ref. 23] solved the speed equation in the 1985 HCM for the weaving section length. Thus, for given conditions, including a desired LOS, the necessary weaving section length could be directly calculated. The authors note that it could be used on collector-distributor roadways, but that LOS criteria have not been established off the freeway mainlanes.

Kuwahara, Koshi, and Suzuki [Ref. 24] collected data from three weaving areas on Japanese freeways, and compared the measured results with the 1965 HCM, 1985 HCM, and the methods proposed by PINY, JHK, and Leisch (all three discussed above regarding the development of the 1985 HCM). The authors found the 1965 HCM to be inadequate for the particular weaving areas selected, the PINY and Leisch methods underestimated the speeds, and the 1985 HCM and JHK methods provided relatively good estimates, with the 1985 HCM slightly outperforming the JHK method. While 1985 HCM speed estimates deviate from observed speeds when lane flows are greater than 1200 pcu/hour-lane in the United States, this deviation was not noted in Japan. The authors provide capacity flows, volume ratios, weaving ratios, length, and configurations in the paper for the six weaving areas studied.

Alexiadis, Muzzey, and MacDonald [Ref. 25] observed that existing speeds in weaving areas in Boston exceeded those predicted by the 1985 HCM weaving method. They re-estimated the coefficients for the speed equations using data collected from 11 sites in the Boston area, resulting in improved speed prediction, which passed a t-test at a 95% confidence level. Because only overall average speed was collected at the freeway sites, a single speed equation representing the average of weaving and non-weaving speeds was estimated.

Alexiadis, et al. [Ref. 25], also estimated two speed equations (weaving and non-weaving speeds) using data from Logan airport access roads. Data from two sites at the airport were used; both were two-sided, Type C weaves, and typical speeds were much lower than normal freeway speeds. The authors replaced the (1+VR) term in the 1985 HCM general speed equation (eqn. 2.3) with (v_{w2}/v), the "cross-weaving ratio" (the smaller weaving volume divided by the total volume in the weave), and re-estimated the parameters. Again, the estimated speeds were much closer to the observed speeds than those predicted by the 1985 HCM equations and parameters. However, when selecting level of service, the cutoff speeds in

the 1985 HCM were used in spite of the low operating speeds (compared to that on freeways). In the re-estimated equations, the numerator was unchanged, resulting in a potential range of 15 to 65 mph, the same as the 1985 HCM.

Vermijs [Ref. 26] used simulation to evaluate capacity for several Type A major weaves and ramp weaves. The simulation model FOSIM was used, which had been developed at the Delft University of Technology in the early 1990s. Four specific factors were considered to have an impact on weaving area capacity: (1) weaving section length, (2) weaving flow, (3) traffic mix, and (4) entering speed. The first three factors were examined in this paper.

The capacity of a weaving section was expected to increase with increasing length, up to "a certain length." Vermijs noted that most lane changes take place within the first 350 meters (1150 feet) of a weaving section (based on limited observations in The Netherlands [Ref. 27]) and speculated that longer weaving sections would not increase capacity. While the study design apparently included weaving areas as short as 100 meters (330 feet), the shortest weaving length reported was 400 meters (1310 feet). The simulation studies showed that weaving section length ranging from 400 to 1000 meters (1310 to 3280 feet) had no significant impact on weaving capacity.

Increasing weaving flow was shown to decrease the capacity of the weaving section. Lastly, the percentage of trucks had a profound impact on capacity, with lower values in terms of vehicles per hour for higher truck percentages. The truck pce (passenger car equivalents) ranged from 2.5 to 3.6, depending on the weaving section configuration and the level of congestion. In addition, the truck pce was higher for weaving sections than basic freeway segments.

Stander and Tichauer [Ref. 28] examined a 220-meter (720-foot) Type A ramp weave in South Africa. The weave consisted of two through lanes plus an auxiliary lane. Traffic volumes entering from the ramp at the beginning of the weave were nearly as high as the entering through traffic. Exiting traffic was much smaller.

The weave was divided into three longitudinal segments of 73 meters (240 feet) each. The bulk of the lighter weaving movement took place in the first segment in all traffic conditions reported. Under moderate traffic conditions, most of the heavier weaving movement also took place in the first segment, but as traffic increased, there were roughly the same number of lane changes in the third segment as seen in the first.

The authors noted that some through (non-weaving) vehicles on the freeway mainlanes were observed changing into the auxiliary lane at the beginning of the weave and changing back into one of the through lanes at the end of the weave. This implies congestion on the mainlanes that may be a result of downstream bottleneck (perhaps due to the addition of the entrance ramp volume onto the two through lanes) rather than capacity conditions due to the weave. This may have also significantly contributed to the larger lane-changing volume in the third segment of the weaving area.

Weaving on Frontage Roads

Weaving on frontage roads can be similar to freeway-type weaving when an exit ramp is followed by an entrance ramp connecting the freeway mainlanes to a parallel one-way frontage road. However, the speed-based methodology in chapter 4 of the 1985 HCM [Refs. 3,5] is inappropriate, as the typical operating speeds correspond only to the poorer levels of service regardless of the volume levels. At-grade intersections and driveways introduce arterial-like weaving characteristics on the frontage roads. Two

recent studies emphasizing the freeway-type weaving on frontage roads are discussed in this section, while arterial weaving is covered in the next section. (The current research did not have sufficient resources to investigate arterial or frontage road weaving beyond this review of the literature.)

Frederickson and Ogden [Ref. 29] examined Type A weaves on frontage roads, which were formed by an auxiliary lane between the exit ramp to the frontage road and the entrance ramp back to the freeway mainlanes. Their procedure is based on data collected at six sites and tested with data from two additional sites, all in Texas. Speed was rejected as a measure of the quality of service since it was found to be insensitive to flow. Although density was found to be strongly related to flow (both on a per lane basis), it, too, was rejected, due to the close relationship between density, flow, and speed. It should be noted that flow and density were directly measured from the video-taped data, and speed was calculated from the flow and density.

Instead, Frederickson and Ogden selected lane changing intensity (LCI) as their principal measure of quality of service. LCI is defined as the number of lane changes per hour divided by the number of lanes in the weaving section and the length of the weaving section. A linear model relating LCI to flow and the number of lanes in the weaving section was developed for each of three weaving section lengths (400 to 600 feet, 600 to 900 feet, and 900 to 1200 feet). Three levels of service were subjectively identified by observation of the videotapes: unconstrained (0 to 3000 lane changes per hour per mile per lane or lcphpmpl), constrained (3000 to 6000 lcphpmpl), and undesirable (more than 6000 lcphpmpl). LOS A and B were associated with the unconstrained range, LOS C and D with constrained, and LOS E and F with undesirable.

This procedure does not address capacity, as the maximum observed flow was approximately 600 passenger cars per hour per lane. In addition, since the flow rate used in the estimation of LCI is found by adding the flow rate from the exit ramp and the frontage road approaching the weaving section then dividing by the number of lanes, relative values of ramp and frontage road flows are not considered. The fraction of weaving vehicles is similarly not considered.

The Texas Transportation Institute (TTI) developed procedures for the Texas Department of Transportation to estimate the level of service on freeway frontage roads. Their focus was on one-way frontage roads, but also examined delays at ramp junctions on two-way frontage roads. Two weaving types were considered: one- and two-sided weaves.

The one-sided weave is the same as the Type A weave in Fredericksen and Ogden [Ref. 29]. Fitzpatrick and Nowlin [Refs. 30,31] used NETSIM to develop a procedure to evaluate level of service, and used the field data from Ref. 29 to calibrate the model. Weaving sections of 100 to 500 meters (330 to 1640 feet) were examined. The weaving volume was taken to be the sum of the exiting and entering traffic, implying that no exiting traffic was allowed to re-enter the freeway (this was not specifically stated). No sources of interruption to the frontage road traffic (such as driveways and cross streets) were assumed to be within the weaving section.

Weaving speed was found to decrease with increased weaving volume, but that it was more sensitive to the number of lane changes than the volume. (The weaving volume was also found to be linearly related to the number of lane changes.) Speed was selected as the principal measure of the quality of service, the authors noting that speed is also used in the HCM [Ref. 5] for arterials, that it is easily understood, and easily measured.

Three levels of operation (unconstrained, constrained, and undesirable) were subjectively identified from a plot of weaving speed vs. number of lane changes. The break points in the slopes were identified at 2000 lane changes/hour and 4000 lane changes/hour. As in Ref. 29, LOSs A and B were associated with unconstrained operations, C and D with constrained, and E and F with undesirable. However, these levels are not comparable with those identified in Ref. 29, as the number of lane changes was used rather than the lane change intensity (lane changes per hour per mile per lane). This distinction is uncertain, since the number of lane changes was not found to vary with the length of the weave.

The speed was also found to be sensitive to the length of the weave for weaving sections less than 300 meters (980 feet). The levels of service mentioned above were selected for weaving sections greater than 300 meters; as such, the authors recommended a desirable minimum weaving length of 300 meters, with a 200-meter (660-foot) absolute minimum. These results were validated at a single site in Houston with data in the unconstrained and constrained regions only. A visual inspection of some of the calibration data was used to verify the breakpoint between constrained and undesirable operations.

A two-sided weaving section [Ref. 32] was defined as the distance between an exit ramp to the frontage road and the downstream intersection. Since the exit ramp typically enters the frontage road from the left, traffic turning right at the downstream intersection was considered to be the weaving traffic; in effect, this is an example of arterial weaving. Four sites were selected to calibrate NETSIM, all with signalized downstream intersections, and with a minimal number of driveways between the ramp terminal and the intersection. None of the sites included a frontage road lane created by the off ramp. The distance required for right-turning drivers to get into the right lane of the frontage road along with the difficulty each driver had in changing lanes were recorded. In addition, the length of queues from the signalized intersection were recorded at three of the sites.

Three cases were simulated: two-lane frontage road, three-lane frontage road, and two-lane frontage road with an auxiliary lane formed by the exit ramp. Simulations were made for combinations of volumes, turning percentages (for both the ramp and frontage road traffic), and ramp-to-intersection (or weaving) distance. Speed and density were candidate MOEs. Speed was taken directly from the NETSIM output, and density was calculated by dividing the flow by the speed. Regression equations for speed and density were then developed. Speed was found to be highly sensitive to the total volume, the fraction of the ramp volume turning right (thus weaving across the frontage road), and the weaving distance, and was thus discarded as the measure to determine LOS. Density was found to be dependent on the total volume and the fraction of traffic turning right, but not the length (since density is defined in terms of unit length). The regression equations were tested at one site, and density was reasonably well estimated. Density was selected as the principal measure for LOS determination.

Examination of the speed-density relationship revealed slope changes at 40 and 100 veh/km-lane (65 to 160 veh/mile-lane), and were used to delimit unconstrained, constrained and undesirable levels of operation, which were again associated with LOS A and B, C and D, and E and F, respectively. These cutoffs were developed assuming moderate cross street traffic and optimally timed traffic signals.

Desirable and minimum ramp-to-intersection spacings were found by solving the regression equations for weaving section length and using densities of 40 and 100 veh/km-lane (65 and 160 veh/mile-lane), respectively. While AASHTO recommends an overall minimum of 105 meters (340 feet), the field studies indicated that the majority of drivers use 60 to 120 meters (200 to 400 feet) to weave across the frontage road. In addition, the queue started to have serious effects on weaving drivers when it backed up to within 90 meters (300 feet) of the ramp. Thus, an overall minimum spacing of 150 meters (490 feet)

was recommended, with tables showing minimum and desirable spacings for a range of frontage road and ramp volumes, the fraction of ramp volume turning right, and the number of frontage road lanes.

Next, chapter 11 (Urban and Suburban Arterials) of the HCM [Ref. 5] was used as a basis for a procedure to estimate level of service on frontage roads [Ref. 33]. Arterial capacity is controlled by signalized intersections, which are covered separately in chapter 9. The significant sources of delay along frontage roads were found to be the cross street intersections (with either signal or stop control on the frontage road) and the ramps. Earlier, Gattis, Messer, and Stover [Ref. 34] developed delay equations for ramp junctions on one- and two-way frontage roads, and found negligible additional delay when auxiliary lanes were used.

Fitzpatrick, et al. [Ref. 33], examined the effects of link length, volume, access density (number of access points, such as driveways, per km), and link type on the link running time. Link type was determined by the downstream terminal of the link: traffic signal, stop sign, exit ramp, or entrance ramp. The dependence of running time on link type was reduced by excluding links with speeds less than 8 km/hour (5 miles/hour). The excluded links were largely those with downstream signals or stop signs; the delay on these links can be estimated using techniques in chapters 9 and 10 (signalized and unsignalized intersections, respectively) of the HCM. Average speed was unrelated to the number of access points with less than 20 access points/ km (32 access points/mile) on a one-way frontage road (16 access points/km, or 26 access points/mile, on a two-way frontage road). Greater numbers of access points resulted in reduced speed.

The level of service over an extended section of frontage road can be determined through a speed estimate based on link travel times (developed in Ref. 33), delays around ramps (developed in Ref. 34), and intersection delays (from the current HCM). The level of service boundaries recommended are those for Class I arterials from chapter 11 of the HCM (range of free-flow speeds: 35-45 mph; 40 mph typical free-flow speed).

The procedures for analysis of one- and two-sided weaving on frontage roads, level of service evaluation of extended frontage road sections, and spacing to metered entrance ramps (from Ref. 36) were summarized in Ref. 35, along with worksheets similar in format to those found in the Highway Capacity Manual.

Arterial Weaving Areas

While the principal source for arterial weaving was discussed in the frontage road section, one additional source was found for non-freeway weaving sections. Iqbal [Ref. 37] concentrated on expressway-type facilities and excluded consideration of traffic signals or stop signs. His methodology essentially covers freeway-type weaves with severe geometrics: low speeds (15 to 40 or 45 mph), short weaving sections (less than 600 feet), horizontal curvature within the weave (up to 40°), and large approach and diverge angles (up to 65°).

Iqbal tested the JHK, 1985 HCM, and Fazio models developed for freeway weaving sections (discussed above) on the non-freeway sites. He also recalibrated the models and retested them. When recalibrating the models, the numerator of the speed equation was reduced to reflect upper speeds of 40, 45, or 55 mph, depending on the type of weave, rather than 65 mph. In addition, a number of other models incorporating the approach angles and horizontal curvature within the weaving section were developed and tested. In all cases, the models predicted weaving and non-weaving speeds. The models specifically developed with the non-freeway data performed significantly better than the freeway models (either with the original

parameters or the recalibrated parameters). Finally, the author selected new speed cutoffs for level of service determination for non-freeway conditions, recognizing that the speed criteria in the 1985 HCM reflected operating conditions on freeways, and, thus, much higher speeds. For this case, LOS F is achieved when the speeds are less than 20 or 25 mph.

References

1. *Highway Capacity Manual,* Highway Research Board, 1950.

2. *Highway Capacity Manual,* Special Report 87, Highway Research Board, 1965.

3. *Highway Capacity Manual,* Special Report 209, Transportation Research Board, 1985.

4. R.P. Roess, "Development of Weaving Area Analysis Procedures for the 1985 Highway Capacity Manual," *Transportation Research Record* 1112, Transportation Research Board, 1987.

5. *Highway Capacity Manual*, Special Report 209, Transportation Research Board, 1994.

6. L.J. Pignataro, et al., *Weaving Areas: Design and Analysis,* NCHRP Report 159, Transportation Research Board, 1975.

7. R.P. Roess, et al., *Freeway Capacity Analysis Procedures, Final Report,* Project DTFH-11-9336, Federal Highway Administration, 1978.

8. R.P. Roess, et al., *Freeway Capacity Procedures, Procedural Manual,* Project DTFH-11-9336, Federal Highway Administration, 1978.

9. J.E. Leisch, *Completion of Procedures for Analysis and Design of Weaving Sections*, Volumes I and II, Federal Highway Administration, 1983.

10. J.E. Leisch, *Capacity Analysis Techniques for Design and Operation of Freeway Facilities,* Report FHWA-RD-74-24, Federal Highway Administration, 1975.

11. *Interim Materials on Highway Capacity,* Transportation Research Circular 212, Transportation Research Board, 1980.

12. W.R. Reilly, J.H. Kell, P.J. Johnson, *Weaving Analysis Procedures for the New Highway Capacity Manual, Technical Report,* Federal Highway Administration, 1984.

13. J. Fazio, N.M. Rouphail, "Freeway Weaving Sections: Comparison and Refinement of Design and Operations Analysis Procedures," *Transportation Research Record* 1091, Transportation Research Board, 1986.

14. J. Fazio, "Geometric Approach to Modeling Vehicular Speeds through Simple Freeway Weaving Sections," *ITE Journal,* Vol. 58, Nr. 4, 1988.

15. M. Cassidy, A. Skabardonis, A.D. May, "Operation of Major Freeway Weaving Sections: Recent Empirical Evidence," *Transportation Research Record* 1225, Transportation Research Board, 1989.

16. M.J. Cassidy, A.D. May, "Proposed Analytical Technique for Estimating Capacity and Level of Service of Major Freeway Weaving Sections," *Transportation Research Record* 1320, Transportation Research Board, 1991.

17. M.-H. Wang, M.J. Cassidy, P. Chan, A.D. May, "Evaluating the Capacity of Freeway Weaving Sections," *Journal of Transportation Engineering,* Vol. 119, Nr. 3, American Society of Civil Engineers, 1993.

18. M.J. Cassidy, P. Chan, B. Robinson, A.D. May, *A Proposed Analytical Technique for Designing and Analyzing Major Freeway Weaving Areas,* Report UCB-ITS-RR-90-Draft, Institute of Transportation Studies, University of California, Berkeley, 1990.

19. B. Ostrom, L. Leiman, A.D. May, "Suggested Procedures for Analyzing Freeway Weaving Sections," *Transportation Research Record* 1398, Transportation Research Board, 1993.

20. J.R. Windover, A.D. May, "Revisions to Level D Methodology of Analyzing Freeway Ramp Weaving Sections," *Transportation Research Record* 1457, Transportation Research Board, 1994.

21. K. Moskowitz, L. Newman, *Traffic Bulletin 4: Notes on Freeway Capacity,* California Department of Public Works, July 1962.

22. D.L. Harkey, H.D. Robertson, "Weaving Analysis for Curved Freeway Segments," *ITE Journal,* Volume 58, Nr. 3, March 1988.

23. M.C. Pietrzyk, M.L. Perez, "Weaving Section Length Analysis: A Planning Design Approach," *ITE Journal,* Volume 60, Nr. 6, June 1990.

24. M Kuwahara, M. Koshi, T. Suzuki, "Capacity and Speed of Weaving Sections of the Tokyo Metropolitan Expressway," *ITE Journal,* Volume 61, Nr. 3, March 1991.

25. V. Alexiadias, P.D. Muzzey, O.J. Macdonald, "Weaving Operations in Boston," *ITE Journal,* Volume 63, Nr. 5, May 1993.

26. R. Vermijs, "New Dutch Capacity Standards for Freeway Weaving Sections Based on Micro Simulation," *Proceedings of the Third International Symposium on Highway Capacity,* R. Rysgaard, editor, Road Directorate, Ministry of Transport, Denmark (publisher), 1998.

27. H. Schuurman, R.G.M.M. Vermijs, *Traffic operation near discontinuities* (in Dutch), Transportation Research Laboratory, Civil Engineering, Delft University of Technology, 1993.

28. H. Stander, C. Tichauer, "Evaluation of Weaving on Freeways with Sub-standard Geometric Characteristics," *Proceedings of the Third International Symposium on Highway Capacity,* R. Rysgaard, editor, Road Directorate, Ministry of Transport, Denmark (publisher), 1998.

29. V.E. Fredericksen, M.A. Ogden, "Proposed Analytical Technique for Analyzing Type A Weaving Sections on Frontage Roads," *Transportation Research Record* 1457, Transportation Research Board, 1994.

30. K. Fitzpatrick, R.L. Nowlin, *One-Sided Weaving Analysis on One-Way Frontage Roads,* Report No. FHWA/TX-96/1393-1, Texas Transportation Institute, Texas A&M University, 1995.

31. K. Fitzpatrick, L. Nowlin, "One-Sided Weaving Operations on One-Way Frontage Roads," *Transportation Research Record* 1555, Transportation Research Board, 1996.

32. R.L. Nowlin, K. Fitzpatrick, *Two-Sided Weaving Analysis on One-Way Frontage Roads,* Report No. FHWA/TX-97/1393-2, Texas Transportation Institute, Texas A&M University, 1996.

33. K. Fitzpatrick, R.L. Nowlin, A.H. Parham, *Development of Level-of-Service Analysis Procedure for Frontage Roads,* Report No. FHWA/TX-97/1393-3, Texas Transportation Institute, Texas A&M University, 1996.

34. J.L. Gattis, C.J. Messer, V.G. Stover, *Delay to Frontage Road Vehicles at Intersections with Ramps,* Report No. FHWA/TX-86/402-2, Texas Transportation Institute, Texas A&M University, 1988.

35. K. Fitzpatrick, R.L. Nowlin, A.H. Parham, *Procedures to Determine Frontage Road Level of Service and Ramp Spacing,* Report No. FHWA/TX-97/1393-4F, Texas Transportation Institute, Texas A&M University, 1996.

36. S. Sharma, C.J. Messer, *Distance Requirements for Ramp Metering,* Report No. 1392-5, Texas Transportation Institute, Texas A&M University, 1994.

37. M.S. Iqbal, "Analytical Models of Weaving Area Operations Under Nonfreeway Conditions," *ITE Journal,* Volume 65, Nr. 7, July 1995.

CHAPTER 3. SIMULATION

Important issues regarding the use of simulation are presented in this chapter. First, the selection of an appropriate simulation model is briefly addressed. The model selected was the most widely used simulation model available at the time of this study. The calibration and validation of the simulation model are also described. It should be noted that the data used in this chapter is described later, in Chapter 5. This somewhat unusual format was selected by the authors in order to present the data collection in its respective place as a part of model development. The issues of simulation, however, overshadow the entire project, and are presented here.

Simulation Approach

Simulation was a key element of this study. Given the time and monetary constraints, adequate field tests for model development were not possible. FRESIM [Ref. 1] was selected because, at the time of the research, it was the only widely-accepted and available microscopic simulation model for freeways. FRESIM was originally developed as a stand-alone model, called INTRAS, but, in later revisions, renamed then incorporated into CORSIM. FRESIM models vehicle movements on a second-by-second basis, with detailed car-following and lane-changing routines.

The version used in this work was one in use by the now-defunct Viggen Corporation, which had taken the officially distributed version of CORSIM and added pre- and post-processors. Later, a new version of CORSIM was released which made several significant changes to the car-following and lane-changing routines. However, the direct cause of these changes was not apparent, and not having access to the source code of the newer version made detailed calibration within the time and budget limitations of the research impossible. As such, the version in use by Viggen was used in this study because access to the source code was vital for this project, permitting as it did the research team to specify second-by-second vehicle position and speed output which allowed the direct calculation of speeds, flows, and densities. The research team was also able to recalibrate embedded routines, for which user access is not possible through the usual input process. In this recalibration process, several iterations could be compiled and tested in a single day.

A short FORTRAN program was written to produce speeds, flows, and densities from the second-by-second vehicle position data in each lane of the weaving area. Average densities were computed by adding the number of cars in each lane every 15 seconds, then averaging the counts over each five minute period. Density was then calculated by dividing this average by the length of the lane (typically, the length of the weaving area). Speed was found by averaging the instantaneous speed of each vehicle within the weaving area every second, resulting in a time-mean speed. Traffic volumes were found by placing simulated system detectors in each lane at several locations.

As described in Chapter 5, field data was collected from videotapes of operations for a range of weaving areas. Density was found in the field studies in the same way it was for the simulation. The number of vehicles by lane within the weaving area was counted every 15 seconds then averaged over each five-minute period. Volumes were found by simply counting the vehicles in each lane as they passed particular points in the weave corresponding to the simulated detector positions. Speed, however, was estimated by measuring the travel time of one vehicle every 30 seconds, which results in a space-mean speed. This speed measurement technique does not yield the same results as that used in the simulation (space-mean speed vs. time-mean speed), however, as indicated in the literature review in Chapter 2,

speed is often an unreliable predictor of traffic conditions and is difficult to estimate from other data. As such, the authors restricted their use of speed in the analysis to the broadest qualitative assessments.

The researchers made an important distinction between two separate evaluations of simulation. In this research, calibration was performed first, in an attempt to make FRESIM work as well as possible for the test sites, adjusting parameters as appropriate to match conditions at the test site. Then, the research evaluated the validity of simulation for use in the research. Note that there was no attempt to develop the simulation for use in creating the end product (a direct evaluation of capacity and level of service in weaving zones), but rather for its supporting role in the research. Research into the development of the use of simulation by the end user would focus first on verification, to show that the simulation faithfully follows the theories of traffic movement on which it lies, and then to validation, to prove that the simulation is usefully realistic, and finally to calibration, which is the end user's responsibility to adjust the parameters of the model to match a particular application case. It should be noted that calibration against a test site is also a part of the development of underlying theories, and therefore is a part of initial verification. This is the context in which calibration was conducted for this research—to manipulate the implementation of theories within FRESIM to produce the most realistic model possible. Then and only then could the researchers evaluate the effectiveness of the resulting simulation.

A typical FRESIM network is shown in Figure 3.1.

Figure 3.1. FRESIM Pilot Study Network.

FRESIM Calibration

Before exploring the calibration of embedded routines, the researchers examined the user-available parameters that affect the performance of traffic in a freeway weaving section. These parameters are

- location of advance warning sign
- adjusting the car-following sensitivity factor
- limiting anticipatory lane changes
- adjusting the maximum acceleration and deceleration rates
- adjusting the mix of trucks

The advance warning sign notifies the simulation model of the point at which vehicles begin to make lane changes in preparation of exiting the freeway. Placing the advance warning sign 1200 feet in advance of the merge point provided a spatial distribution of lane changes which agreed very closely to the data from the pilot study, as shown in Figure 3.2.

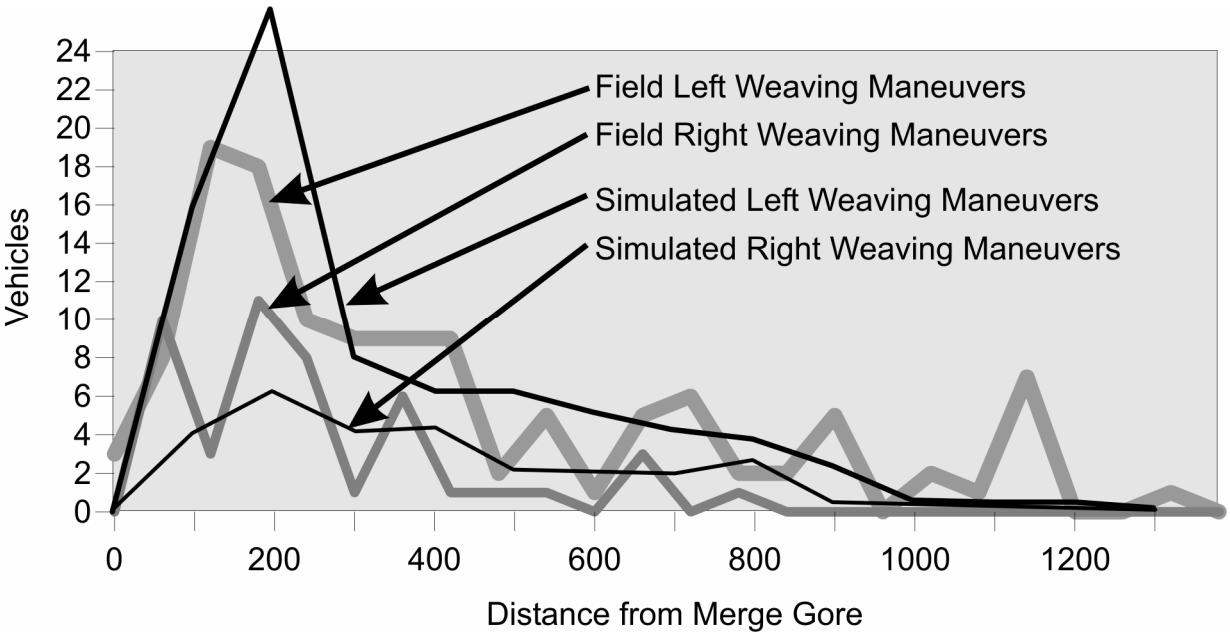

Figure 3.2. Simulated and Observed Spatial Distribution of Lane Changes

In general, the densities found in FRESIM at capacity conditions were lower than those found in the field. At capacity, the researchers observed a density of 71 vehicles per lane-mile in the pilot study, but FRESIM reported a density of only 37 vehicles per lane-mile under the same volume conditions. A density of 47 vehicles per lane-mile was found in a sub-capacity sample of the field data with the same weaving ratio, but 8 to 10 % lower flows.

Driver performance characteristics were adjusted to evaluate their impact on density. A substantial increase in driver sluggishness (achieved by tripling the car-following sensitivity factor) did not increase the density to the observed values, but did appreciably reduce the capacity with queues forming over the entire length of the upstream links. However, when changes in the car-following sensitivity factor were made on a link-specific basis (a modification of standard FRESIM, see below), this factor was found to be quite useful in modeling the immediate weaving section.

Desired speed had an impact on the operational characteristics within the weaving area. Setting the desired speed to 35 mph allowed the simulated speed and density to match that observed in the pilot study; however, since speed and density will not be known *a priori,* this is not a reasonable calibration factor. However, it does point to an issue regarding the simulation model's response to desired speeds.

Vehicle mix also had an impact on operational characteristics, allowing one to "calibrate" by varying the vehicle mix. This also is an unreasonable calibration factor, but does verify previously observed impacts of the fraction of heavy vehicles on operational characteristics on freeways, as documented in the Highway Capacity Manual. Explicit consideration of the fraction of trucks in the development of weaving area capacity models is beyond the scope of this study, but must be pursued in refinement of these models.

Anticipatory lane changes allow the simulated vehicles to change lanes in advance of the merge point to avoid congestion at the merge and change back into the weaving lanes to complete an exit maneuver. Very few drivers attempted this action in the field studies, with the vast majority completing their lane

changes within the first 500 feet of the weave. However, variation of this parameter had little impact on the simulation results.

Detailed Calibration at Two Sites

The researchers attempted detailed calibration of the simulations of two data sets that were part of the original JHK/FHWA data collection effort. One was located on the Baltimore-Washington Parkway in Maryland, and the other one was located on US-101 in California. These two data sets were used because the demand equaled or exceeded capacity within the time period over which the data were collected. These data were collected using time-lapse aerial photography at one-second intervals. These data were reduced to provide vehicle trajectories consisting of vehicle longitudinal and lateral positions, also at one-second intervals. The FRESIM model also has the capability of writing vehicle position information on a second-by-second basis to a peripheral file.

The researchers then developed a computer program to provide longitudinal distributions of lane-change maneuvers for each five-minute time period in the data sets. The program also provided origin-destination volumes, density, and speed assessments. This program worked similarly to the post-processor of FRESIM output as previously described.

The researchers corrected several problems arising from modifications made to facilitate graphical animation output in the CORSIM package. These modifications, in the subroutines FGAP and EMGNCY, attempted to eliminate the possibility of an exiting vehicle missing the off-ramp. The added code caused unexpected queuing in the middle of the weaving zone as vehicles became trapped by refusing to proceed but being unable to get to the exit ramp. These conditions were never observed in the field but appeared in simulations of capacity conditions. The researchers bypassed these modifications in the code of the computer program.

The researchers also made modifications to FRESIM to provide additional calibration tools. The first allowed the modification of the following distance on a link-by-link basis, and the second allowed changing the minimum deceleration in mandatory lane changes. The researchers also examined the minimum assumed deceleration of the lead vehicle in a lane-changing situation.

Following Distance

The following distance (and, hence, the capacity) can be modified on a link-specific basis through an added field on card type 20 (columns 41-44). The desired change is provided as a percentage of the nominal value. Thus, an entry of 0 (the default value) or 100 will result in no change, while, for example, an entry of 110 leads to every element of the following distance array being multiplied by 1.1.

A number of runs for each data set were performed with different values of the following distance on the weaving link. The purpose of these runs was to match the observed capacity of the merge lane. This was done by observing which value most closely matched the observed longitudinal speed distribution in the merge lane, particularly when it appeared that a queue was beginning to form. The presence of a queue was determined by observing when the speed reductions appeared to be propagating upstream from one time period to the next.

The research found that factors of 130% and 95% applied to the following distance for the Baltimore-Washington Parkway and US-101 data sets, respectively, allowed the simulation results to closely match the observed data. These results were not surprising, considering that the two sites differ greatly in terms

of design speed, existence of shoulders, proximity of lateral structures, and so on. The 1994 Highway Capacity Manual provides capacity corrections for such factors.

Minimum Deceleration in Mandatory Lane Changes

The second modification allowed us to modify the value of the minimum deceleration for computing the value of the acceptable risk in mandatory lane changing. A field was added in columns 25-28 to optional card type 70 to accommodate this capability. The variable provided by FRESIM is ZMNDEC. The impact of this variable was investigated on the two data sets already calibrated for capacity. The researchers hoped to determine if the field-observed longitudinal lane changing distributions between the auxiliary lane and the adjacent through lane could be replicated in FRESIM. The tested range included -5 (the default), -0.1, 2, and 5 feet/sec^2. Results indicated that the effect of this variable is not observable, indicating that this variable has little effect on the distribution of longitudinal lane changes. Therefore, it also had little effect on the values of capacity, speed, or density.

This modification, however, exposed an incorrect use of the variable ZMNDEC to control coast-down deceleration (applied when a vehicle enters a link with a lower free-flow speed than its current speed). This occurred when the positive values mentioned above were applied and resulted in very high speeds being observed. The researchers replaced the use of the variable ZMNDEC for controlling coast-down deceleration with the variable ZMNAC, which is the maximum deceleration allowed for the car-following rule in FRESIM (and, hence, must always be negative).

Minimum Deceleration of the Lead Vehicle during a Lane Change

Lastly, the researchers examined the impact of an existing but undocumented variable (optional card type 70, columns 21-24), which defines the minimum assumed deceleration of the lead vehicle in a lane-changing situation. The value was changed from the default of -5 to -7.5 feet/sec^2. This change was found to have a strong effect on the longitudinal lane-changing distribution from the auxiliary lane to the adjacent through lane, but a much weaker effect on the distribution in the other direction. Both effects were seen in both data sets. The value of -7.5 ft/sec^2 led to a result more closely resembling the field data, and this was used in the simulations later in the research. As with the previous parameters, this parameter had little effect, however, on the predicted capacity and associated density and speed, so that no modification to the capacity calibration appeared necessary.

Sensitivity Analysis of Calibration Parameters at One Site

Using the same IH-580 site in Alameda that was used for capacity analysis, the researchers conducted a test of the three calibration parameters. The sample used reflected sub-capacity conditions. The results of the sensitivity test are contained in Table 3.1.

Speed Limit	(Card 68) Car-Following Sensitivity	(Card 20) Following Distance	Sign Distance	Speed, mph Lane 1	Speed, mph Lane 9	Volume (vph) Lane 1	Volume (vph) Lane 9	Number of Vehicles Lane 1	Number of Vehicles Lane 9	Density (veh/mi-ln) Lane 1	Density (veh/mi-ln) Lane 9
55						1344	1956			50.0	29.0
55	1.05	100%	3000	46.3	49.2	1644	1968	10.4	5.7	42.9	23.5
55	1.05	**70%**	3000	49.8	51.9	1692	1956	10.9	4.9	45.0	20.2
55	1.05	**80%**	3000	48.3	51.6	1704	1944	10.8	4.8	44.6	19.8
55	1.05	**90%**	3000	46.0	49.9	1680	1944	11.0	5.1	45.4	21.0
55	1.05	**100%**	3000	46.3	49.2	1644	1968	10.4	5.7	42.9	23.5
55	1.05	**110%**	3000	43.9	49.2	1716	1956	10.9	5.7	45.0	23.5
55	1.05	**120%**	3000	38.1	46.7	1728	1944	11.6	6.3	47.9	26.0
55	1.05	**130%**	3000	28.8	26.6	1656	1476	13.9	9.7	57.3	40.0
55	**1.65**	100%	3000	25.9	30.9	1332	1320	13.9	6.8	57.3	28.1
55	**1.05**	100%	3000	46.3	49.2	1644	1968	10.4	5.7	42.9	23.5
55	**0.55**	100%	3000	49.7	51.7	1776	1956	10.7	5.4	44.1	22.3
55	1.05	100%	**1500**	43.2	47.4	1512	1956	11.1	5.8	45.8	23.9
55	1.05	100%	**2000**	45.4	49.2	1752	1956	10.5	6.1	43.3	25.2
55	1.05	100%	**2500**	45.2	49.6	1788	1956	10.8	6.2	44.6	25.6
55	1.05	100%	**3000**	46.3	49.2	1644	1968	10.4	5.7	42.9	23.5

Highlighted row indicates field-observed values
Shaded areas represent base calibration
Boldface indicates range of values under test

Table 3.1. Sensitivity Analysis of FRESIM Calibration Parameters

The car-following sensitivity factor was not analyzed in the previous section, but the researchers did a broad evaluation of its sensitivity. Only extreme changes in its value appeared to have a substantial effect on simulated density.

Following distance was shown in the previous section to have a significant effect on simulated density and capacity. Over a range of reasonable values, including those that provided the best fit for the Baltimore-Washington Parkway (95%) and the US-101 (130%) data sets, the results showed that this parameter had a significant effect on density.

The research had explored the so-called position of the advance warning sign (really the first point at which simulated drivers are aware of the need to prepare for their exiting maneuver), and found it to have little effect on capacity. The sensitivity test also showed only a small variation of simulated density over a range of values.

FRESIM Validation

To validate FRESIM for use as a research tool, the research compared simulated and observed density. As preciously discussed, the intent of the research plan was to use simulation in support of a level-of-service model and field data to support a capacity model. Thus, while capacity was considered during calibration as a measure of when calibration had been achieved, it was not considered during validation because the capacity model would not be based on simulation results.

As a check on density estimation, the researchers compared the calculated density (using the method discussed in later chapters) with observed density, for both calibrated and uncalibrated simulations of field conditions.

The validation process can also measure the sensitivity of the simulation to variations in calibration. Table 3.2 lists the results of simulation for sites on I-580 in Alameda, California and for the Baltimore-Washington Parkway and US-101. The first of these was used in the sensitivity analysis described above, but was not otherwise calibrated to match density results. The second two sites received detailed calibration for density, and are shown shaded in the table.

Figure 3.3 shows a scatter plot of observed vs. simulated density from the results in Table 3.2. The square symbols are the uncalibrated simulation samples, and the diamond symbols are the calibrated samples. In all cases, uncalibrated FRESIM is too pessimistic about the density of the traffic, with simulated densities greater than observed densities. This result reflects the error in the sensitivity factor, which also causes FRESIM to underestimate capacity. The magnitudes of these errors range up to two levels of service, using the LOS thresholds defined for ramp merges. The specific values are indicated in the unshaded portion of Table 3.2. The shaded portion of that table shows samples that received full calibration. These samples show that properly calibrating the sensitivity factor improves the estimation of capacity as well as density. The validity of the simulation in these samples is good. The correlation between observed and simulated density for the calibrated samples is indicated by an R^2 of 0.62, though the regression line does show some skew. The regression line crossed the ideal line at its midpoint within the samples, but the slope is a little shallower than the ideal line. This is most likely a reflection of the relatively narrow range of densities in the field data being used as a comparison. Within this range, the regression line does not vary from the ideal line more than about 10%.

Figure 3.4 combines the results of the chart and the table to show simulated and observed density with respect to levels of service.

For Type A Major weaves, too little field data existed to allow a statistical evaluation of the validity of simulation. Only three five-minute samples of field data were available. These three samples, however, were plotted against the large number of simulations as an indicator that they fell within the range of simulation values. These results are plotted in Figure 3.5. This plot only attempts to indicate that it would not be reasonable, in the absence of more detailed data, to reject the validity of the simulation model out of hand.

In summary, CORSIM was calibrated to accurately predict density in the critical lanes of Type A ramp weaves. The model also appeared to reflect the operation of Type A major weaves, at least in the critical lanes, however, the limited number of field studies did not allow a rigorous comparison.

Time Period	Site	Observed Density	Simulated Density	LOS Observed	LOS Simulated	LOS Error
5	Alameda '89	28.7	39.2	D	E	-1
10	Alameda '89	29.3	40.4	D	E	-1
15	Alameda '89	34.7	48.3	D	E	-1
20	Alameda '89	30.6	45.0	D	E	-1
25	Alameda '89	34.7	45.0	D	E	-1
30	Alameda '89	31.0	35.1	D	E	-1
35	Alameda '89	27.2	39.6	C	E	-2
40	Alameda '89	29.7	39.6	D	E	-1
115	Alameda '89	25.8	36.3	C	E	-2
120	Alameda '89	29.3	35.1	D	E	-1
15	Alameda '87	29.4	33.3	D	D	0
30	Alameda '87	31.8	33.3	D	D	0
45	Alameda '87	39.9	41.1	E	E	0
60	Alameda '87	38.3	41.5	E	E	0
75	Alameda '87	38.2	41.1	E	E	0
5	Alameda '88	38.2	46.3	E	E	0
10	Alameda '88	35.1	45.4	E	E	0
55	Alameda '88	32.8	35.1	D	E	-1
60	Alameda '88	27.9	34.6	C	D	-1
1	BW Pkwy	28.2	26.8	D	C	1
2	BW Pkwy	28.1	30.7	D	D	0
3	BW Pkwy	28.8	31.7	D	D	0
4	BW Pkwy	26.9	31.4	C	D	-1
5	BW Pkwy	30.2	31.0	D	D	0
6	BW Pkwy	34.2	38.4	D	E	-1
7	BW Pkwy	32.4	35.3	D	E	-1
8	BW Pkwy	28.3	31.1	D	D	0
9	BW Pkwy	33.6	36.4	D	E	-1
10	BW Pkwy	34.6	38.0	D	E	-1
1	US-101	39.8	34.6	E	D	1
2	US-101	32.0	31.3	D	D	0
3	US-101	29.4	31.2	D	D	0
4	US-101	27.1	27.4	C	C	0
5	US-101	29.4	27.8	D	C	1
6	US-101	35.6	35.2	E	E	0
7	US-101	35.6	41.0	E	E	0
8	US-101	37.8	37.6	E	E	0
9	US-101	40.4	36.7	E	E	0
10	US-101	38.0	44.6	E	E	0
11	US-101	45.8	39.0	E	E	0
12	US-101	43.8	41.8	E	E	0
	Mean Density	32.99	36.93			
	Standard Deviation	4.94	5.42		Mean LOS Error	-0.4

Shaded Values Show Detailed Calibration

Table 3.2. Observed vs. Simulated Density for Calibrated and Uncalibrated Samples

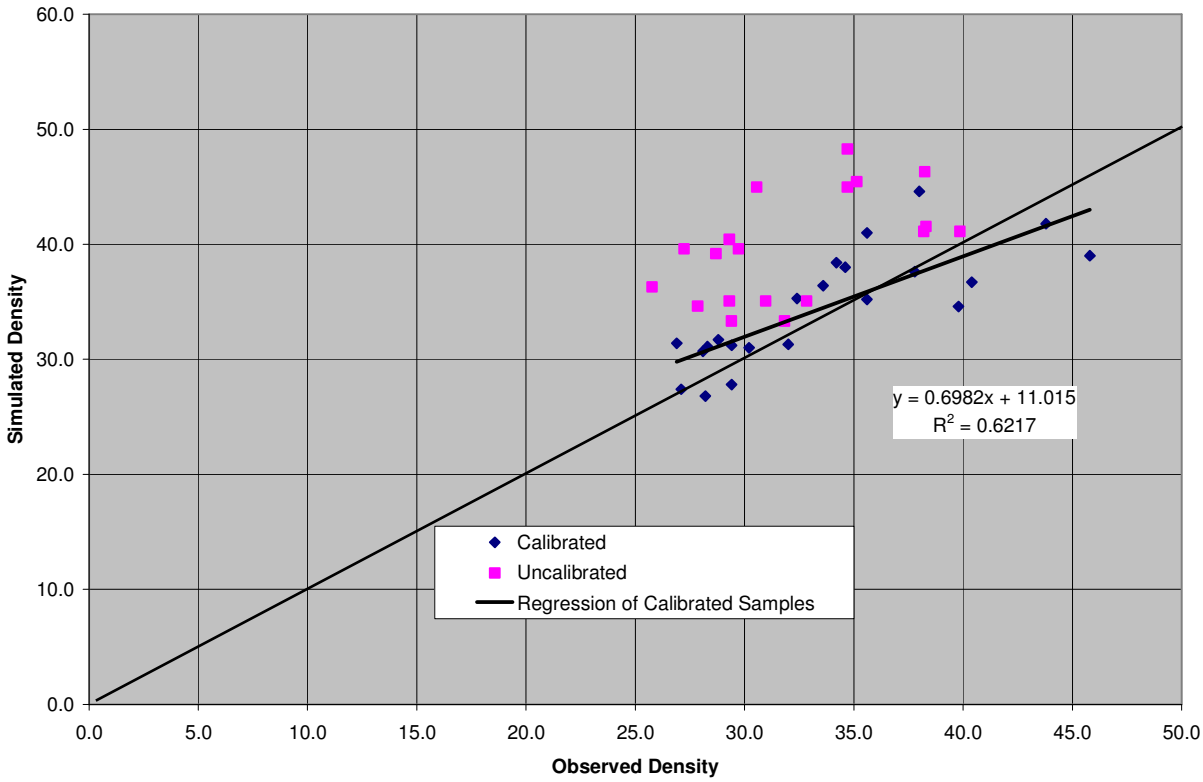

Figure 3.3. Observed vs. Simulated Density, Validation of Calibrated Samples

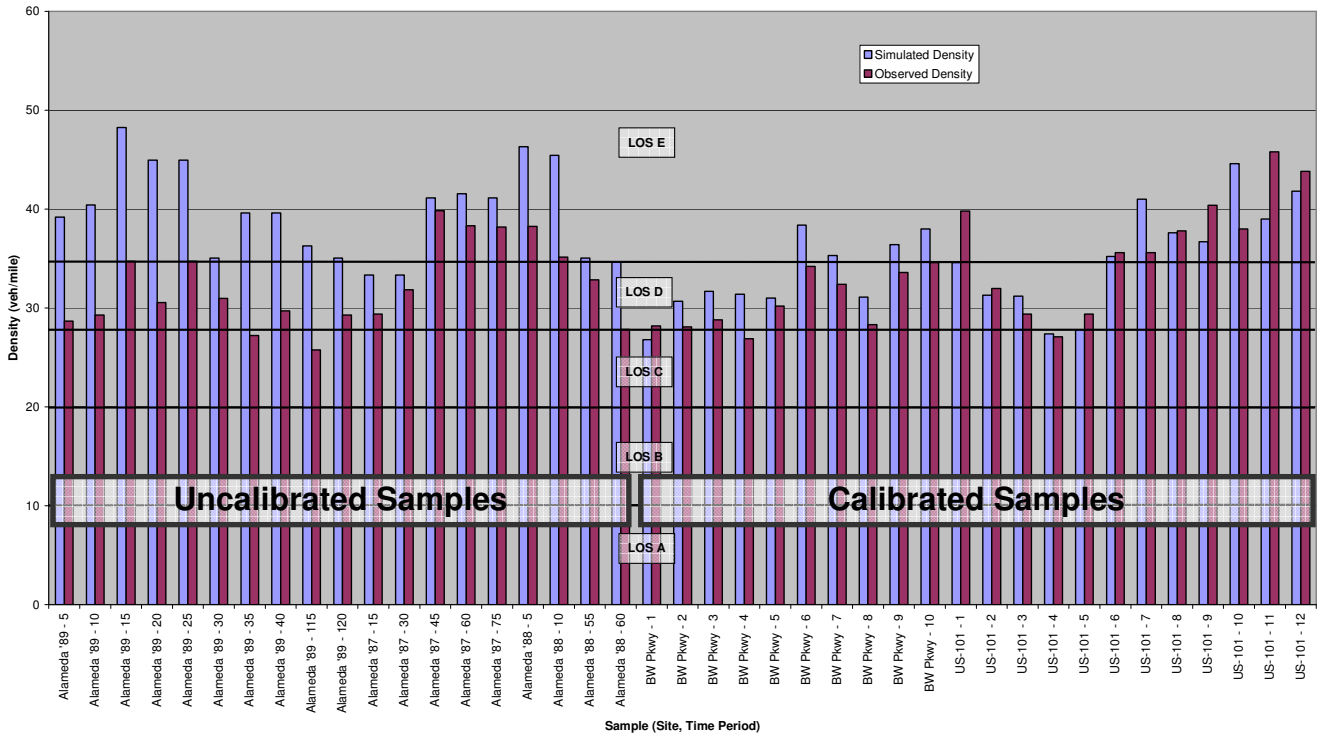

Figure 3.4. Observed vs. Simulated Density, Level of Service Prediction

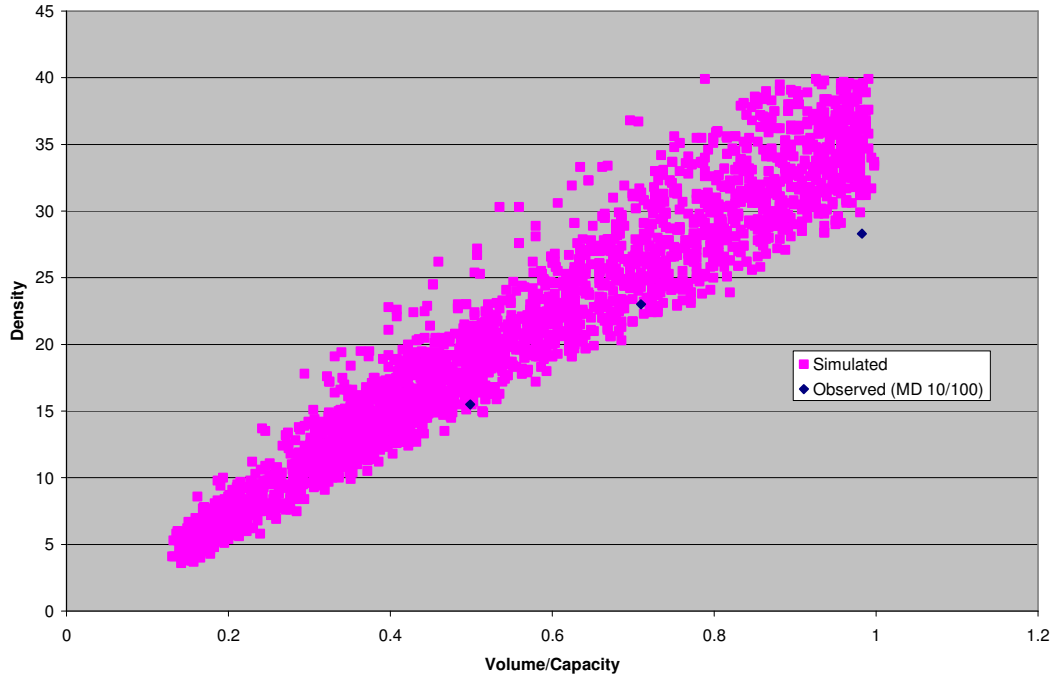

Figure 3.5. Simulated and Observed Density for Type A Major Weaves

References

1. CORSIM Reference Manual (TSIS Volume 3), Version 5.0, Federal Highway Administration, 2001.

PART II. TYPE A WEAVING ZONES

CHAPTER 4. PROPOSED CAPACITY MODELS

The development of a capacity model for Type A weaves is presented in this chapter. First, the initially proposed model is described, followed by a probability-based capacity model. Data from the pilot study (described in Chapter 5) indicated that one of the assumptions in the initial model was incorrect. This chapter is concluded with a description of the weaving model developed in this project.

Individual Weaving Region Model

A new physical model was initially proposed based on the assumption that, at capacity, weaving maneuvers are evenly distributed along the length of the weaving zone. As such, the weaving zone can be divided into individual weaving regions, each roughly the length of a single lane change maneuver. The weaving traffic is evenly distributed over the entire weaving area, so that each individual weaving area has the same lane-changing and non-lane-changing volumes. Within each individual weaving region, non-lane-changing cars could travel side-by-side, with a capacity of two cars. Lane-changing cars would only be able to pass through the individual weaving regions one at a time.

The lane changing maneuvers in the average individual weaving region and the non-lane-changing volumes are separately quantified, resulting in the following equations:

$$q_{lc} = \frac{(V_1 + V_2)L_w}{L}$$

$$q_{nlc} = (V_1 + V_2) - q_{lc}$$

where

q_{lc} = the flow of weaving vehicles that change lanes in the average individual weaving region

q_{nlc} = the flow of weaving vehicles that do not change lanes in the average individual weaving region

V_1 = the volume of vehicles weaving to the right

V_2 = the volume of vehicles weaving to the left

L_w = the length of the average individual weaving region

L = the length of the weaving zone

The lane changers are assumed to pass through the individual weaving region one at a time and the others pass through side-by-side, and actual weaving volumes can be converted into equivalent through volumes (in the weaving lanes) with the following equation:

$$q_{eff} = 2q_{lc} + q_{nlc}$$

where

q_{eff} = the effective weaving volume in equivalent through vehicles

With the weaving volume expressed in equivalent through vehicles, the weaving saturation level can be calculated by dividing by the capacity of two through lanes.

A critical parameter in the equation is L_W, which is the length of the average individual weaving region. Then, the number of weaving regions available in the weaving zone could be found, which would lead to an estimate of the capacity. However, this research has shown that virtually all weaving is accomplished in approximately the first 500 feet of the weaving area for single-lane weaves. While this would imply an L_W of about 500 feet, the downstream "weaving areas" were starved for demand.

A Probabilistic Capacity Model

The initial model postulated two conditions, the first being two cars side by side, with a capacity of two, and the second a single car changing lanes, with a capacity of one. In practice these two conditions are only two possibilities. In addition to these, either of the two lanes may be starved for demand, either because of upstream weaving maneuvers, or simply because one entering flow is smaller than the other. Also, neither lane may be occupied. If one attempts to define capacity at the merge gore, which seems evident from field observations, then one can define all possible scenarios in these lanes.

The probability model predicts capacity in the weaving zone only (i.e. right lane on the freeway and the auxiliary lane). The researchers have assumed that the inner freeway lanes are not impacted significantly by the turbulence in the weaving zone, so that their individual capacity is close to that of a comparable basic freeway segment, though this assumption was not studied explicitly.

The concept of the model is similar to the original version that is founded on the principle of the number of potential lanes that are available under each arrival scenario, of which there are now nine. Summing across all scenarios gives the expected number of lanes available in the weaving zone. It is further assumed that weaving vehicles will yield to non-weaving vehicles (if present). Further, a weaving vehicle effectively occupies both lanes even if a gap is present. Single non-weaving vehicles occupy one lane, with the gap in the other lane potentially available for only non-weaving vehicles in the other stream. These concepts are further explained in each scenario below.

Variable Definitions:

These variables define each traffic stream by both location and destination, and are necessarily different from the terms used in other parts of this report. For this reason, the following terms will be used in this section only.

V_F = Freeway volume in right mainlane
V_{FW} = Weaving freeway volume in right mainlane
V_R = Ramp volume
V_{RW} = Weaving ramp volume
C_F = Freeway right mainlane capacity
C_R = Ramp roadway capacity
P_F = Probability that a freeway vehicle in right mainlane is present at the ramp gore
P_R = Probability that a ramp vehicle is present at the ramp gore
P_{FW} = Probability that a present freeway vehicle is weaving
P_{RW} = Probability that a present ramp vehicle is weaving
N_w = Number of lanes available in the weaving zone
$E(N_w|i)$ = Expected number of lanes available in the weaving zone in scenario (i)
Prob(i) = Probability that scenario (i) occurs

Simple estimates of the above four probabilities are given below:
$P_F = V_F / C_F$; $P_R = V_R / C_R$; $P_{FW} = V_{FW} / V_F$ and $P_{RW} = V_{RW} / V_R$

Scenario Probabilities and Expected Values—Descriptions and Computations

Scenario 1

Two weaving vehicles are simultaneously present at the merge gore

Prob (1)= $P_F P_R P_{FW} P_{RW}$

$E(N_w| 1)= 1$ (one weaving vehicle will yield to the other)

Scenario 2

Two non-weaving vehicles are simultaneously present at the merge gore

Prob (2)= $P_F P_R (1-P_{FW}) (1-P_{RW})$

$E(N_W|2)=2$ (both vehicles pass side-by-side)

Scenario 3

A freeway non-weaving and ramp weaving vehicle are simultaneously present at the ramp gore.

Prob (3)= $P_F P_R (1-P_{FW}) P_{RW}$

$E(N_W|3)= 1$ (ramp vehicle will yield)

Scenario 4

A freeway weaving and ramp non-weaving vehicle are simultaneously present at the ramp gore.

Prob (4)= $P_F P_R P_{FW} (1-P_{RW})$

$E(N_W|4)= 1$ (freeway vehicle will yield)

Scenario 5

Single ramp weaving vehicle present—no freeway vehicles in lane 1

Prob (5)= $(1-P_F) P_R P_{RW}$

$E(N_W|5)= 1$ (gap unusable—one weaving vehicle can cross the crown line)

Scenario 6

Single freeway weaving vehicle present—no ramp vehicles

Prob (6)= $P_F F_W (1-P_R)$

$E(N_W|6)= 1$ (same as scenario 5)

Scenario 7

Single, on-ramp non-weaving vehicle present—no freeway vehicles in lane 1

Prob(7)= $(1-P_F) P_R (1-P_{RW})$

In this case the adjacent gap could be available for a non-weaving vehicle on the freeway—a weaving freeway vehicle would have to yield to the ramp vehicle. Therefore the expected number of available lanes is dependent on the probability of serving a freeway non-weaving vehicle

$E(N_W|7)= 2-P_{FW}$

Scenario 8

Single, freeway non-weaving vehicle present—no ramp vehicles

Prob(8)= $P_F (1-F_W) (1-P_R)$

This is similar to scenario 7, with the notation reversed

$E(N_W|8)= 2-P_{RW}$

Scenario 9

No vehicles present in the merge gore

Prob (9)= $(1-P_F) (1-P_R)$

This is perhaps the most interesting scenario. Since capacity is of primary interest, the *potential* number of lanes available in this case depends on the pattern of weaving and non-weaving vehicles in both streams. Potentially two lanes are available if all traffic is non-weaving. In all cases where there is weaving traffic (in one or both streams), only one lane will be available.

$E(N_W|9)= 1+ (1-P_{FW}) (1-P_{RW})$

From these scenarios, the weaving zone capacity, C_w, is computed from the following:

$$C_w = C_F \sum_{i=1}^{9} E(N_w \mid i)\text{Prob}(i)$$

It can be shown that the sum of probabilities 1 through 9 add up to one. Further, the model is internally consistent at the boundaries, yielding a single lane capacity when $P_{FW}=P_{RW}=1.0$, and a two lane capacity when $P_{FW}=P_{RW}= 0.0$. Thus all model predictions will vary from one to two lanes.

Application to Houston I-610 Site

The probabilistic capacity model has been applied to the Houston site, but the results were not promising. For the capacity sample, the model predicted capacity about 15% below the measured flow, but the cause of the problem has not been pursued. One possibility is that the model ignores the willingness of drivers in weaving zones to accept shorter than normal headways, especially when weaving. In addition, it, like the initial model, assumes that weaves are made throughout the weaving area.

The Merge-Point Capacity Model

The original model depended on the ability of drivers to select their weaving location such that they would perform the maneuver uniformly down the weaving zone at capacity. The idea was that a driver would first attempt to weave immediately and if not able to would proceed to the next individual weaving region. In practice, some drivers will come to a stop at the merge point to wait for a gap. If the traffic in the first main lane is heavy, they will have to wait for a while, and will block other vehicles on the ramp. The capacity point in the pilot study was the first 100 feet of the weaving zone. As traffic regained speed after passing the capacity point, those drivers unable to weave immediately would then weave.

One phenomenon was completely ignored by the first model. Because the volume in the left lane of the weaving area (right lane of mainlanes) was observed in the field to be much higher than in the right lane (entrance ramp), the right lane was under-saturated and the speeds were often much higher. The originally proposed model considered two conditions: vehicles changing lanes and vehicles traveling side by side. Two additional conditions were observed: a single vehicle in the left lane and a single vehicle in the right lane (though the latter was quite rare). If the volume in the right lane were higher, the results might have shown more cases of a single vehicle in the right lane.

Rather than characterize the weaving area as two lanes that are penalized by cars changing lanes, the researchers have developed an approach where the weaving zone is one lane, with one lane of capacity. That lane of capacity may be enhanced by those opportunities for two cars to move side by side and then further enhanced by their willingness to accept shorter headways.

A hypothetical model was formulated to consider this approach. The traffic volumes affecting the capacity of the weave are the cars that must change lanes in the weaving lanes and the cars entering the weaving lanes. The capacity of a single lane is then factored up by the inverse of the ratio of cars that must change lanes to the cars in the weaving zone. The hypothetical model is:

$$VR_w = \frac{V_1 + V_2}{V_{rl} + V_{ramp}}$$

$$C_w = (2 - VR_w)(2300)$$

where

VR_w = the ratio of weaving volume over all cars ***in the weaving zone***

C_w = the capacity in the weaving zone (right main lane plus auxiliary lane)

V_{rl} = the volume in the rightmost lane of the left entering roadway

V_{ramp} = the volume on the ramp

$V_1 + V_2$ = the total number of vehicles that must change lanes

In effect, this is a familiar formulation for highway capacity, where a basic capacity value is modified by a correction factor. The lane capacity of 2300 passenger cars per hour is used as a representative single lane capacity from the HCM chapter on basic freeway segments. With this formulation, the above model looks like this:

$$C_w = f_{VR} C_l$$

where

f_{VR} = adjustment factor based on ratio of weaving volume to total volume

C_l = capacity of a single lane

By defining VR_w as the ratio of *the cars that must change lanes* to total cars entering the weaving lanes, this model could be used for Type B weaves. In a Type B weave one of the two weaving flows does not have to change lanes to reach their destination. Therefore, by defining V_1 and V_2 as the left and right weaving cars that must change lanes, the weaving flow that does not have to change lanes in a Type B weave is zero.

This formulation of the model still ignores the possibility that drivers will accept shorter headways at higher weaving volumes. A second adjustment factor was added to adjust the basic lane capacity upward under conditions of high flow. As will be seen in subsequent chapters, this phenomenon was suggested by field data. The form of this model will be refined in Chapter 6, which will estimate empirical parameters based on the field data discussed in the next chapter. For now, it is sufficient to present the overall form of the model, as follows:

$$C_w = f_{VR} f_{lc} C_l$$

The second adjustment factor, f_{lc}, adjusts the lane capacity upward to account for shorter headways in high-demand conditions.

Summary

In summary, the individual weaving region model was not satisfactory because it did not account for the merge point congestion blocking access to downstream portions of the weaving zone. It assumed that drivers could choose to make their weave at any convenient point, but at capacity this choice is constrained by the choice of the driver in front of them.

The probabilistic capacity model explicitly evaluates all possible conditions rather than the two considered in the individual weaving region model. In practice, it underestimated capacity considerably, possibly because it does not model the willingness of drivers to accept shorter headways in high-density weaving environments. It also assumes that weaving maneuvers can be made anywhere, but observation of weaving traffic suggests that weaving motorists make their maneuvers as close to the merge point as possible.

The merge point capacity model is explicitly based on the assumption that motorists desire to complete their weaving maneuver as soon as possible, and allows the capacity of the merge point to be adjusted upward to account for the tendency of motorists to accept shorter headways in high-density weaving situations. The remaining research addressed itself to refining the merge point capacity model based on

simulation and field studies. That refinement is reported in Chapter 6, after a presentation of supporting field studies.

CHAPTER 5. FIELD STUDIES

Data from five Type A weaving areas was used in the development of the capacity model and in the calibration of the simulation model. Details of data collection and reduction are provided in this chapter.

Data at two sites, one ramp weave and one major weave, was collected as part of this study. Also, two sites were selected from a data set collected by JHK for the FHWA in the early 1980s, both ramp weaves. Finally, one site was selected from a set of data provided by the California Department of Transportation (Caltrans), also a ramp weave. Data from the California site was reduced by the research team from the video tapes provided by Caltrans.

Pilot Study

To provide the basis for evaluating and refining candidate capacity models, a pilot study was conducted on southbound Interstate Highway 610 in Houston. The southbound freeway carries four basic lanes. The weaving zone is a Type A ramp weave, between the entrance ramp at Westheimer Road and the exit ramp at Richmond Avenue. The weaving zone is about 1300 feet long and apparently operates at capacity, with minor queuing upstream from the merge gore, and no congestion downstream. The layout of the pilot study is shown in Figure 5.1.

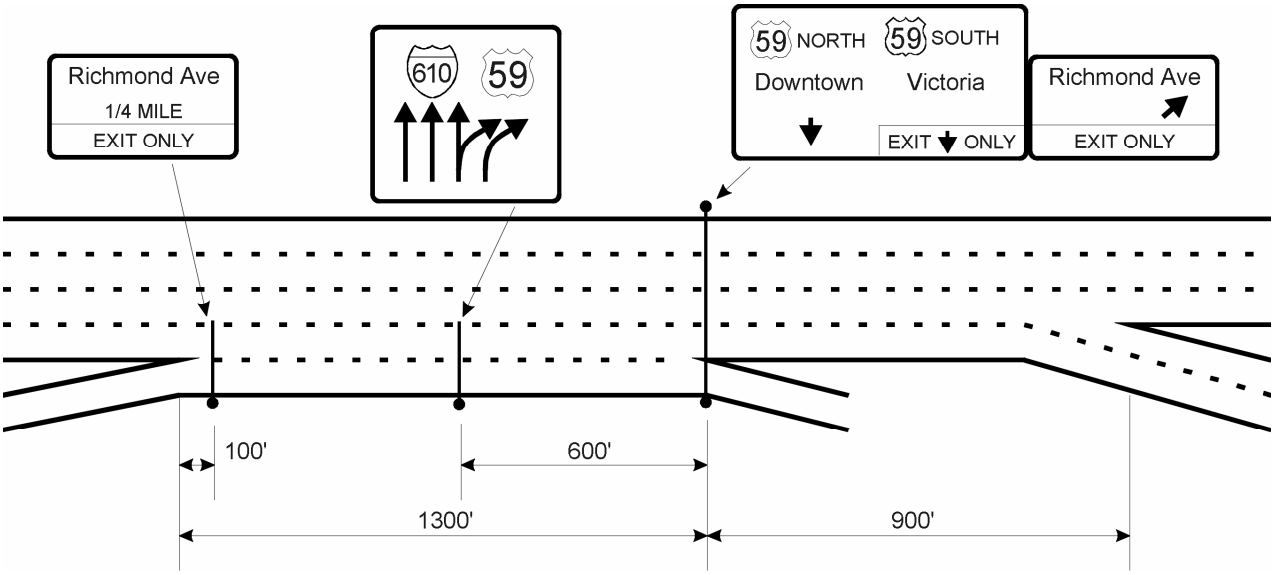

Figure 5.1. Layout of Pilot Study.

One characteristic of the site that is less than ideal is the proximity of a downstream major freeway split. The relative popularity of the movement to the right at this split may have encouraged some through drivers to use the lanes in the weaving zone when otherwise they may have moved left to avoid it. Another potential problem was that entering traffic intending to continue on IH-610 had to move an additional lane to the left, which may have encouraged them to make their initial weaving maneuver early. In practice, this phenomenon was not observed.

A nearby suburban skyscraper, the Transco Tower, provided a unique vantage point that was used to collect video data of the entire weaving zone. Two hours of video data were recorded on December 26, 1996, starting at about 3:10 PM. The Transco Tower is located about 500 feet west of the freeway, and researchers collected data from the 47th floor, which is about 500 feet up. The image contains the entire

weaving zone from the tip of the merge gore markings to the tip of the grass diverge gore. Using markings along in the shoulder, the weaving zone was divided into 60-foot sections for recording location, and the camera provided a video-editing time code accurate to the video frame. A sample video frame is shown in Figure 5.2 (the actual video image was somewhat sharper than the captured frame in the figure).

Figure 5.2. Typical video image from Houston pilot study

The initial examination at the data immediately rejected the notion that weaving maneuvers will be uniformly distributed along the weaving zone at capacity. Figure 5.3 shows the spatial distribution of weaving maneuvers within the weaving lanes in the pilot study, and shows that about 85% of the maneuvers took place in the first 400-500 feet. These results seem to indicate that the length of the weaving zone has no effect on the *capacity* of the weave beyond a certain minimum value. At capacity, speeds are low and relatively uniform across lanes, which makes lane changes easier over a shorter distance. In fact, in all phases of the research it was apparent that weaving drivers attempted their maneuvers as early as possible.

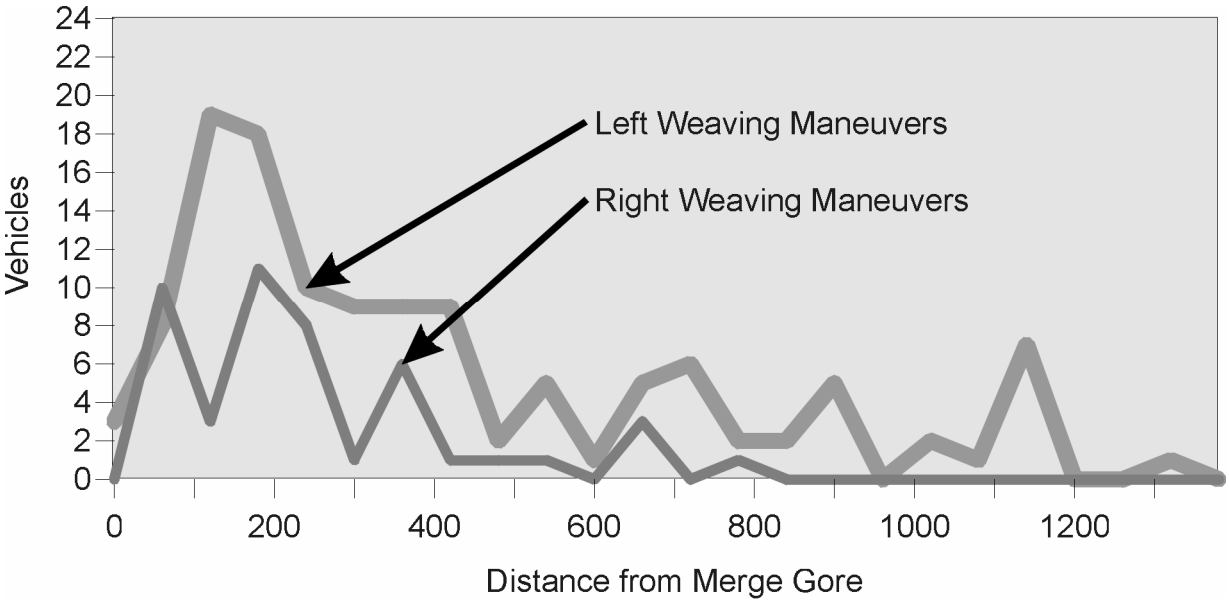

Figure 5.3. Distribution of Weaving Maneuvers

The desirable length of the weaving zone therefore seems to be a function of free-flow quality of service and safety rather than conditions at capacity. Capacity itself will be a function of traffic demand only, assuming weaving zones of adequate length. As reported previously, these results coincide very closely with those observed in California. For this site, it was apparent that a weaving zone of adequate length to allow safe lane changes at free-flow speed would not constrain the capacity of the weaving zone.

The data also showed considerable variation in speed for individual vehicles as they passed through the weaving area. Speeds were lowest immediately downstream of the merge point. Once most of the lane changes were made, vehicles increased their speeds as they moved through the weaving area. This suggests that speed is a poor indicator of capacity flow.

MD 10/100 Interchange

Data for Type A Major weaves were collected by Skycomp, Inc. using aerial photography. The limited resources of the project imposed severe discipline on both the quantity and complexity of data that could be collected. The researchers determined that if vehicles could be located by lane, and assigned to 100-foot sections, their movements could be tracked sufficiently to determine the origin-destination matrix of the traffic, the location of lane changes, and the approximate speed and density of traffic. The objective, as stated previously, was to provide a wide range of observations and use simulation to provide the depth necessary to develop new methods. The field observations would be used to demonstrate the reality of the simulation, and reported in Chapter 3.

The Maryland Route 10 and Route 100 interchange southeast of Baltimore is a Type A Major weaving zone. This site was the only Type A Major weave for which field data was gathered.

The data collection process for this site, and also for the field sites for Type B and C weaves reported in Part III, was as follows:

1. Sites were marked in 100-foot sections, called bins. The marking of the sites involved staking a contrasting panel to the ground at the roadside, or painting a marking on a paved shoulder.

2. Photographs were made of the entire study area using cameras that automatically made an exposure every three seconds. The photographer would switch cameras at the end of a 36-exposure roll of film, and an assistant would change the rolls of film. The camera marked the time on each frame.

3. Photographs were made over a period of an hour.

4. After the photographs were made, three five-minute periods were selected for further data collection. These periods were selected to provide, if possible, two samples of capacity flow and one sample of sub-capacity flow. In the end, capacity conditions proved rare in the sites selected, and therefore difficult to observe.

5. For each 5-minute period, each entering vehicle was tracked from one photograph to the next, noting the lane and bin.

6. The researchers wrote several simple computer programs to analyze these data to determine origins and destinations, entering lane volumes, lane change positions, and density in each lane.

JHK/FHWA Data

The JHK data consists of vehicle trajectory points at one-second intervals for a period of one hour. The data was collected using time-lapse aerial photography and consists of data records for each photographic frame that provide the longitudinal location, the lateral location, the vehicle type, the vehicle identification number and an estimated lane for each vehicle which was digitized. Speeds of each vehicle were obtained from the distance traveled between frames. The data collection was designed so that there was no congestion at the start. There are six weaving data sets among a total of twelve collected data sets. Because of the detail of the data, all demand data can be obtained and any and all measures of effectiveness can be computed. Two sites from this data collection effort were used for the development of capacity and level of service models for Type A weaves. The remaining sites are described in Appendix I.

Baltimore-Washington Parkway NB at Interstate Highway 495 in Prince Georges County, Maryland. A schematic is shown in Figure 5.4. Congestion level starts at observed level of service B and ends at E.

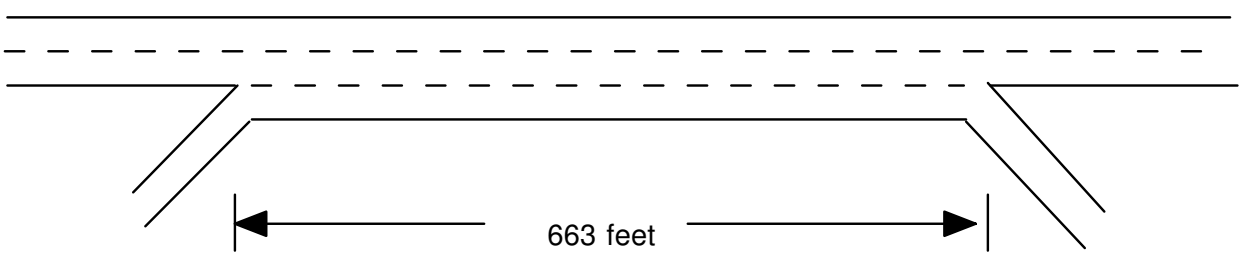

Figure 5.4. Baltimore-Washington Parkway at IH-495

US Highway 101 westbound (WB) at Topanga Canyon Boulevard in Los Angeles, California. A schematic of this section is shown in Figure 5.4. It should be noted that this section is in a construction zone and has reduced lane width and shoulder width over part of the section. Congestion levels were observed from level of service C to D.

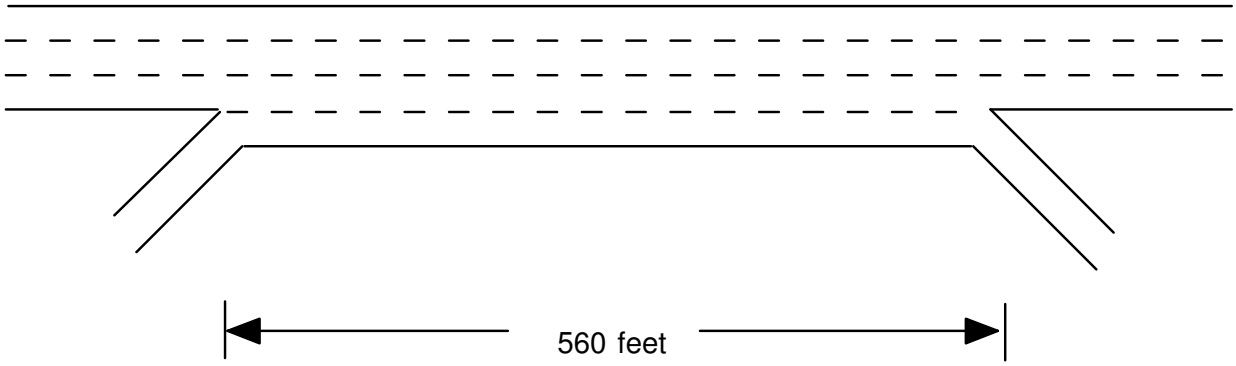

Figure 5.4. US-101 Westbound at Topanga Canyon Blvd.

California Department of Transportation Data

All of the California Department of Transportation (Caltrans) data sets [1] are for simple ramp weaves where there is a one-lane on-ramp entering the freeway, a full auxiliary lane that connects to a one-lane off-ramp. The data consists of count and speed data collected using video. The volume data was collected at five-minute intervals over a one-hour period, while the speed data was collected for only the first three five-minute intervals. The volume data is distinguished by vehicle type and is by lane and by origin/destination pair. In addition, vehicle counts in the lane next to the auxiliary lane are made every fifteen-seconds and averaged every five minutes to obtain a density estimate. Estimates of congestion level are based on vehicle counts, not passenger car equivalents (PCE), resulting in low estimates.

The analysis of these studies reported in Ref. 1 did not provide sufficient detail for us to use for capacity estimation or for simulation validation. The study was interested only in non-capacity conditions, and data reduction stopped when capacity conditions were detected. Consequently, the researchers contacted the California Department of Transportation and obtained the videotapes for detailed analysis within this project. Figure 5.5 shows a typical view of the video camera. The view is severely foreshortened, but the researchers were able to collect origin-destination, count, density, and some speed data from the tapes.

Figure 5.5. Capacity Flow Conditions on IH-580.

The only site that provided useful capacity flow data was IH-580 in Alameda, which is near Oakland in the bay area. Data from this site were collected over a three-year period. In this phase of the work, only this site was used, but all sites were reduced. The remaining sites are described in Appendix I.

Interstate Highway 580 EB from Oakland Avenue to Grand Avenue, in the San Francisco, California bay area. This site is shown in Figure 5.6. Data were collected at two different times. In the second time period, there are two hours of collected data which were used in this research. Congestion levels vary from C to F, based upon observed densities, over the time period.

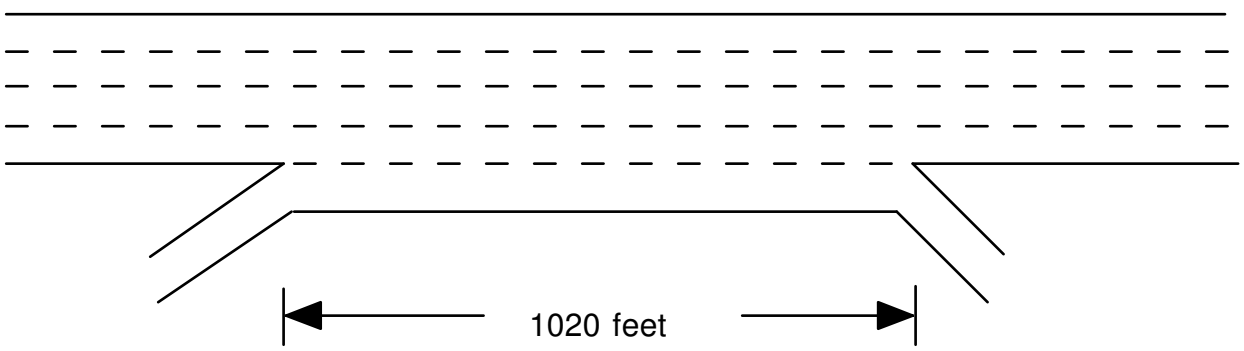

Figure 5.6. IH-580 Eastbound, Oakland Avenue to Grand Avenue, San Francisco Bay Area

References

1. "Weaving Data, 1987," California Department of Transportation, Sacramento, California.

CHAPTER 6. CAPACITY MODEL REFINEMENT

The proposed capacity model at the end of Chapter 4 is developed and its parameters are estimated in this chapter.

Several candidate capacity models were introduced in Chapter 4, with the Merge Point Model providing the best description of the field data in the pilot study. The Merge Point Model is based on a single adjustment factor that modifies the basic lane capacity upward to account for increased capacity resulting from times when vehicles travel side by side.

$$C_w = f_{VR} C_l$$

where

f_{VR} = adjustment factor based on ratio of weaving volume to total volume

C_l = capacity of a single lane

The volume ratio adjustment factor, f_{VR}, is the ratio of weaving volume to total volume subtracted from 2, or ($2-VR_W$). The subtraction ensures that the correction factor is a number between 1 and 2. A capacity of 2300 vehicles per hour per lane is taken as representative of a single lane capacity. Expanding the above general equation yields:

$$VR_w = \frac{V_1 + V_2}{V_{rl} + V_{ramp}}$$

$$C_w = (2 - VR_w)(2300)$$

where

VR_w = the ratio of weaving volume over all cars ***in the weaving zone***

C_w = the capacity in the weaving zone (not the whole freeway section)

V_{rl} = the volume in the rightmost lane of the left entering roadway

V_{ramp} = the volume on the ramp

$V_1 + V_2$ = the total number of vehicles that must change lanes

Figure 6.1 shows a bar chart that compares the results of this model with observed capacity flows at each of 28 5-minute samples taken from the Houston data (labeled IH 610), the California data (labeled Alameda), and the JHK data (labeled BW Parkway).

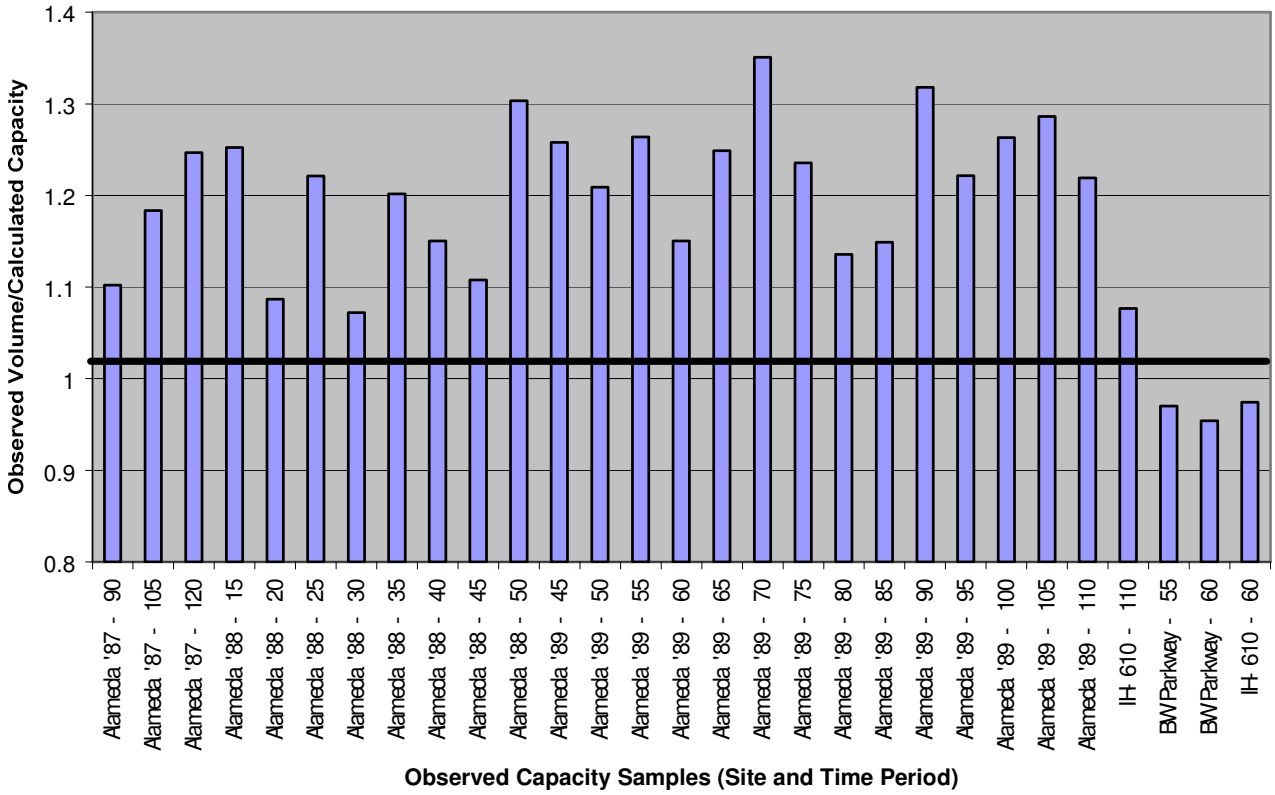

Figure 6.1 Capacity Model with Volume Ratio Adjustment

As the figure illustrates, a number of samples showed much higher traffic volume than the capacity predicted by the model. In order to characterize the errors of the model (i.e., identify potential missing terms), a regression analysis was performed on the incorrect calculated volume/capacity ratios against various parameters. The ratio of weaving to total volume, VR_w, is a variable in the model, and was first compared against the v/c ratio, as shown in Figure 6.2.

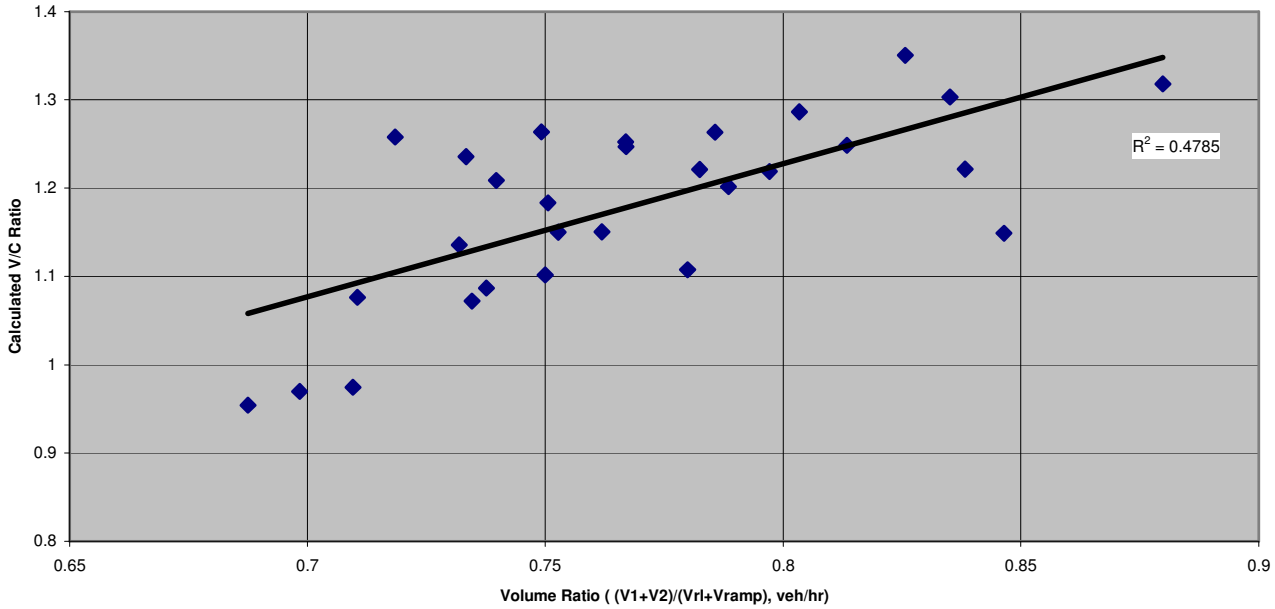

Figure 6.2. Calculated V/C Correlation with Volume Ratio

Then the total input volume was plotted against the calculated v/c ratio, as shown in Figure 6.3, resulting in a better fit.

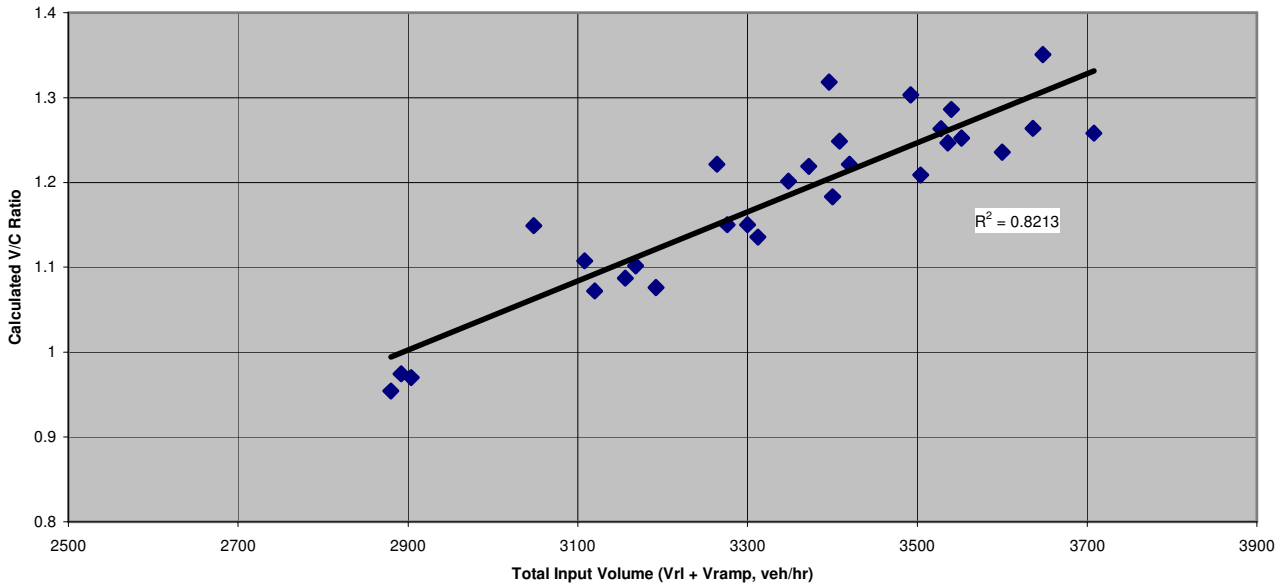

Figure 6.3. Calculated V/C Correlation with Total Input Volume

Finally, the calculated v/c ratio was compared against the total weaving volume, as shown in Figure 6.4, providing the best fit of the variables.

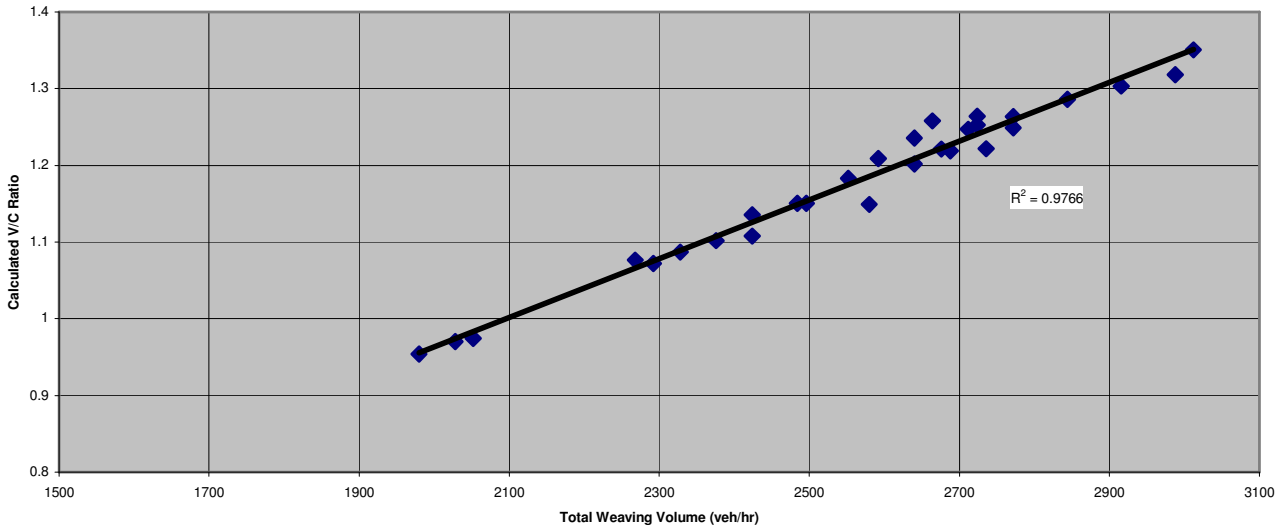

Figure 6.4. Calculated V/C Correlation with Total Weaving Volume

This indicates that drivers accept shorter headways in weaving conditions, and the greater the weaving volume, the shorter the headways they will accept. Based on the residual analysis, a second adjustment factor was added to the equation, as earlier described in Chapter 4.

$$C_w = f_{VR} f_{lc} C_l$$

After testing several forms for f_{lc}, the one shown below was selected. The two values in the equation, 2142 and 2370, were estimated to provide the best fit. The fitted model is shown in Figure 6.5.

$$f_{VR} = 2 - VR_w = 2 - \frac{V_1 + V_2}{V_{rl} + V_{ramp}}$$

$$f_{lc} = \left(1 + \frac{V_1 + V_2 - 2142}{2370}\right)$$

$$C_w = \left(2 - \frac{V_1 + V_2}{V_{rl} + V_{ramp}}\right)\left(1 + \frac{V_1 + V_2 - 2142}{2370}\right)(2300) \qquad (6.1)$$

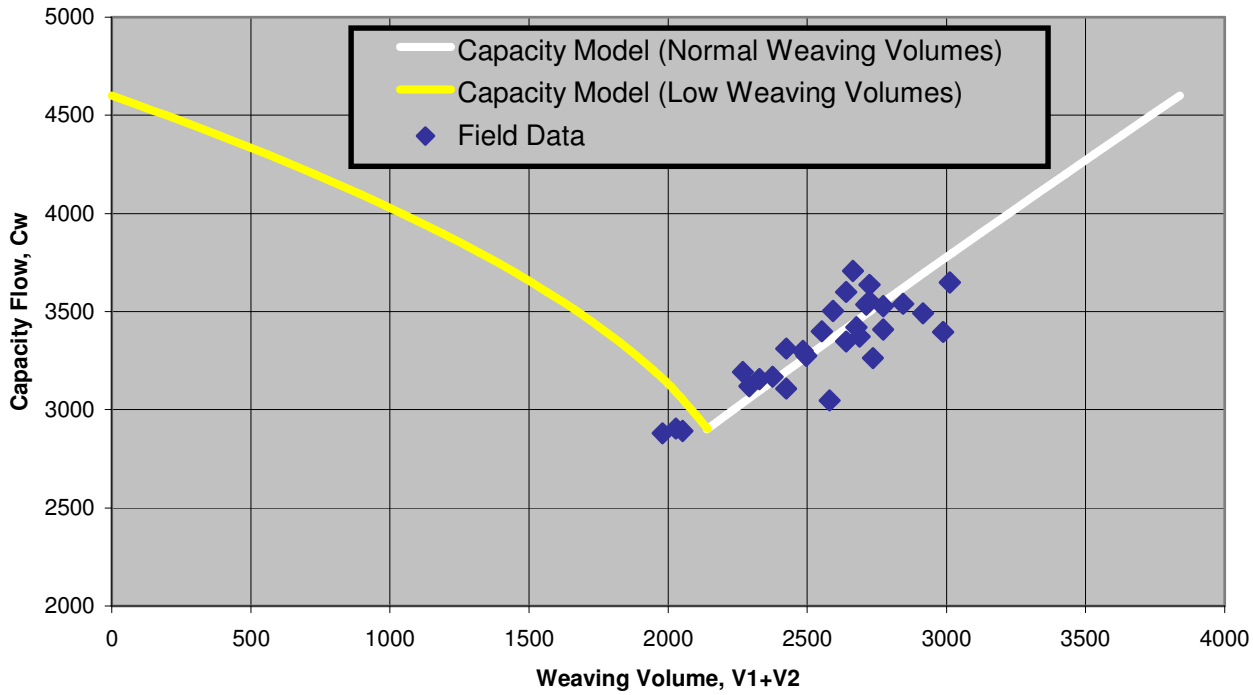

Figure 6.5. Merge Point Capacity Model—Initial Parameter Estimation

When total weaving volume is less than 2142 vehicles per hour, the lane capacity factor (f_{lc}) should be set to 1. Note 2142 is the minimum level at which vehicles are expected to reduce headways with increasing flow. Three of the samples represented sub-capacity flow, and were therefore excluded from the curve fitting.

Figure 6.5 shows the expected capacity of the weaving lanes for a range of weaving flows. The white line represents the entire model, Equation 6.1, for weaving flows in excess of 2142 vehicles per hour. The darker line represents capacity for smaller weaving flows. In this case, drivers are not assumed to accept shorter headways while changing lanes.

The two empirical constants in the f_{lc} term of Equation 6.1 were found by minimizing the sum of squared errors between calculated and observed capacity, as shown in Figure 6.6.

The capacity equation was evaluated for the full range of input and weaving volumes, and the results are shown in Figure 6.7. Note that the shaded triangular area at the bottom of the chart is where total volume is greater than capacity, and that the boundary occurs at V/C = 1.0. This area is triangular because the lane capacity factor (f_{lc}) is set to one when weaving flows are less than 2142 vehicles/hour, and increases as weaving flows increase above this value.

The upper right half of Figure 6.7 represents conditions when the weaving volume is greater than the total volume. One should recall that the total volume is the volume in the weaving lanes only (right lane of mainlanes and entrance ramp) and that the volume ratio is the weaving volume divided by the total volume. By definition, the weaving volume can not be greater than the total volume.

Thus, the unshaded portions of Figure 6.7 represent the possible solutions where the total volume is less than capacity. It should be noted that, for feasible solutions where volume is less than capacity (V/C <

1.0), the reported volume-to-capacity ratio can not be used to estimate the remaining capacity, as the additional volume necessary to reach capacity would depend on whether the additional volume is weaving.

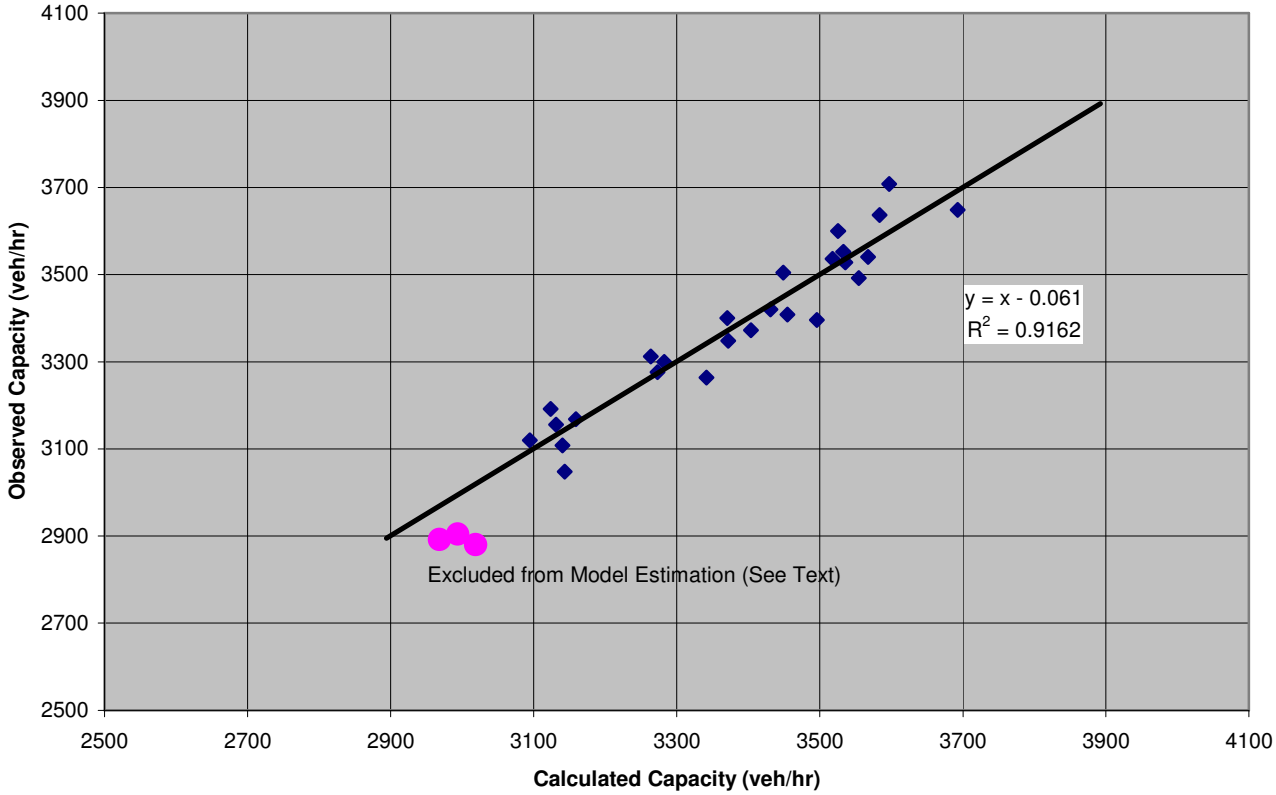

Figure 6.6. Comparison of Calculated and Observed Capacity using Final Capacity Model

Weaving Volume (V1 + V2)

Total Volume (Vrl + Vramp)	0		400		800		1200		1600		2000		2400		2800		3200		3600		4000	
	Cw	V/C	Cw	V/C	Cw	Vt/Cw	Cw	V/C	Cw	V/C	Cw	V/C	Cw	V/C	Cw	V/C	Cw	V/C	Cw	V/C	Cw	V/C
1	4600	0.00																				
100	4600	0.02																				
200	4600	0.04																				
300	4600	0.07	1533	0.20																		
400	4600	0.09	2300	0.17																		
500	4600	0.11	2760	0.18	920	0.54																
600	4600	0.13	3067	0.20	1533	0.39																
700	4600	0.15	3286	0.21	1971	0.36	657	1.07														
800	4600	0.17	3450	0.23	2300	0.35	1150	0.70														
900	4600	0.20	3578	0.25	2556	0.35	1533	0.59	511	1.76												
1000	4600	0.22	3680	0.27	2760	0.36	1840	0.54	920	1.09												
1100	4600	0.24	3764	0.29	2927	0.38	2091	0.53	1255	0.88	418	2.63										
1200	4600	0.26	3833	0.31	3067	0.39	2300	0.52	1533	0.78	767	1.57										
1300	4600	0.28	3892	0.33	3185	0.41	2477	0.52	1769	0.73	1062	1.22	392	[illegible]								
1400	4600	0.30	3943	0.36	3286	0.43	2629	0.53	1971	0.71	1314	1.07	729	[illegible]								
1500	4600	0.33	3987	0.38	3373	0.44	2760	0.54	2147	0.70	1533	0.98	1020	1.47	[illegible]	[illegible]						
1600	4600	0.35	4025	0.40	3450	0.46	2875	0.56	2300	0.70	1725	0.93	1275	1.25	[illegible]	[illegible]						
1700	4600	0.37	4059	0.42	3518	0.48	2976	0.57	2435	0.70	1894	0.90	1500	1.13	1037	1.64	391	4.34				
1800	4600	0.39	4089	0.44	3578	0.50	3067	0.59	2556	0.70	2044	0.88	1700	1.06	1306	1.38	739	2.43				
1900	4600	0.41	4116	0.46	3632	0.52	3147	0.60	2663	0.71	2179	0.87	1879	1.01	1547	1.23	1051	1.81	391	4.86		
2000	4600	0.43	4140	0.48	3680	0.54	3220	0.62	2760	0.72	2300	0.87	2040	0.98	1763	1.13	1331	1.50	743	2.69		
2100	4600	0.46	4162	0.50	3724	0.56	3286	0.64	2848	0.74	2410	0.87	2186	0.96	1959	1.07	1584	1.33	1061	1.98	391	5.37
2200	4600	0.48	4182	0.53	3764	0.58	3345	0.66	2927	0.75	2509	0.88	2319	0.95	2137	1.03	1815	1.21	1351	1.63	746	2.95
2300	4600	0.50	4200	0.55	3800	0.61	3400	0.68	3000	0.77	2600	0.88	2439	0.94	2300	1.00	2025	1.14	1615	1.42	1070	2.15
2400	4600	0.52	4217	0.57	3833	0.63	3450	0.70	3067	0.78	2683	0.89	2550	0.94	2449	0.98	2218	1.08	1857	1.29	1368	1.75
2500	4600	0.54	4232	0.59	3864	0.65	3496	0.72	3128	0.80	2760	0.91	2652	0.94	2586	0.97	2395	1.04	2080	1.20	1641	1.52
2600	4600	0.57	4246	0.61	3892	0.67	3538	0.73	3185	0.82	2831	0.92	2747	0.95	2713	0.96	2559	1.02	2286	1.14	1894	1.37
2700	4600	0.59	4259	0.63	3919	0.69	3578	0.75	3237	0.83	2896	0.93	2834	0.95	2830	0.95	2711	1.00	2477	1.09	2128	1.27
2800	4600	0.61	4271	0.66	3943	0.71	3614	0.77	3286	0.85	2957	0.95	2915	0.96	2939	0.95	2852	0.98	2654	1.06	2345	1.19
2900	4600	0.63	4283	0.68	3966	0.73	3648	0.79	3331	0.87	3014	0.96	2990	0.97	3040	0.95	2983	0.97	2818	1.03	2547	1.14
3000	4600	0.65	4293	0.70	3987	0.75	3680	0.82	3373	0.89	3067	0.98	3060	0.98	3134	0.96	3105	0.97	2972	1.01	2735	1.10
3100	4600	0.67	4303	0.72	4006	0.77	3710	0.84	3413	0.91	3116	0.99	3126	0.99	3223	0.96	3219	0.96	3116	0.99	2912	1.06
3200	4600	0.70	4313	0.74	4025	0.80	3738	0.86	3450	0.93	3163	1.01	3188	1.00	3306	0.97	3327	0.96	3251	0.98	3077	1.04
3300	4600	0.72	4321	0.76	4042	0.82	3764	0.88	3485	0.95	3206	1.03	3246	1.02	3384	0.98	3428	0.96	3377	0.98	3233	1.02
3400	4600	0.74	4329	0.79	4059	0.84	3788	0.90	3518	0.97	3247	1.05	3300	1.03	3457	0.98	3522	0.97	3496	0.97	3379	1.01
3500	4600	0.76	4337	0.81	4074	0.86	3811	0.92	3549	0.99	3286	1.07	3352	1.04	3526	0.99	3612	0.97	3609	0.97	3517	1.00
3600	4600	0.78	4344	0.83	4089	0.88	3833	0.94	3578	1.01	3322	1.08	3401	1.06	3592	1.00	3696	0.97	3715	0.97	3647	0.99
3700	4600	0.80	4351	0.85	4103	0.90	3854	0.96	3605	1.03	3357	1.10	3446	1.07	3653	1.01	3776	0.98	3815	0.97	3770	0.98
3800	4600	0.83	4358	0.87	4116	0.92	3874	0.98	3632	1.05	3389	1.12	3490	1.09	3712	1.02	3852	0.99	3910	0.97	3887	0.98
3900	4600	0.85	4364	0.89	4128	0.94	3892	1.00	3656	1.07	3421	1.14	3531	1.10	3767	1.04	3924	0.99	4001	0.97	3998	0.98
4000	4600	0.87	4370	0.92	4140	0.97	3910	1.02	3680	[illegible]	3450	[illegible]	3571	1.12	3820	1.05	3992	1.00	4086	0.98	4103	0.97
4100	4600	0.89	4376	0.94	4151	0.99	3927	1.04	3702	[illegible]	[illegible]	[illegible]	[illegible]	[illegible]	[illegible]	1.06	4057	1.01	4168	0.98	4203	0.98
4200	4600	0.91	4381	0.96	4162	1.01	3943	1.07	3724	1.13	3505	1.20	3643	1.15	3918	1.07	4119	1.02	4246	0.99	4299	0.98
4300	4600	0.93	4386	0.98	4172	1.03	3958	1.09	3744	1.15	[illegible]	[illegible]	[illegible]	[illegible]	3964	1.08	4178	1.03	4320	1.00	4389	0.98
4400	4600	0.96	4391	1.00	4182	1.05	3973	1.11	3764	1.17	3555	1.24	3710	1.19	4007	1.10	4234	1.04	4390	1.00	4476	0.98
4500	4600	0.98	4396	1.02	4191	1.07	3987	1.13	3782	1.19	3578	1.26	3741	1.20	4049	1.11	4288	1.05	4458	1.01	4559	0.99
4600	4600	1.00	4400	1.05	4200	1.10	4000	1.15	3800	1.21	3600	1.28	3770	1.22	4088	1.13	4339	1.06	4523	1.02	4638	0.99

Volume Ratio > 2

Weaving Volume > Total Volume

Total Volume > Capacity

Capacity

Figure 6.7. Numerical Range of Capacity Values

The purpose of the capacity model is two-fold: 1) to assess the difference between LOS E and LOS F, and 2) to provide a useful measure of potential capacity for the current conditions as a means of obtaining a V/C ratio. The V/C ratio provides the entry point into a further level of service evaluation. It is worth repeating that actual capacity is based on the mix of weaving and non-weaving volumes, and therefore cannot be estimated in sub-capacity conditions, because the mix of volumes at capacity cannot be predicted.

Two regimes for capacity are defined. Capacities with higher weaving flows are based on clear field data, and indicated that drivers accept shorter headways under the pressure of weaving. As weaving volumes increase, so does the capacity.

At lower weaving flows, drivers were assumed to not accept shorter headways, with the boundary condition of a capacity of two lanes if the weaving volume is zero. The point of intersection in figure 6.5 is where the model with this assumption meets the fitted curve for higher weaving flows.

The problem with Equation 6.1 is that it is only defined for input volumes exceeding 3000 vehicles per hour. FRESIM either halted or became unstable when simulating these conditions (see Figure 6.8, showing the range of conditions that could be simulated). For Type A weaves, the conditions under which

the weaving zone reaches capacity are fairly narrow. In reviewing potential scenarios above the input volume of 3000 vehicles/hour, the conditions became unrealistic. In these scenarios, the weaving volumes are low (less than about 2000 vehicles/hour). For example, a situation where the total input volume is 4000 and the weaving volume is 1000 requires 3000 non-weaving vehicles/hour. The entering volumes may be distributed at about 2200 vehicles/hour on the main lane and 1800 vehicles/hour on the entering ramp. A large percentage of these motorists must therefore be going straight through, even on the auxiliary lane. If 500 vehicles enter the mainlanes and 500 vehicles exit, then the result will be 1000 weaving vehicles. Conditions such as these, even if they could operate, are assumed to be extremely rare in the field. Such cases will inevitably be operating at LOS E or F.

The table shown in Figure 6.7 was constructed based on the assumption that the capacity of a Type A weaving zone with no weaving volume would be that of two lanes. But it became apparent that this was an unrealistic condition. For ramp weaves especially, if there is no weaving volume there is no reason to use the ramp (except for rare cases of using an auxiliary lane to bypass a frontage-road signal). Thus, the researchers moved away from the assumption that at zero volume a Type A weave had two lanes of capacity, and to the assumption that it has only one lane of capacity. This is an arbitrary determination to keep the values plausible, considering that below capacity the only point to calculating capacity is as an entry point for determining level of service.

Thus, for weaving volumes that are zero, the capacity is assumed to be 2300 vehicles/hour. As weaving volumes increase, the capacity increases with it, under the assumption that each entering vehicle will be able to merge normally, up until the total input volume reaches that level that represented true capacity conditions, i.e., 3000 vehicles per hour.

This led the research to defining capacity in three regimes. The first regime covered conditions where the weaving volume was less than 700 vehicles per hour. For this condition, the capacity was defined at 2300 plus the weaving volume. When the weaving volume reached 700, the capacity reaches 3000, and that is the point at which capacity conditions are possible. Therefore, for conditions where the weaving volume exceeded 700 vehicles per hour, but the total input volume was less than 3000 vehicles per hour, the research defines the capacity at 3000 vehicles per hour. For conditions where the total volume exceeds 3000, the capacity model includes the adjustments for shorter headways as developed in Equation 6.1.

The following is a complete representation of the final Merge Point Capacity Model.

For total weaving volumes, V_w, less than 700 veh/hour:

$$C_w = 2300 + V_w$$

For $V_w \geq 700$ veh/hour **and** total entering volume on the weaving lanes, $V_t \leq 3000$ veh/hour:

$$C_w = 3000$$

For $V_t > 3000$ veh/hour:

$$C_w = (2 - VR_w)\left(1 + \frac{V_w - 2142}{2370}\right)(2300)$$

Capacity is not defined for weaving volumes greater than 3700 veh/hour

The previous discussion stated that simulation proved impossible for conditions in Type A ramp weaves where the total input volume exceeded 3000 vehicles per hour. Samples were determined by factoring field conditions in the calibrated simulation. Each of 12 five-minute time periods in each simulation was scaled up and down to cover the range of volumes. The input volumes were scaled across the range of

20% to 140% in 20% increments. The volume ratio (weaving volume/total input volume *in the weaving lanes*) was scaled from 10% to 100%, in increments of 10%. The intent was to cover the entire solution space, not to represent the likelihood of any given scenario. Samples that resulted in zero weaving volumes were rejected. Samples resulting in critical-lane densities higher than 40 were assumed to be beyond capacity flow and were rejected. The samples that exceeded capacity-level density showed total input volumes less than 3000 vehicles per hour. The range of simulated conditions is depicted in Figure 6.8.

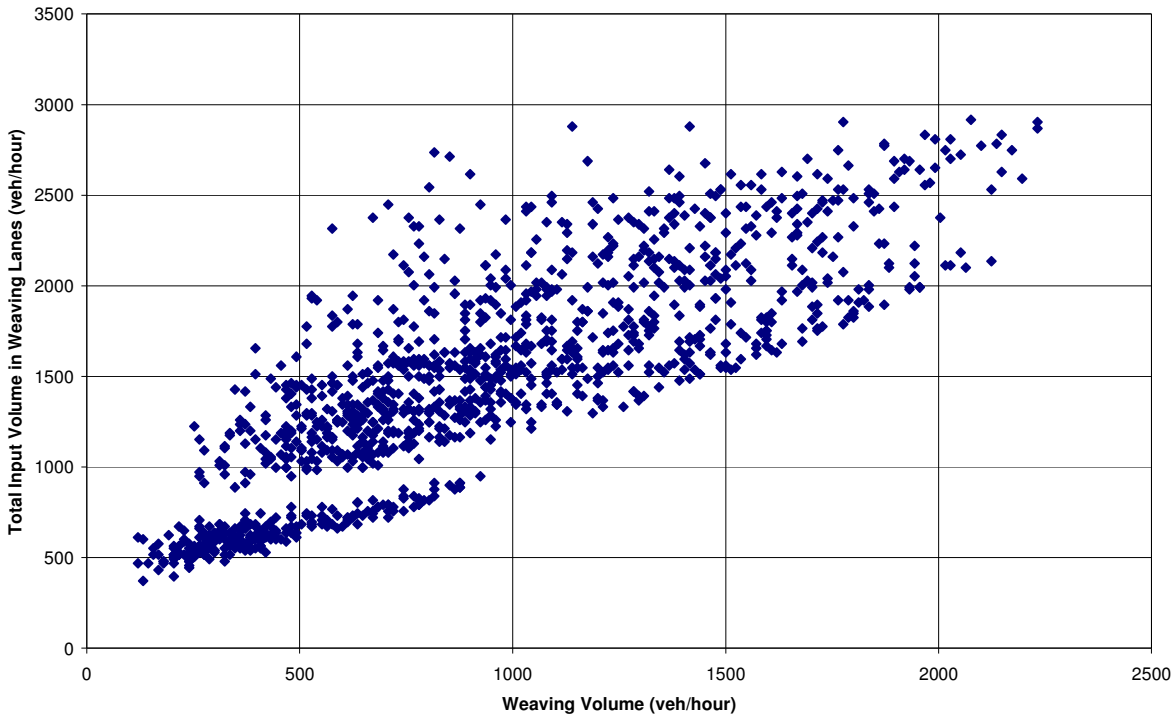

Figure 6.8. Simulated Conditions for Ramp Weaves

For Type A Major weaves, the simulation indicated that the limit on capacity flow was a little higher than for ramp weaves. As Figure 6.9 shows, CORSIM was able to simulate conditions up to a total input volume of about 3500 vehicles/hour. Otherwise, the capacity model is assumed to be the same as for ramp weaves.

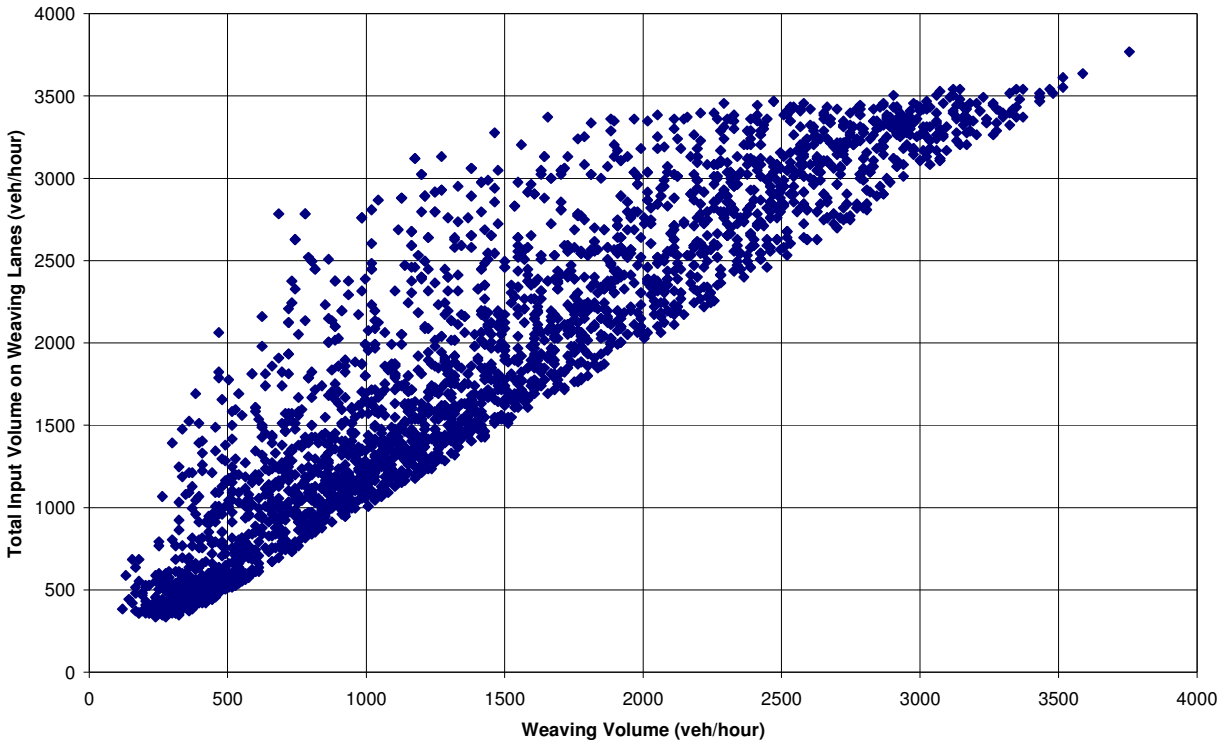

Figure 6.9. Simulated Conditions for Type A Major Weaves

The capacity model for Type A Major weaves can therefore be stated as:

For total weaving volumes, V_w, less than 1200 veh/hour:

$$C_w = 2300 + V_w$$

For $V_w \geq 1200$ veh/hour **and** total entering volumes on the weaving lanes, $V_t \leq 3500$ veh/hour:

$$C_w = 3500$$

For $V_t > 3500$ veh/hour:

$$C_w = (2 - VR_w)\left(1 + \frac{V_w - 2142}{2370}\right)(2300)$$

Capacity is not defined for weaving volumes greater than 3700 veh/hour

Base capacity values are set at 2300 vehicles/hour, with no modification or adjustment.

The capacity models for Type A weaves can also be represented as surfaces, as shown in Figure 6.10 for ramp weaves and 6.11 for major weaves. The three regimes of the capacity models are seen as three distinct surfaces that intersect at the boundary conditions. The calculated capacity is only true capacity on the portion of the surfaces where the input volume exceeds 3000 vehicles per hour. The capacity on the flat surfaces and on the near surface that goes down to zero weaving volumes is *potential capacity,* useful as entry values into the level of service model.

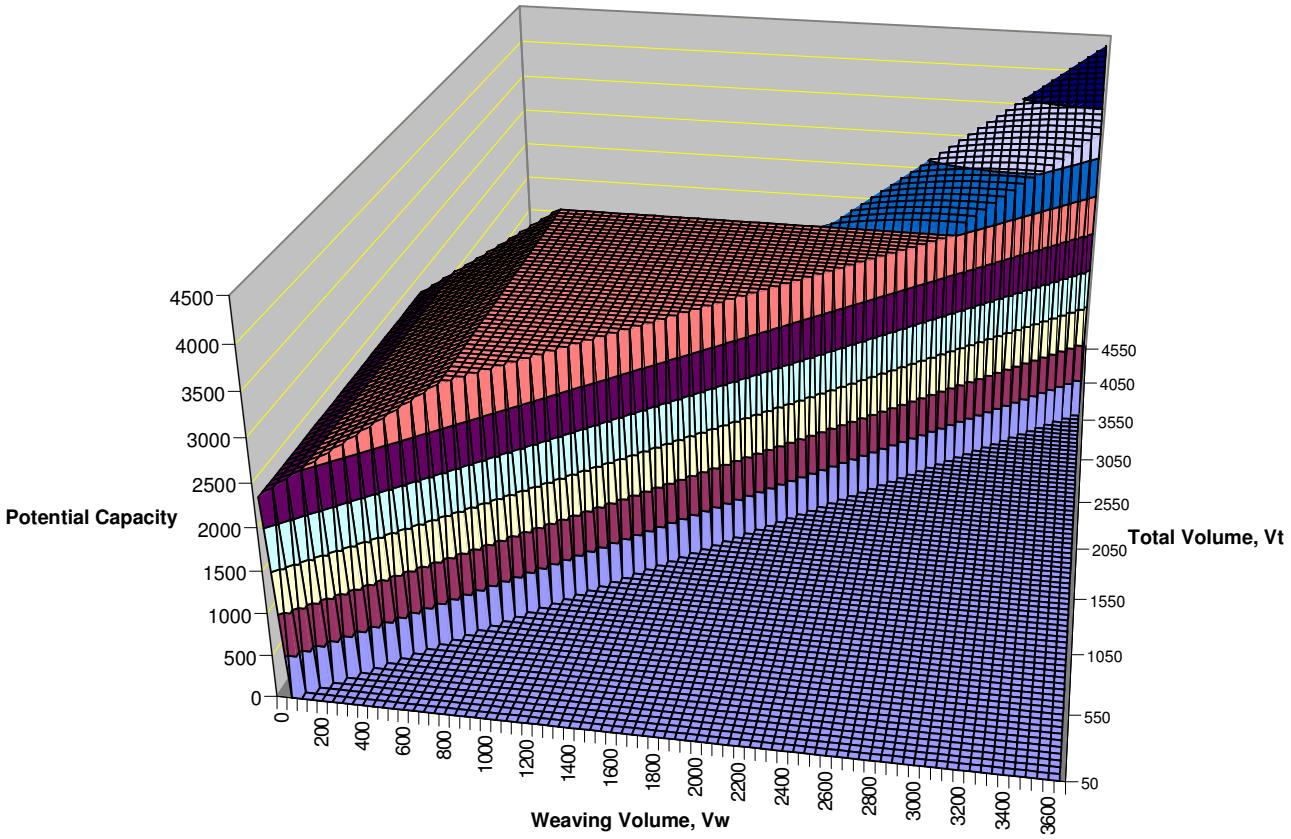

Figure 6.10. Capacity Model for Ramp Weaves

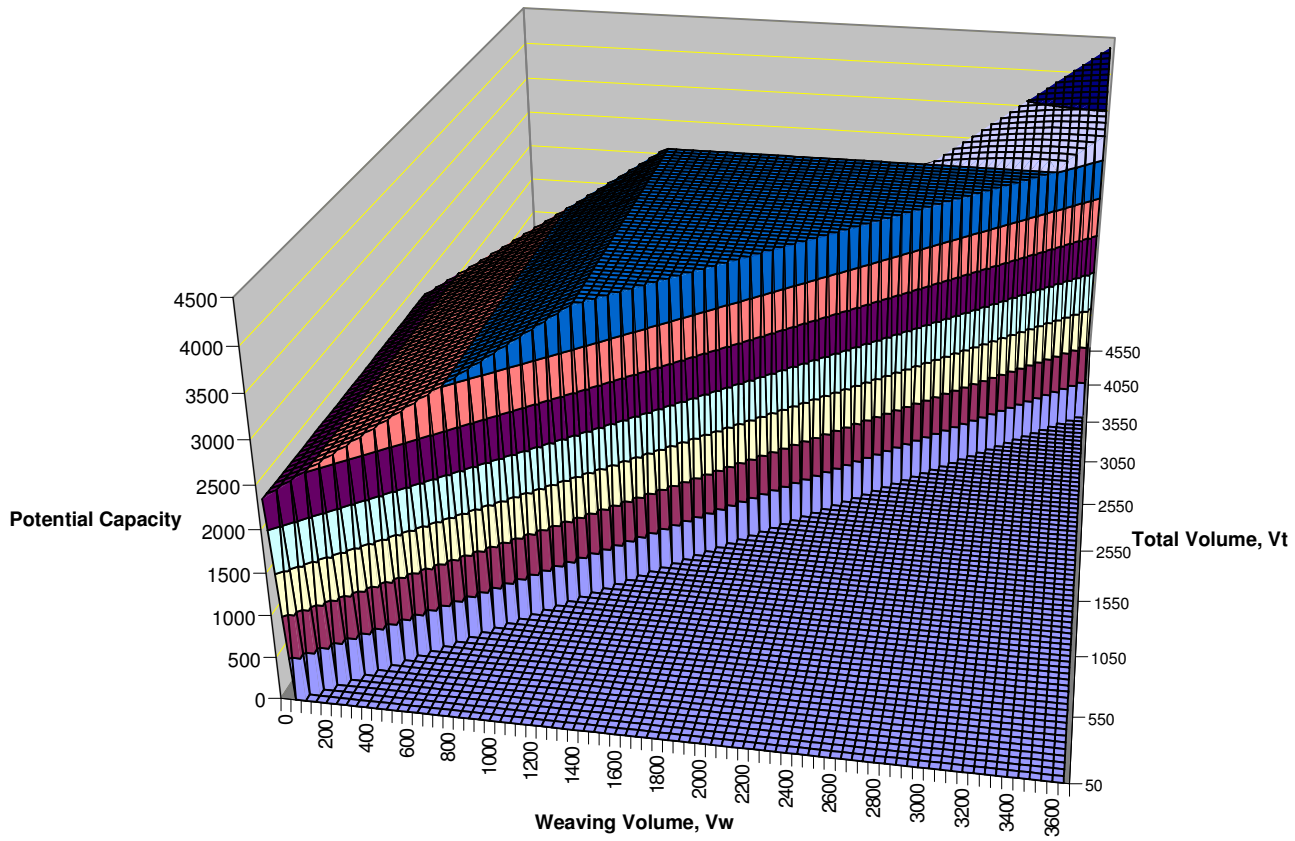

Figure 6.11. Capacity Model for Type A Major Weaves

Summary

A proposed capacity model for Type A ramp weaves was developed in this chapter. At higher weaving volumes, i.e., greater than approximately 2100 vehicles/hour, the model is based on field data, where drivers were observed to accept shorter headways during their weaving maneuvers. Capacity conditions were not seen in the field for lower weaving volumes, however, calibrated simulation runs suggested a capacity of approximately 3000 vehicles/hour for weaving flows less than 2100 vehicles/hour. The researchers further assumed that, at the boundary condition of zero weaving volume, the capacity would be that of a single lane, since it seems unlikely that at low weaving volumes, both the right lane of the mainlanes and the entrance ramp would be running at capacity.

The proposed capacity model for Type A major weaves was developed in the same manner. It is similar to that for ramp weaves, except simulation indicated a capacity of approximately 3500 vehicles/hour for lower weaving volumes. It should be noted that the behavior noted for ramp weaves where drivers accept shorter headways when weaving volumes are high was not directly observed for major weaves, however it seems reasonable to assume that it would occur. The simulation appears to hint at this behavior at very high weaving volumes.

The proposed capacity model is used as a starting point in the next chapter to identify the various levels of service.

CHAPTER 7. LEVEL OF SERVICE

The use of density is explored in this chapter as a means to distinguish between the various levels of service. Density is the preferred means to define levels of service in the freeway chapters of the Highway Capacity Manual as it directly related to the drivers' perception of how crowded (and, thus, congested) the freeway is. The density used herein was found directly from the simulation model by averaging the number of vehicles within the weave in the selected lane(s) and dividing by the length of the weaving section.

A model to estimate density for capacity and sub-capacity conditions is developed in this chapter for Type A ramp weaves and Type A major weaves. The volume-to-capacity ratio, individual weaving flows, total weaving flow, and total flow are all considered as potential indicators of density. The section on density presents the range of tests and evaluation performed on the density model.

Models for space mean speed are also briefly investigated.

Density

An initial plot of field-measured density against calculated V/C (as shown in Figures 7.15. and 7.16) suggested a correlation between the two that might be useful in creating a model. The form of the model that produced the greatest correlation was a second-order polynomial in the form of

$$y=ax^2 + bx + c$$

where x is the V/C ratio, y is the critical lane density, and a, b, and c are coefficients. The intercept, c, is constrained to be zero, so that the model will yield nil density at V/C = 0. The analyses set forth in this chapter found parameters of a=13.2 and b=29 for ramp weaves, and a=0.2 and b=37 for Type A Major weaves. These analyses consider a range of issues, including the effect of length, direction of weave, a test to find any correlation of residuals with unconsidered factors, the transformation of the data to a form that preserves homoscedasticity (a requirement for regression analysis), and a statistical analysis of the final models.

The final model of density for ramp weaves is

$$D_w = 13.2(V/C)^2 + 29(V/C)$$

And the final model of density for Type A Major weaves is

$$D_w = 0.2(V/C)^2 + 37(V/C)$$

All of the tests in this section were performed using these models.

Length

The impact of the length of ramp weaves is shown in Figure 7.1. No relationship was found in sub-capacity conditions beyond 400 feet. In capacity conditions, shorter weaving zones displayed a higher density, but this is caused by the dilution of the density by the presence of relatively empty lane between the merge and diverge points. Because the downstream lanes are starved for demand by the queuing at the

merge point (which characterizes capacity flow), longer weaving lanes will yield lower average densities in capacity conditions. This result does not mean that such weaving zones operate more effectively. The conclusion is that the length of the weaving zone is limited by safe operation at high speeds, rather than by relationship to capacity or service measures. The length of Type A weaving zones should therefore be controlled by the needs of design-speed traffic. The samples included in Figure 7.1 include those with excess demand that were subsequently excluded from the density and speed models.

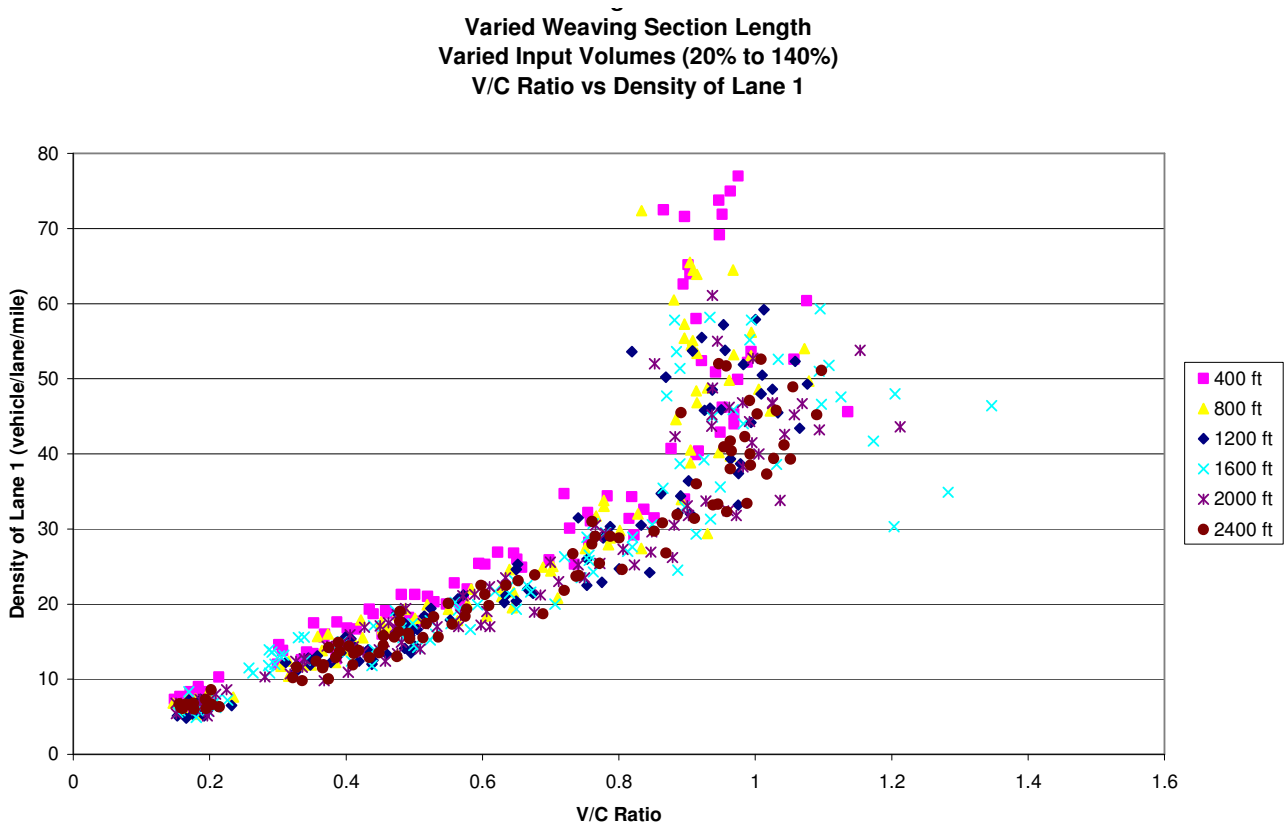

Figure 7.1. Density and Weaving Zone Length

Direction of Weave

Average density was plotted against the right weave/left weave ratio (V_1/V_2) for ramp weaves (Figure 7.2) and major weaves (Figure 7.3), both Type A weaves. No correlation is apparent.

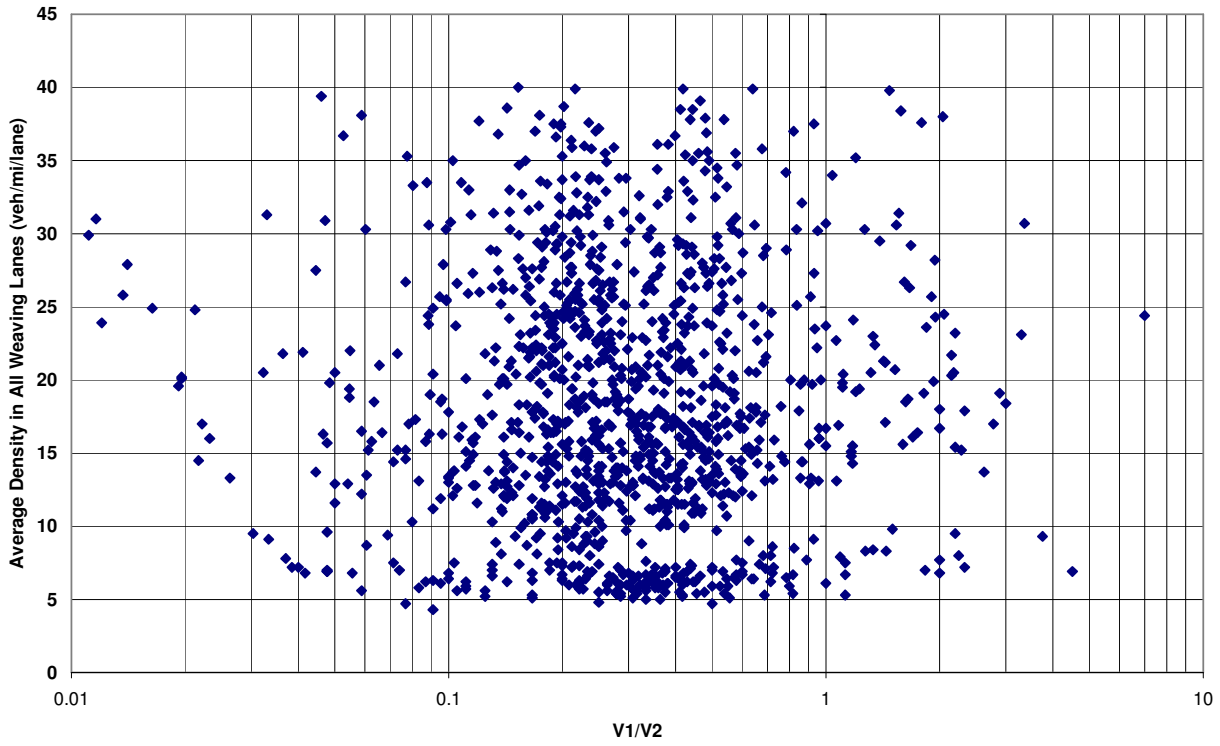

Figure 7.2. Density and Ratio of Right to Left Ramp Weaves

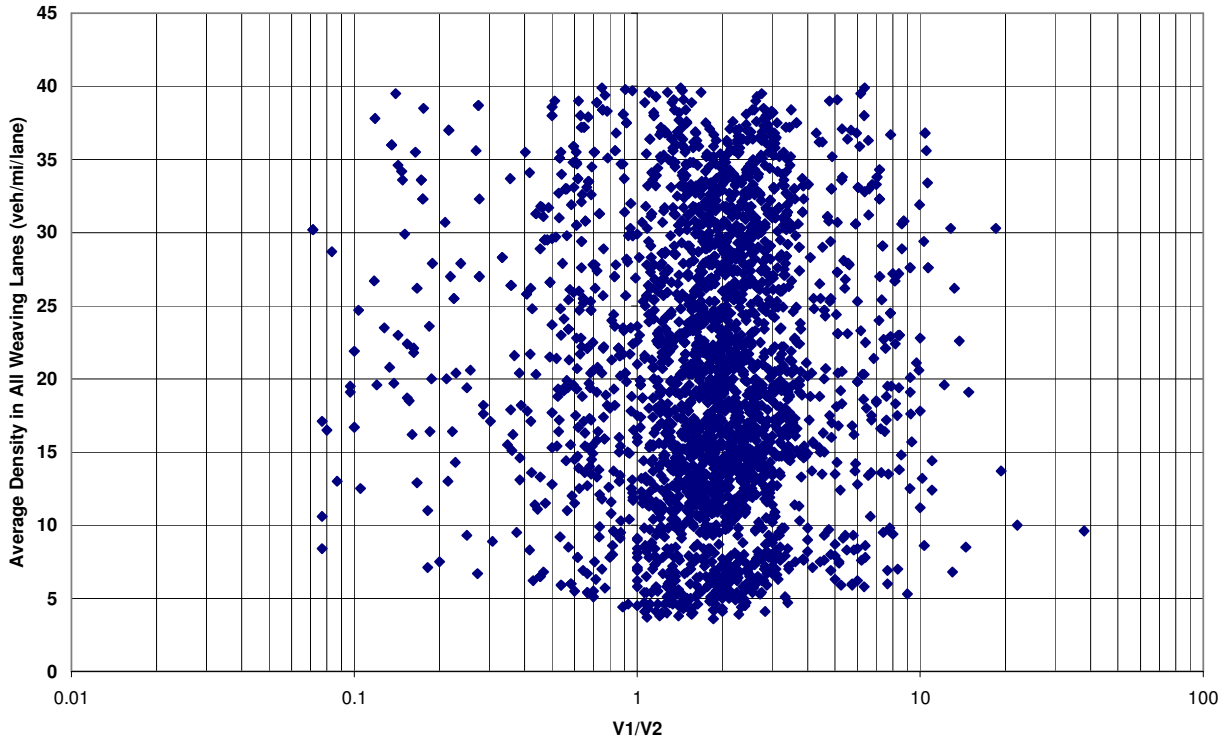

Figure 7.3. Density and Ratio of Right to Left Type A Major Weaves

Residual Analysis

The density model was analyzed to search for factors that might affect density other than the volume/capacity ratio. This analysis was performed by plotting the error of the density model (based on V/C) against a range of other parameters:

- V_1/V_2, the right weave/left weave ratio (Figure 7.4 for ramp and 7.8 for A Major weaves)
- V_1+V_2, total weaving volume (Figure 7.5 for ramp and 7.9 for A Major weaves)
- V_{rl}, volume in the right main lane (Figure 7.6 for ramp and 7.10 for A Major weaves)
- VR_W, volume ratio (Figure 7.7 for ramp and 7.11 for A Major weaves)

The plots show that the residuals of the V/C-based density model show no apparent correlation with other available input parameters.

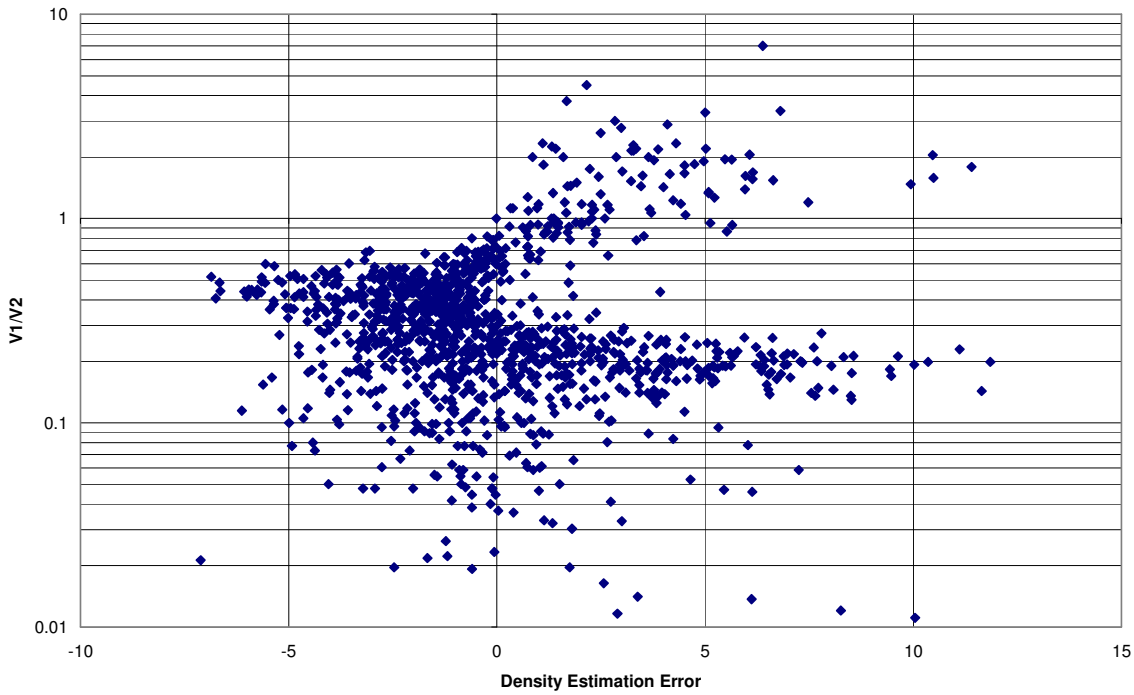

Figure 7.4. Density Model Residuals for Ratio of Right to Left Ramp Weaves

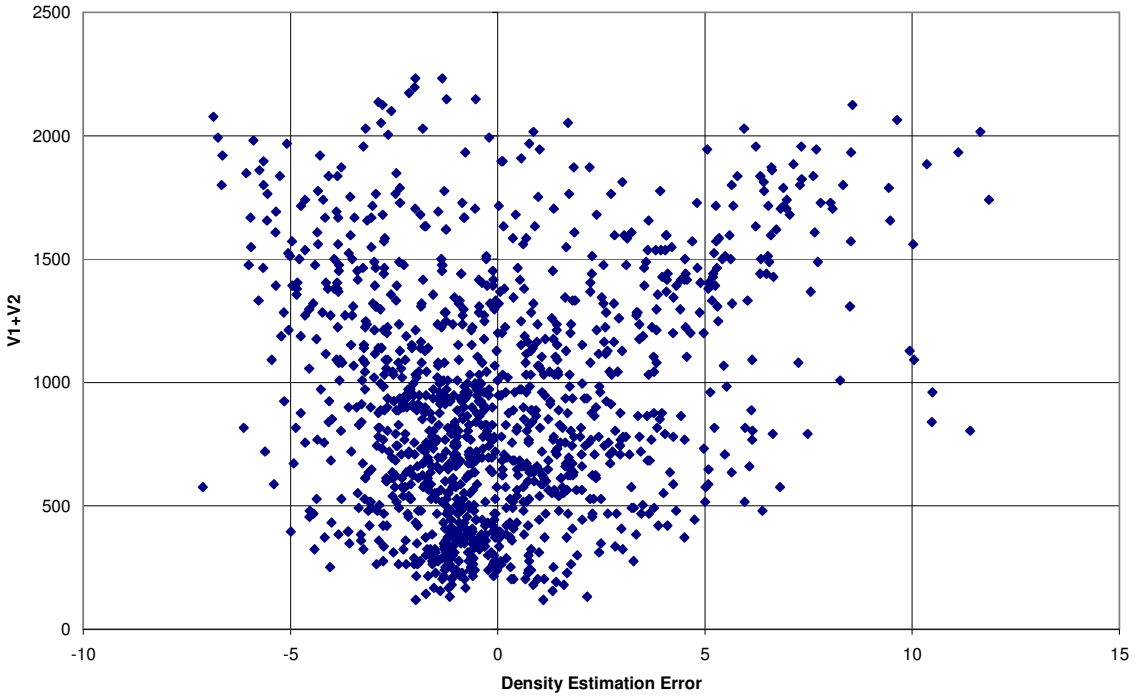

Figure 7.5. Density Model Residuals for Ramp Weave Total Weaving Volume

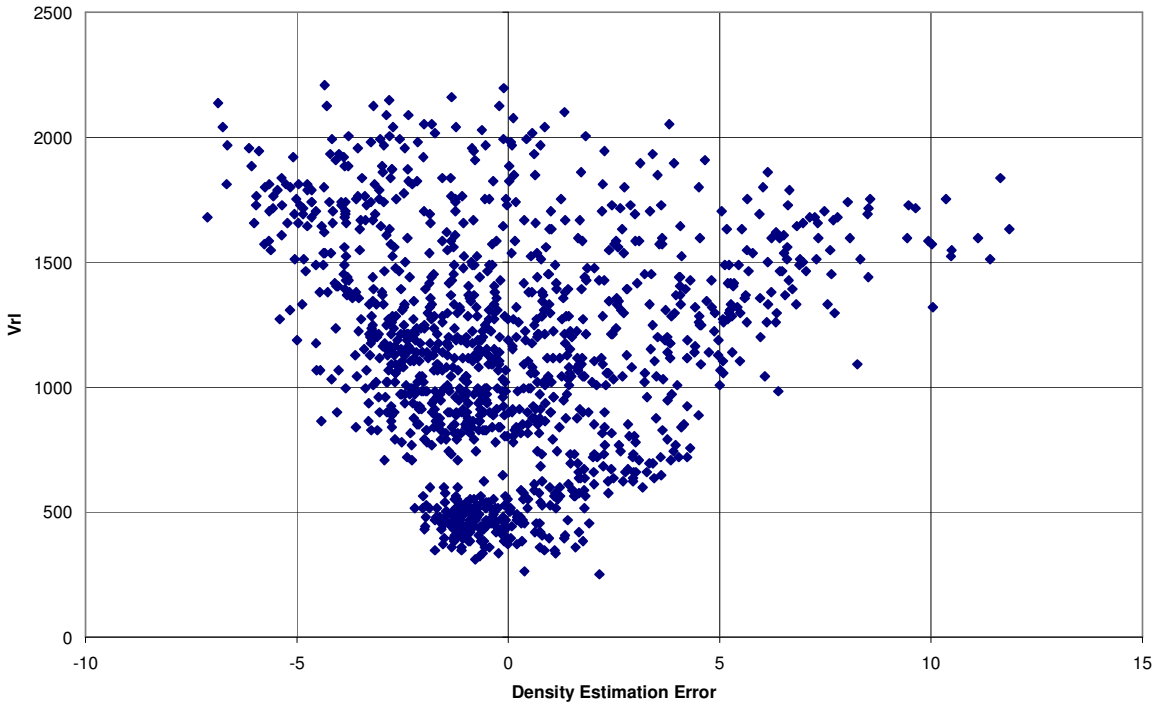

Figure 7.6. Density Model Residuals for Volume in Right Main Lane at Ramp Weaves

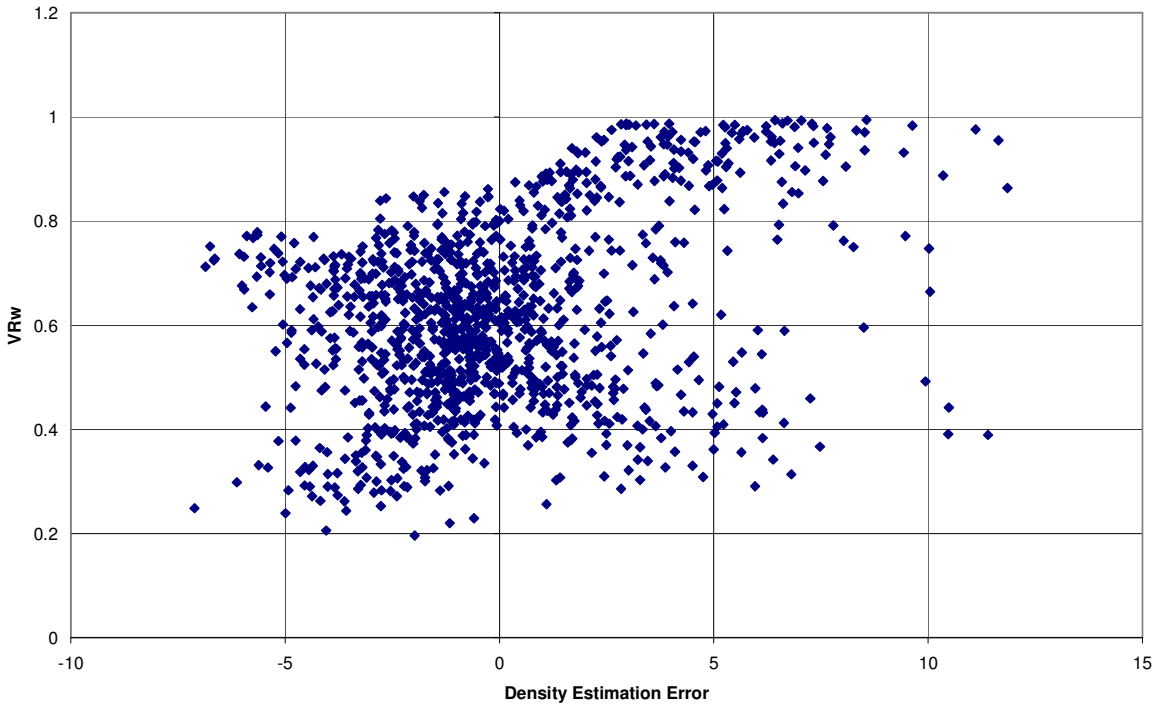

Figure 7.7. Density Model Residuals for Volume Ratio at Ramp Weaves

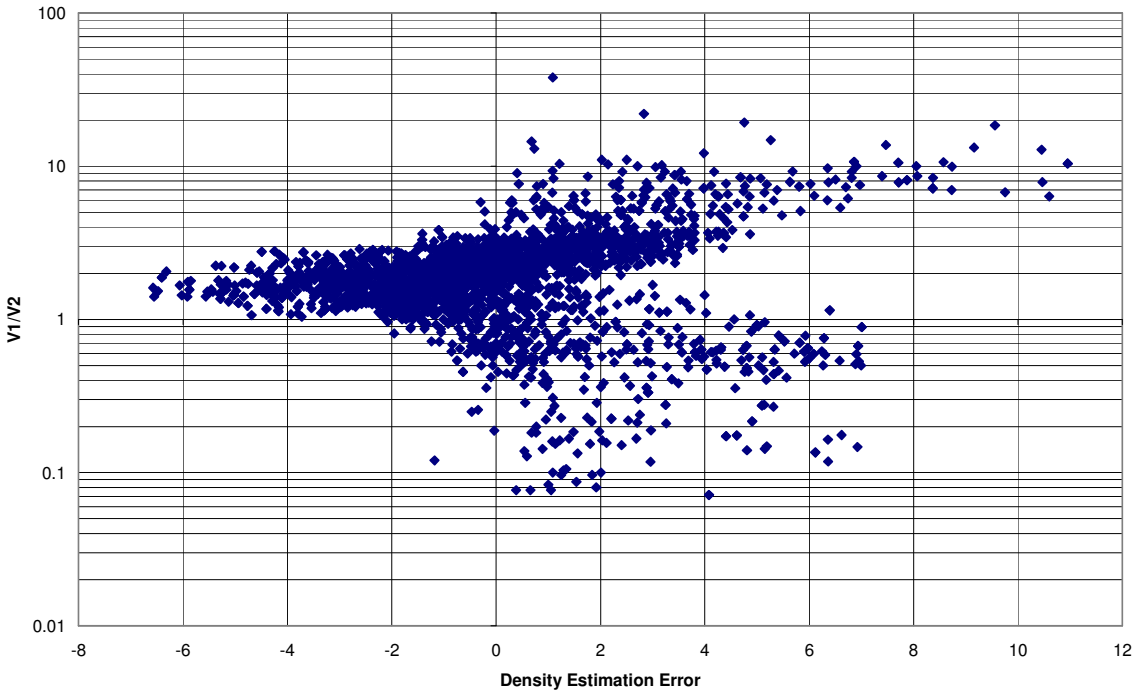

Figure 7.8. Density Model Residuals for Right and Left Type A Major Weaves

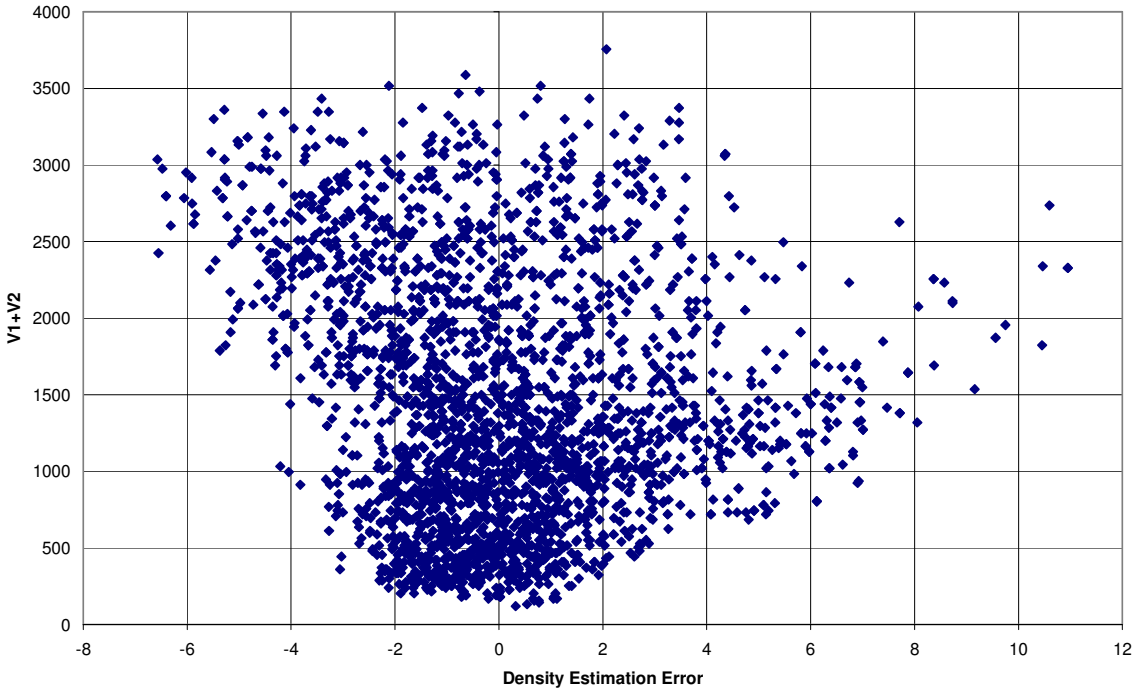

Figure 7.9. Density Model Residuals for Type A Major Weave Total Weaving Volume

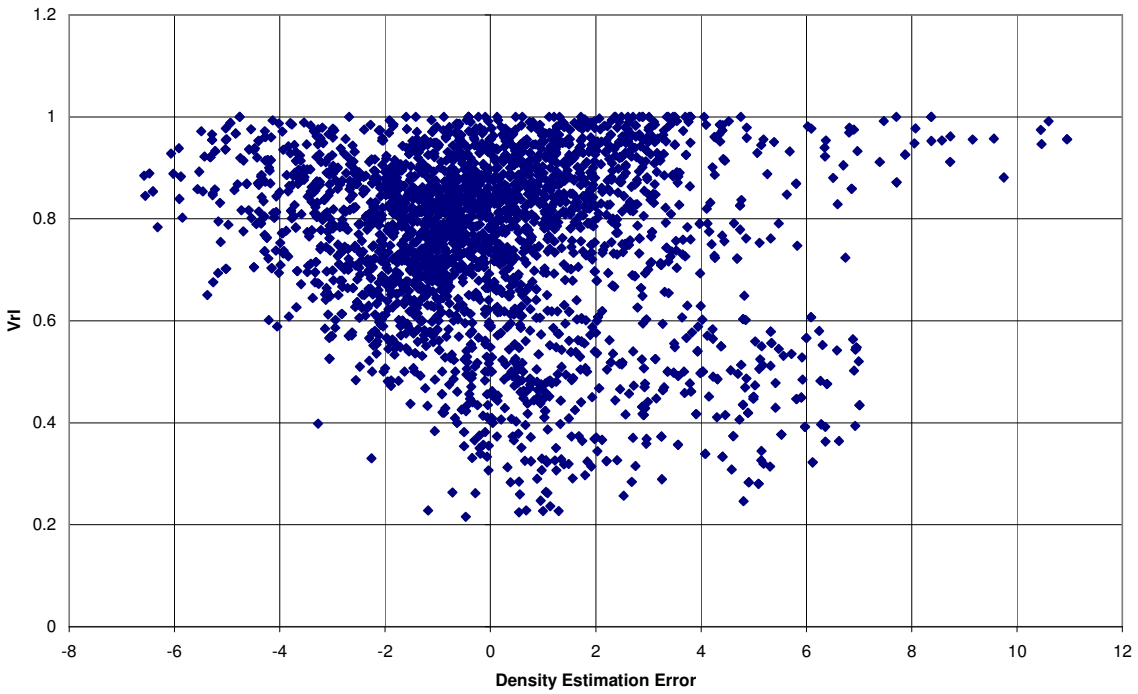

Figure 7.10. Density Model Residuals for Volume in Right Main Lane at Type A Major Weaves

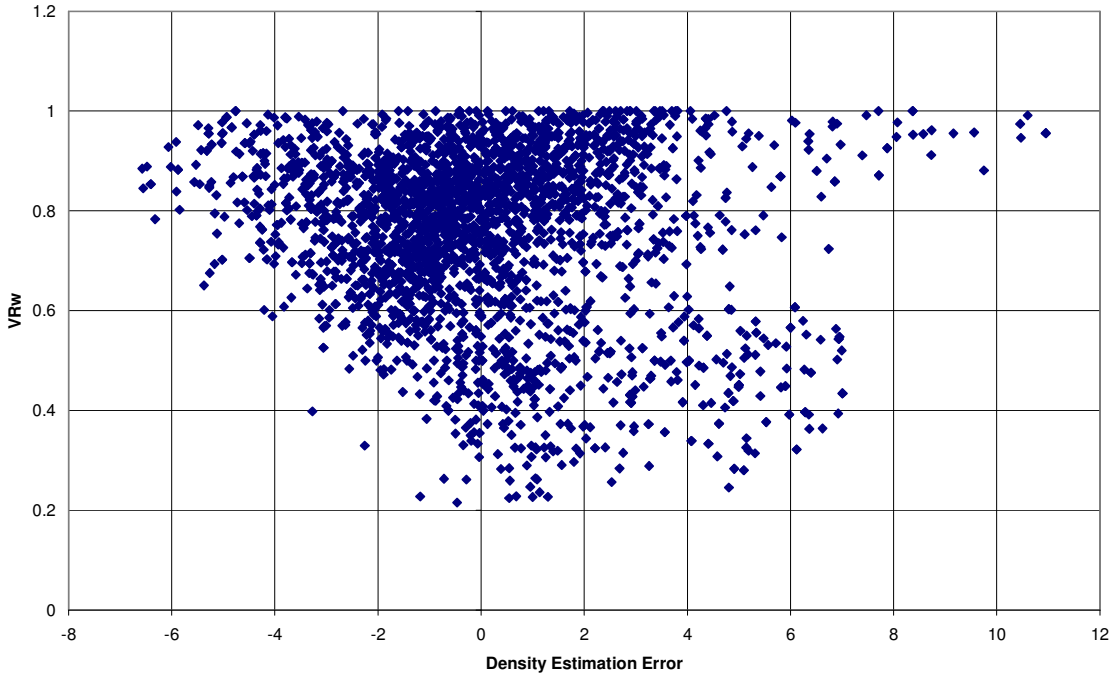

Figure 7.11. Density Model Residuals for Volume Ratio for Type A Major Weaves

Homoscedasticity

The density model itself showed very strong apparent correlation between volume/capacity ratio and critical lane density. But the variance of density varied with different values of the volume/capacity ratio, a condition known as *heteroscedasticity*. As such, an assumption of homoscedasticity, normally assumed in regression analysis, was not valid. Without it, a least-squares regression is no longer a minimum-variance unbiased estimator, but it is still an unbiased estimator [3]. Being able to use statistics, such as confidence limits from regression analysis, that require a minimum-variance unbiased estimator, required a transformation of the data to achieve homoscedasticity.

In order to achieve homoscedasticity, the researchers scaled the data points up by a multiplier. The multiplier needed to be larger at lower values and smaller at higher values of V/C. The researchers therefore chose a multiplier determined by dividing the predicted density into 40, the assumed highest value of density. This factor was then multiplied by each data point to achieve a factored value. A perfect density model would always produce a factored density of 40. Therefore, the most desirable model is that which produces factors that when applied to the data allow a linear regression line of the factored data to be $D_{w,\ factored} = 40$. Figure 7.12 shows the factored density model for ramp weaves and Figure 7.13 for A Major weaves.

The regression equations for V/C vs. the factored density for ramp and major weaves are shown within the graphs. In both cases, the x variable represents V/C and y represents the factored density. A casual review of the two equations reveals that, for the entire range of V/C, the calculated factored density will be very close to 40. Dashed lines representing two standard errors above and below the regression line are shown in the figures. The vast majority of the plotted points fall within two standard errors of the regression line, and these figures indicate that homoscedasticity may be assumed.

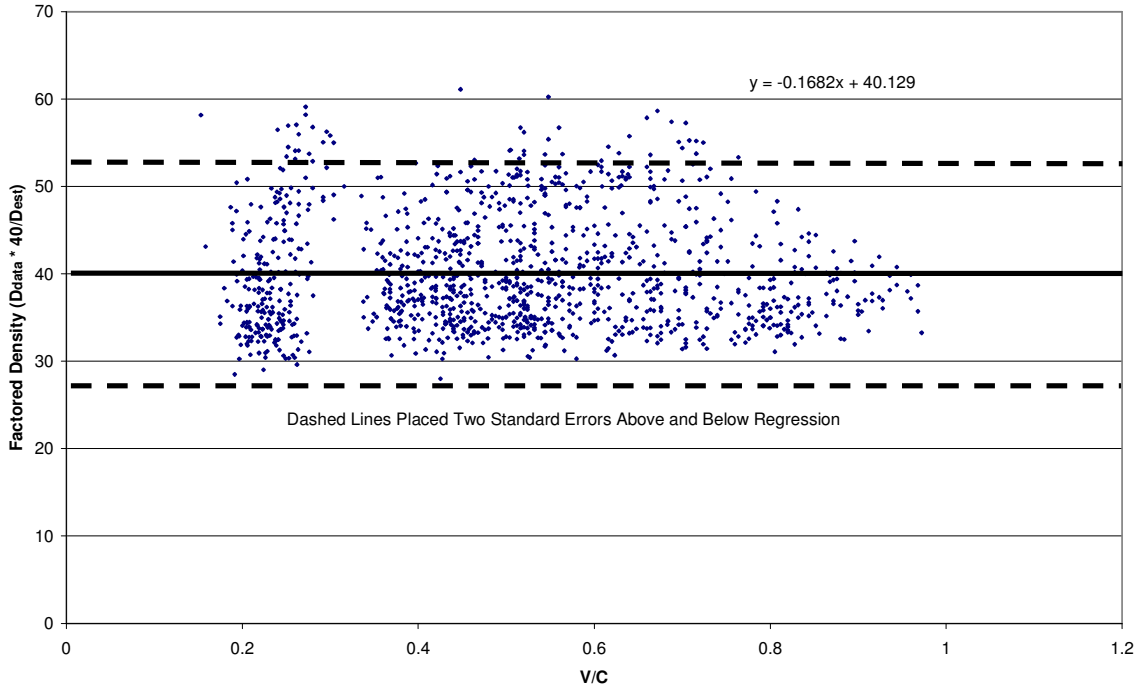

Figure 7.12. Factored Density Model for Ramp Weaves

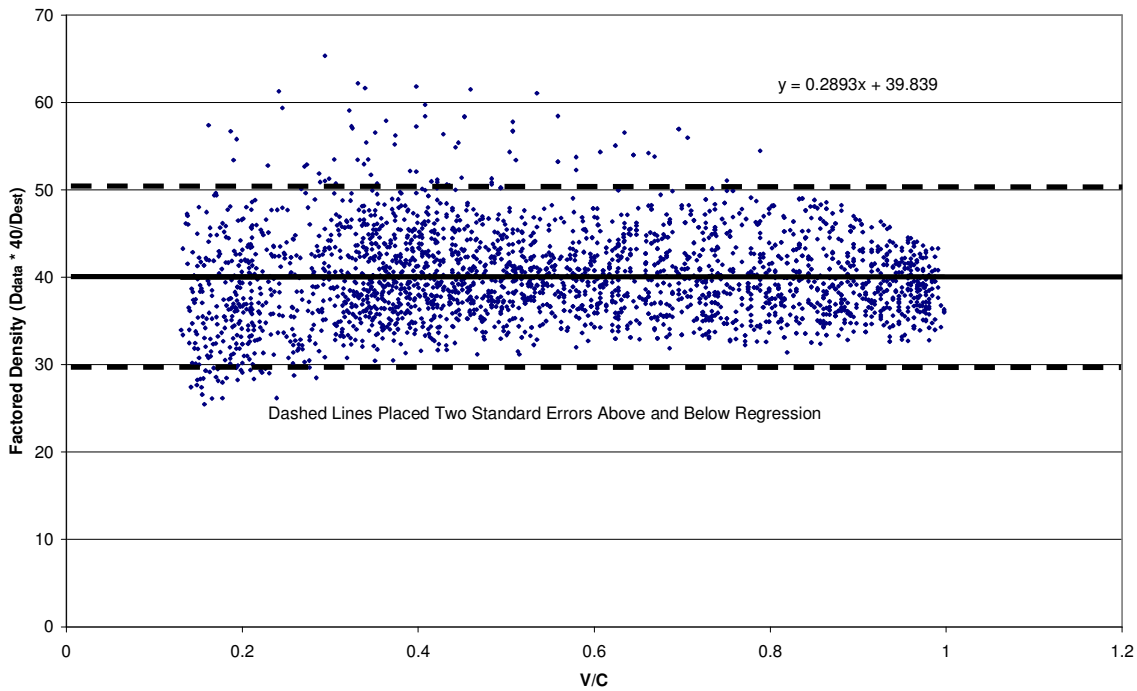

Figure 7.14. Factored Density Model for Type A Major Weaves

Parameter Sensitivity and Statistics

To achieve the final factored model, the coefficients of a function relating the unfactored density to V/C were found. As previously mentioned, a second-order polynomial in this form was selected:

$y=ax^2 + bx + c$

where x is the V/C ratio, y is the critical lane density, and a, b, and c are coefficients. The intercept, c, is constrained to be zero, so that the model will yield nil density at V/C = 0.

The point of the sensitivity analysis is to ensure that the selected parameters are both accurate and sufficiently precise. One measure of parameter quality is the mean error of the resulting model. An additional objective is to determine if the parameters in the unfactored model also provide a reasonable factored model, so that the statistics of the homoscedastistic factored regression become usable. Thus, the parameters are also evaluated against the ideal factored density model, which is $D_{w,\ factored} = 40$.

Table 7.1 shows the variation of the factored linear regression with different values of a and b for ramp weaves. Table 7.2 shows the variation of the factored linear regression for A Major weaves. In both cases, the parameters with the least error in the unfactored density model resulted in very close approximations of $D_{w,\ factored} = 40$ in the factored model. The search for the best parameters was restricted to three significant figures.

For ramp weaves, the parameter values of a=13.2 and b=29.0 yielded a linear regression of the factored data of $D_{w,\ factored} = -0.1682x + 40.13$. For A Major weaves, a nearly linear model worked best, even with unfactored values. Therefore, a = 0.2 and b = 37.0.

a (b = 29.0)	Mean Unfactored Error in Density Model	Factored Linear Regression (y=factored density, x=V/C, ideal is y=40)
13.0	0.061	y = 0.0106x + 40.15
13.1	0.319	y = -0.0790x + 40.14
13.2	0.003	y = -0.1682x + 40.13
13.3	-0.026	y = -0.2568x + 40.12
13.4	-0.055	y = -0.3450x + 40.11
b (a = 13.2)		
28.8	0.104	y = -0.2512x + 40.40
28.9	0.053	y = -0.2094x + 40.26
29.0	0.003	y = -0.1682x + 40.13
29.1	-0.048	y = -0.1274x + 40.00
29.2	-0.098	y = -0.0870x + 39.86

Table 7.1. Sensitivity of Density Model Coefficients, Ramp Weaves

a (b = 37.0)	Mean Unfactored Error of Density Model	Factored Linear Regression (y=factored density, x=V/C, ideal is y=40)
0	0.093	y = 0.5020x + 39.84
0.1	0.055	y = 0.3953x + 39.84
0.2	0.017	y = 0.2893x + 39.84
0.3	-0.021	y = 0.1839x + 39.84
0.4	-0.060	y = 0.0792x + 39.84
b (a = 0.2)		
36.8	0.130	y = 0.2897x + 40.06
36.9	0.074	y = 0.2895x + 39.95
37.0	0.017	y = 0.2893x + 39.84
37.1	-0.040	y = 0.2890x + 39.73
37.2	-0.096	y = 0.2888x + 39.86

Table 7.2. Sensitivity of Density Model Coefficients, Type A Major Weaves

Because the weighted values are linearly correlated and are homoscedastic, a simple correlation coefficient describes the degree of correlation, and confidence limits may be determined based on the standard error of the estimate. The correlation coefficient, R^2, for the ramp weave model was 0.87, and 0.93 for A Major weaves. These and other statistics are shown in Table 7.3.

Type	R^2	Unfactored Mean Error (veh/mile)	Factored Standard Error (scaled to 40)	95% Confidence Limits
A Minor (Ramp Weaves)	0.87	0.003	6.44	+/- 32.2%
A Major Weaves	0.93	0.017	5.05	+/- 25.2%

Table 7.3. Statistical Results of Density Model

The confidence limits shown in Table 7.3 are based on the assumption that the dependent variable, density, is normally distributed with respect to the independent variable, V/C. The plot of factored density shows that this is not the case. In fact the data is skewed such that the data shows less scatter below the model and greater scatter above the model. Consequently, the lower confidence limit is a little too low and the upper limit a little too high. But the confidence limits are provided to give the user an indication of the spread of the data, and the current results provide this information adequately.

Figure 7.15 shows the final unfactored density model for ramp weaves, including the data points and the confidence limits. The model predicts a density of nil when V/C = 0, and a density of 42.2 vehicles/mile at capacity.

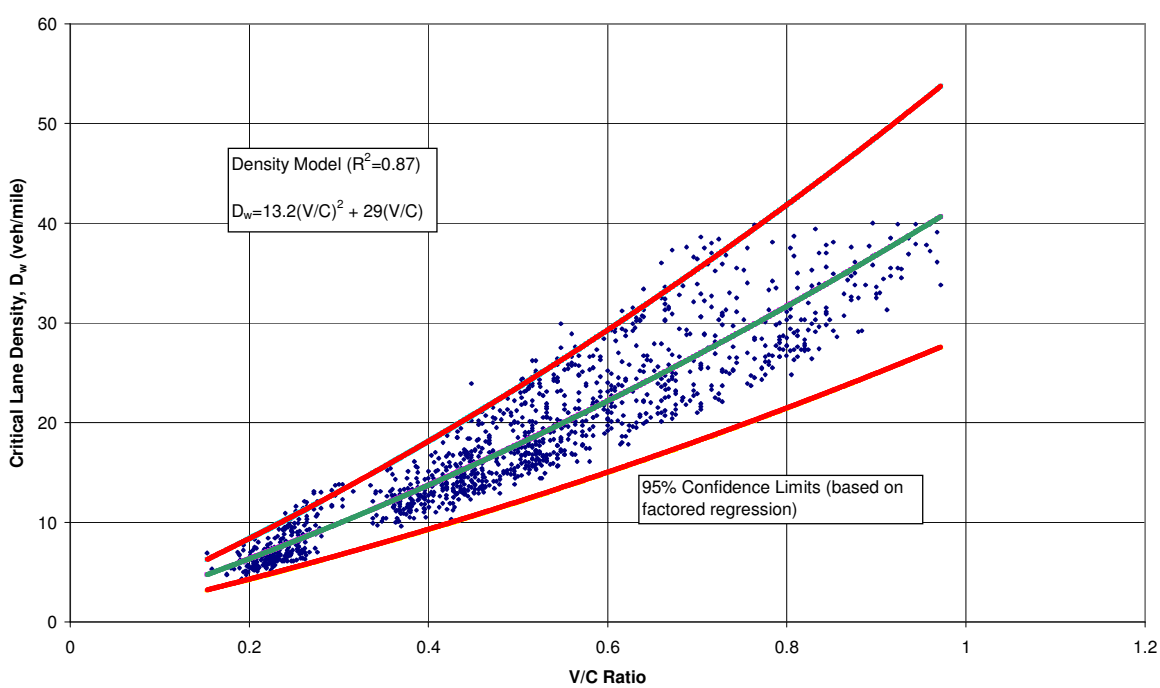

Figure 7.15. Critical Lane Density vs. V/C Ratio for Ramp Weaves

Figure 7.16 shows the unfactored density model for A Major weaves. The density at capacity is 37.2 vehicles/mile, which is a little lower than for ramp weaves. This may be caused by the increased ability of vehicles to vacate the weaving lanes.

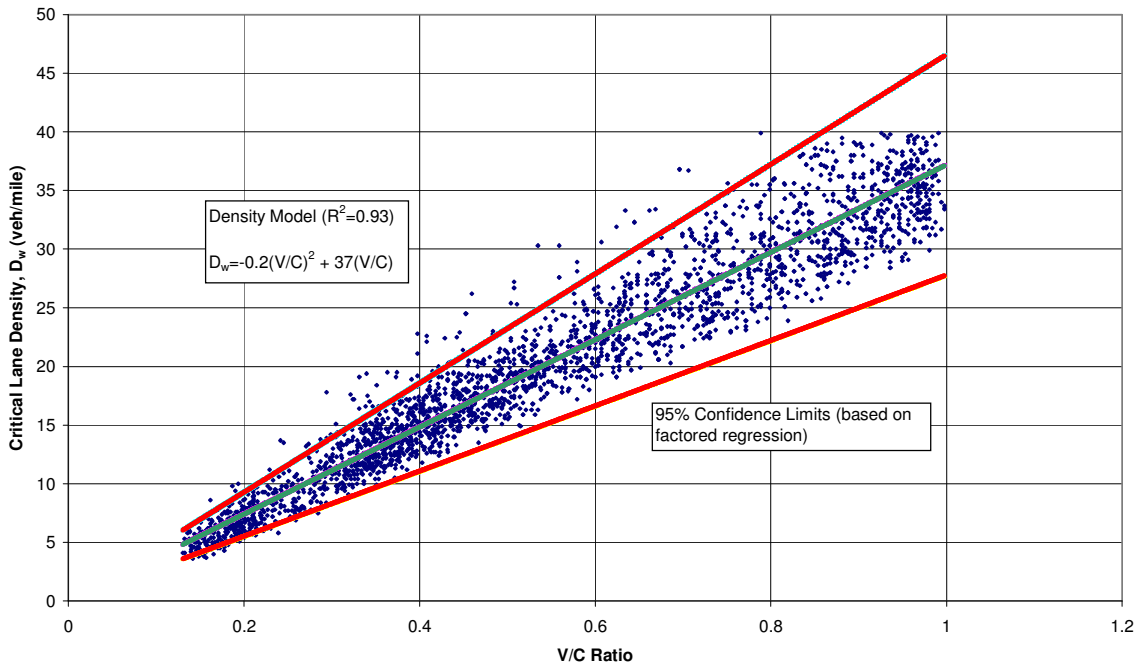

Figure 7.16. Critical Lane Density vs. V/C Ratio for Type A Major Weaves

Summary

The final density models have been shown to represent measured and simulated density based only on the V/C ratio. The correlation with V/C is strong, and there is no apparent correlation to other available input values. Factoring density data into the presumed maximum density provided a model for which regression was the maximum likelihood estimator, making it possible to report statistical confidence limits on the resulting density model. The final model of density for ramp weaves is

$$D_w = 13.2(V/C)^2 + 29(V/C)$$

And the final model of density for Type A Major weaves is

$$D_w = 0.2(V/C)^2 + 37(V/C)$$

Speed

Statistics on the space-mean speed of vehicles in the weaving lanes were recorded from the simulation. Speed is considered a secondary service measure, based on its poor LOS prediction ability, especially at higher levels of service. Space-mean speed was determined by dividing the total entering volume in the weaving lanes by the average density in the weaving lanes (*not* the critical lane density) for both the field data and the simulations. Vehicles that entered a weaving lane were assumed to stay in a weaving lane throughout the length of the weaving zone.

Figure 7.17 shows the speed model for ramp weaves, based on a simple polynomial regression of the speed. Figure 7.18 shows speed data for A Major weaves. R^2 was 0.68 for ramp weaves, and 0.86 for major weaves. No further statistical analysis was attempted.

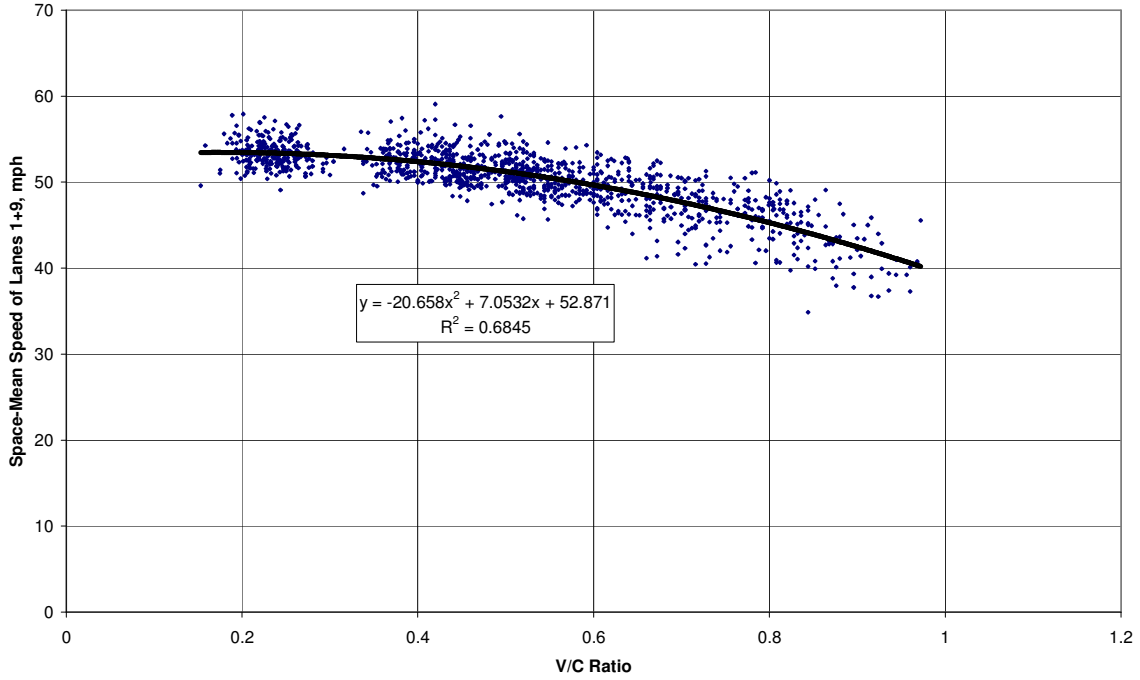

Figure 7.17. Space-Mean Speed in Weaving Lanes vs. V/C Ratio for Ramp Weaves

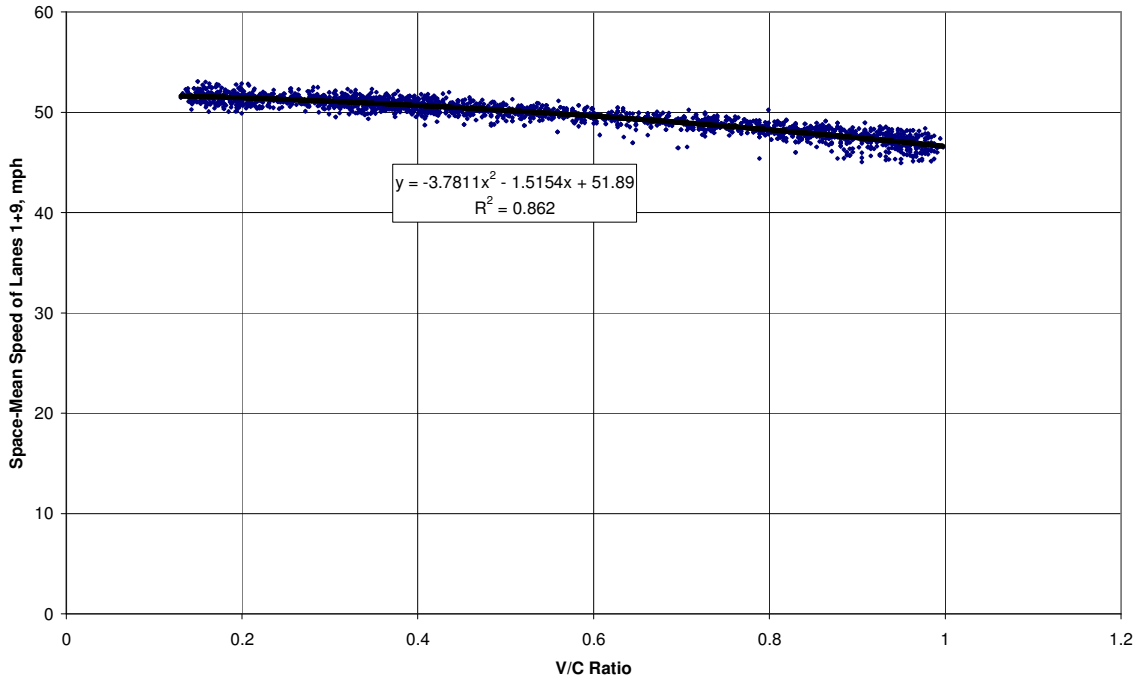

Figure 7.18. Space-Mean Speed in Weaving Lanes vs. V/C Ratio for Type A Major Weaves

For ramp weaves, the resulting speed model is

$S_w = -20.7(V/C)^2 + 7.05(V/C) + 53$

And for A Major weaves is

$S_w = -3.78(V/C)^2 - 1.52(V/C) + 52$

Supporting Simulation and Field Studies

The density and speed models for ramp weaves were primarily based on the highly detailed and comprehensive simulation, using FRESIM, of a site on the Baltimore-Washington Parkway. The simulation was calibrated to the site as reported in Chapter 3. The analysis used 1211 five-minute samples that met the criteria for use. The density and speed models for Type A Major weaves were based on the detailed simulation of 2768 five-minute samples. Calibration was based on three detailed five-minute samples taken in the field along Maryland Route 100.

Calibration and validation results were discussed in Chapter 3.

Solution Surfaces

Because V/C, and therefore density and speed, is directly related to the information on the potential capacity plot (Figures 6.10 and 6.11), the surface of each of volume/capacity ratio, density, and speed can also be shown as surfaces. These plots help visualize the solution space for the level of service models. Type A ramp weaves are shown in Figures 7.19 through 7.21, and Type A Major weaves are shown in Figures 7.22 through 7.24.

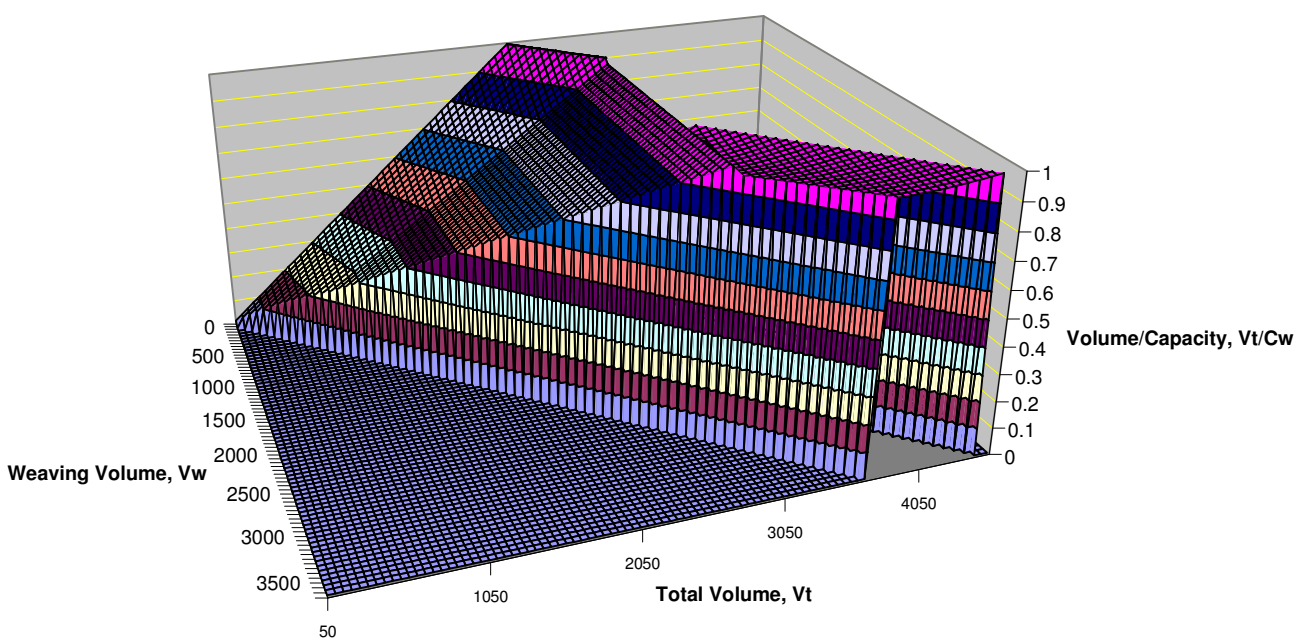

Figure 7.19. Volume/Capacity Ratio Solution Surface for Ramp Weaves

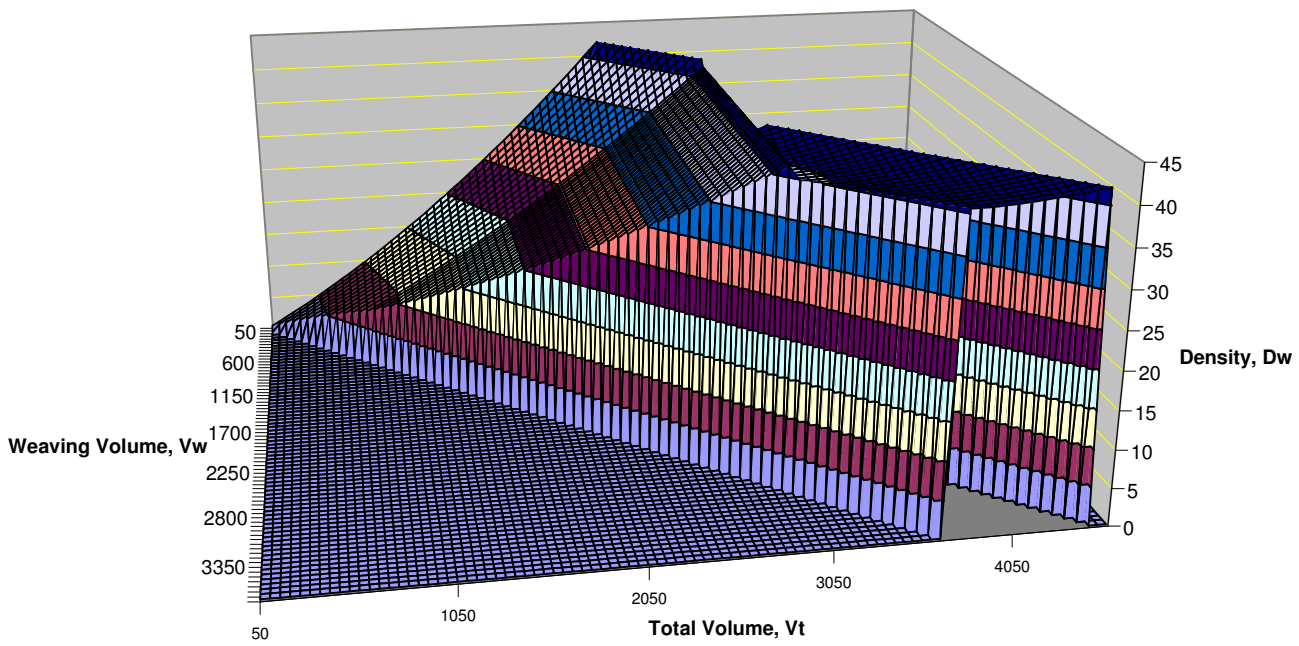

Figure 7.20. Critical Lane Density Solution Surface for Ramp Weaves

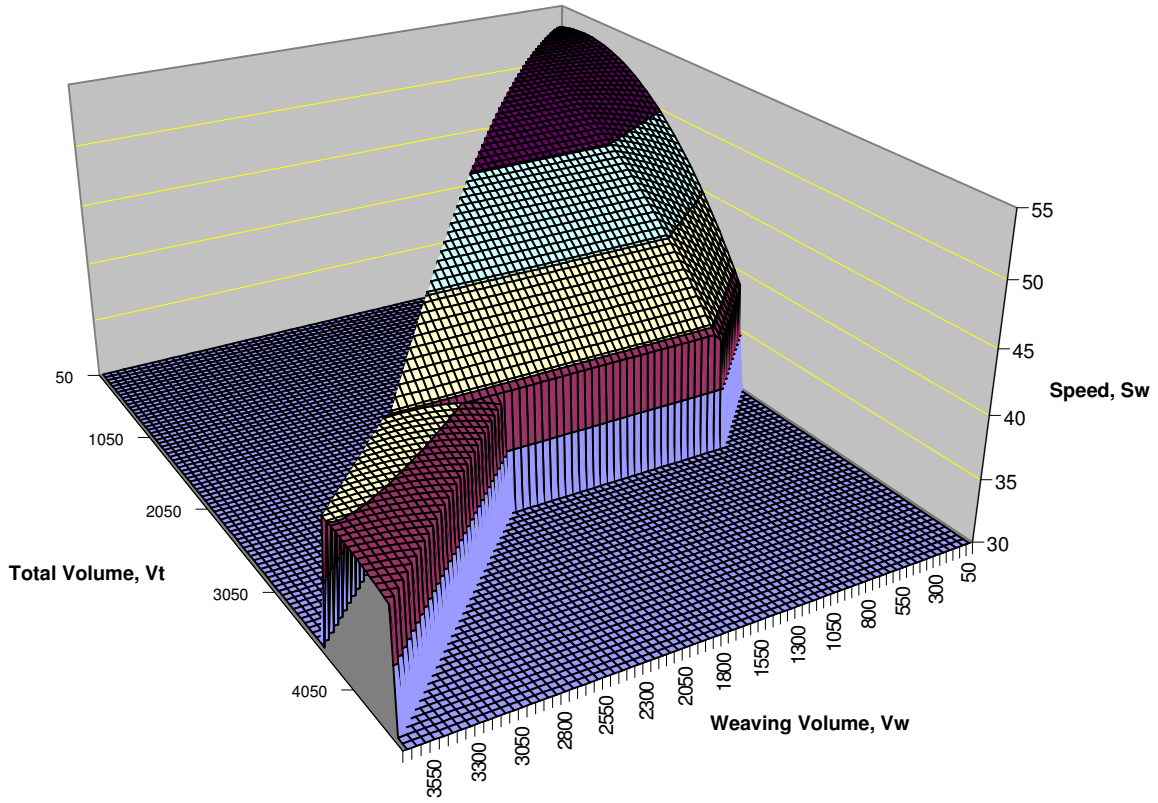

Figure 7.21. Space-Mean Speed Solution Surface for Ramp Weaves

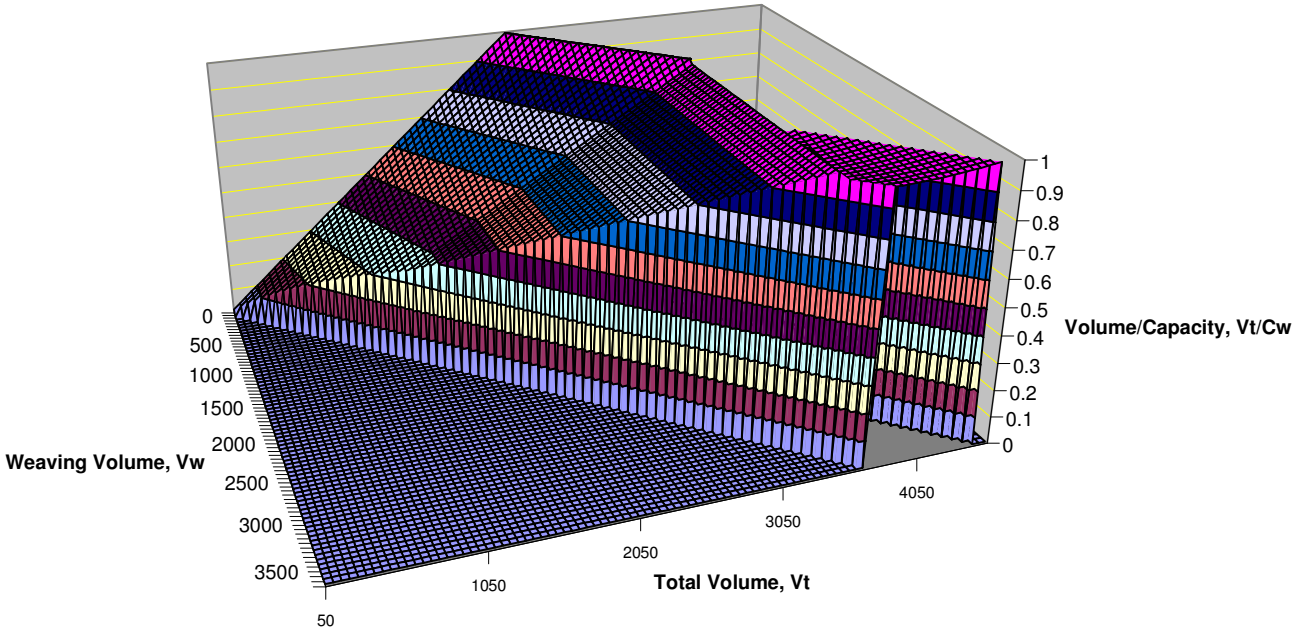

Figure 7.22. Volume/Capacity Ratio Solution Surface for Type A Major Weaves

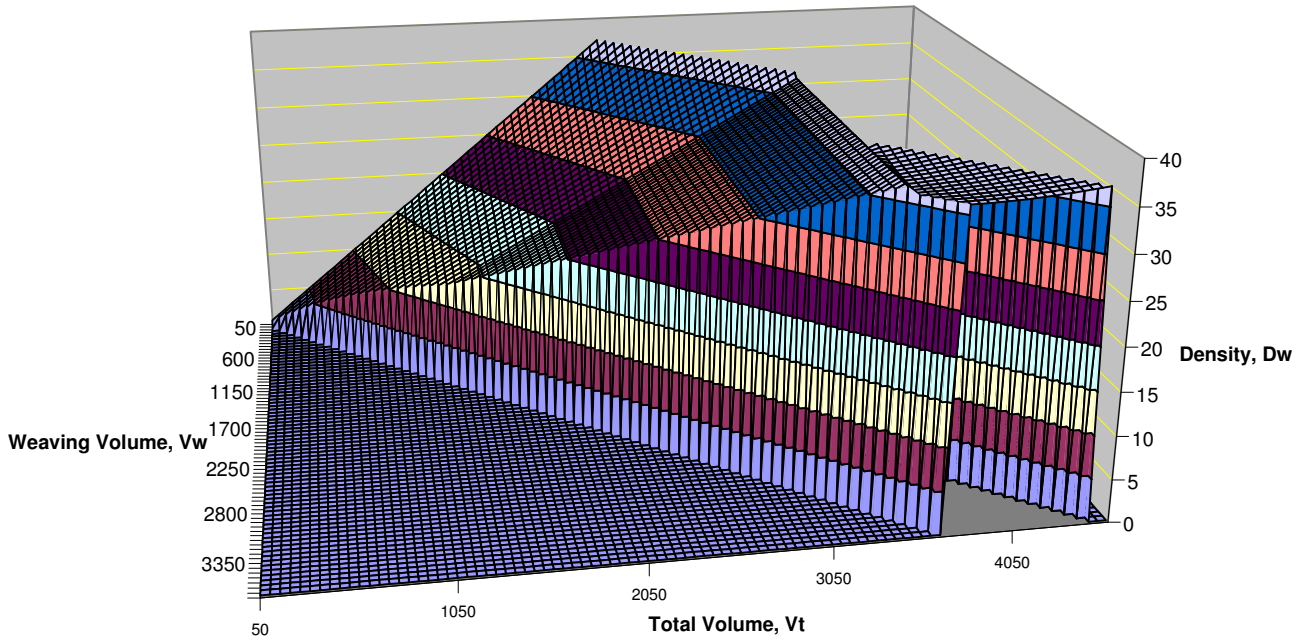

Figure 7.23. Critical Lane Density Solution Surface for Type A Major Weaves

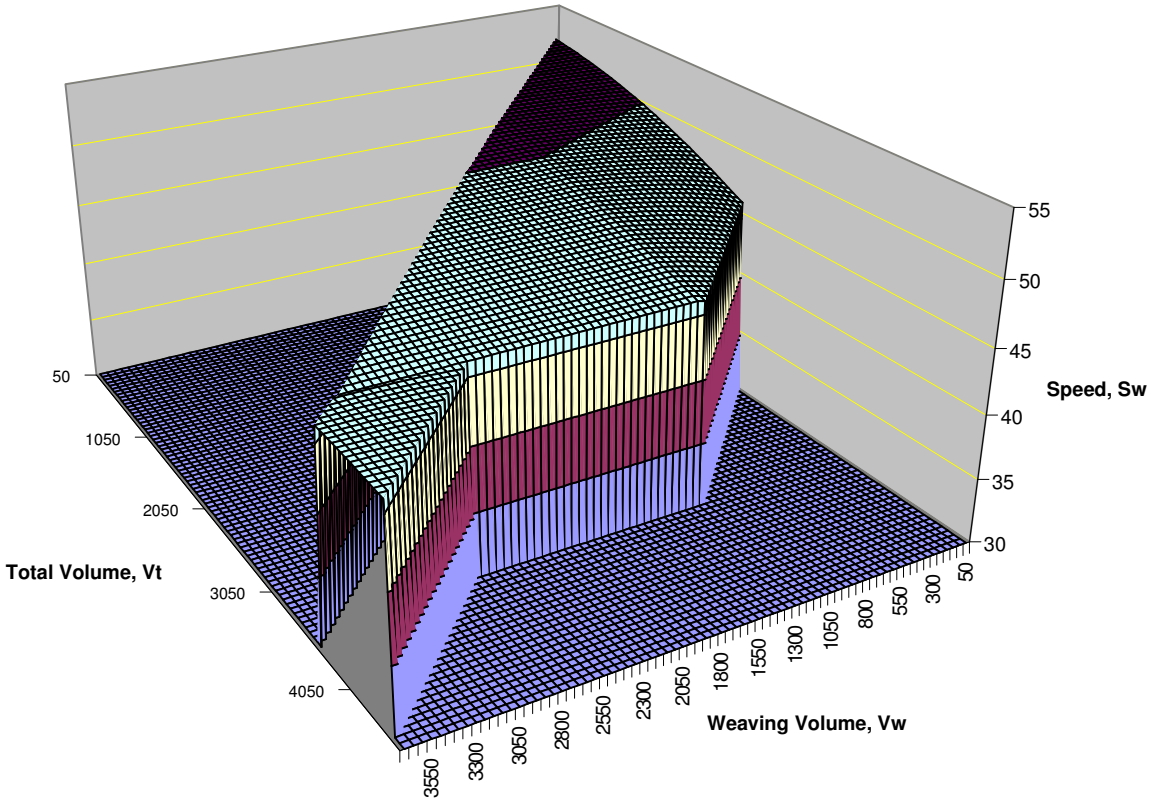

Figure 7.24. Space-Mean Speed Solution Surface for Type A Major Weaves

References

1. Denney, R., J. Williams, and M. Chowdury, *The Development of a Capacity Model for Ramp Weaves,* manuscript, 1998.

2. Denney, R., J. Williams, S. Cohen, and N. Rouphail, *Capacity and Quality of Service of Weaving Zones—Interim Report,* NCHRP 3-55(5), February, 1998, with additional materials of April 1998.

3. Neter, Wasserman, & Kutner, **Applied Statistical Models**, 2nd edition, Irwin,1985.

PART III. TYPE B AND C WEAVING ZONES

CHAPTER 8. FIELD STUDIES

The work performed on Types B and C weaves is described in this part. Data collection is covered in Chapter 8, and preliminary simulation results are reported in Chapter 9. As mentioned at the beginning of this report, project resources did not allow for the completion of capacity and level of service models for Types B and C weaves, however, extensive simulations were performed, and these results are reported herein to document this work.

This chapter covers data collection and some data reduction for Types B and C weaves which was completed for this study. A total of five sites were selected, one Type B and four Type C weaves. All six sites are in Texas, five in the Dallas/Fort Worth area and one in San Antonio. As mentioned earlier, weaving areas operating at capacity are relatively rare. Many of those that appear to be at capacity are merely experiencing congestion due to downstream bottlenecks. Thus, the researchers were not generally successful in finding Type B and Type C weaving zones that provided an observable capacity problem.

First, the geometry of the six sites is described, followed by an examination of the longitudinal distribution of lane changes throughout the weaves. This is a crucial factor in calibrating the simulation model, as it captures the lane changing behavior of the drivers. It also shows whether drivers tend to make their lane changes as early as possible, as was found with Type A weaves.

The figures for the six sites show the lane numbers (in circles), and the bin numbers in squares. The weaving area was divided into 100-foot segments (bins) for reducing the data from the aerial photos. This allowed us to track the location of lane changes throughout the weave. The data collection procedure was the same as used for the Type A major weave at Maryland routes 10 and 100, described in Chapter 5.

Type B

A Type B weaving area is formed in the southbound lanes of SH 121 between the SH 114 entrance and the exit for southbound SH 360 in Grapevine, Texas. The weaving area consists of three mainlanes on SH 121, an added lane from the single lane entrance from William D. Tate Avenue, and a two-lane exit for SH 360, one of which is a shared lane. This weaving area is illustrated in Figure 8.1. Entering traffic must move at least one lane to the left to remain on the mainlanes.

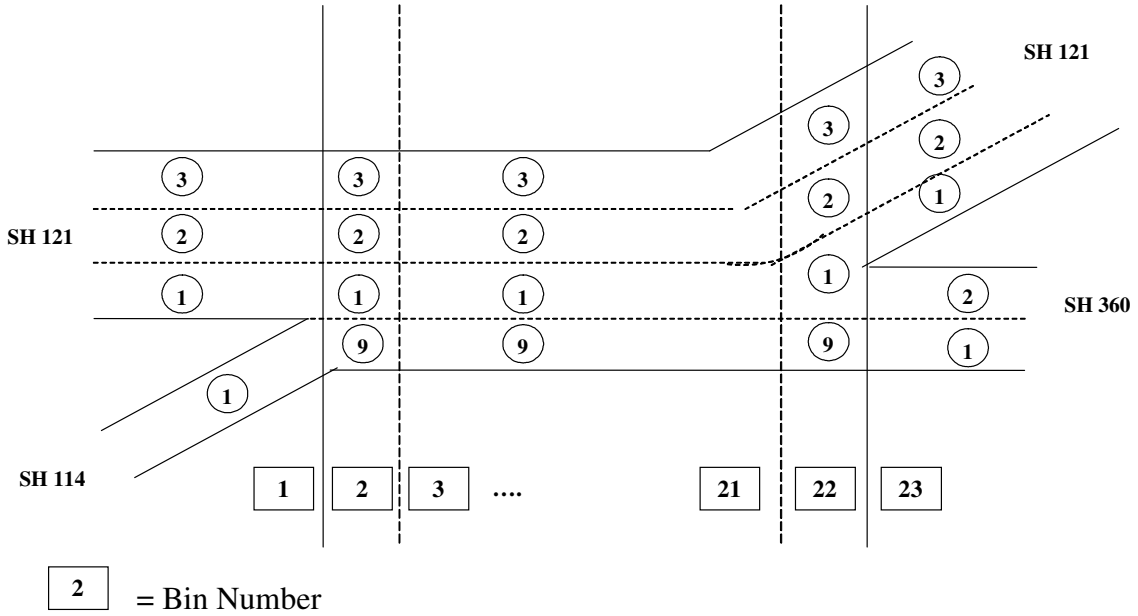

Figure 8.1. Southbound State Highway 121 (Texas), Type B

Type C

Type C weaves can be classed into three general configurations, and at least one field site was selected for each. The first consists of a weaving area with a single lane entrance ramp followed by a two-lane exit ramp. In this case, entering traffic that wishes to stay on the mainlanes must move two lanes to the left. Westbound IH 30 between the Hulen Street entrance and the exit for Camp Bowie Blvd. (US 377) in Fort Worth, Texas, was selected to represent this type of weave, and is illustrated in Figure 8.2

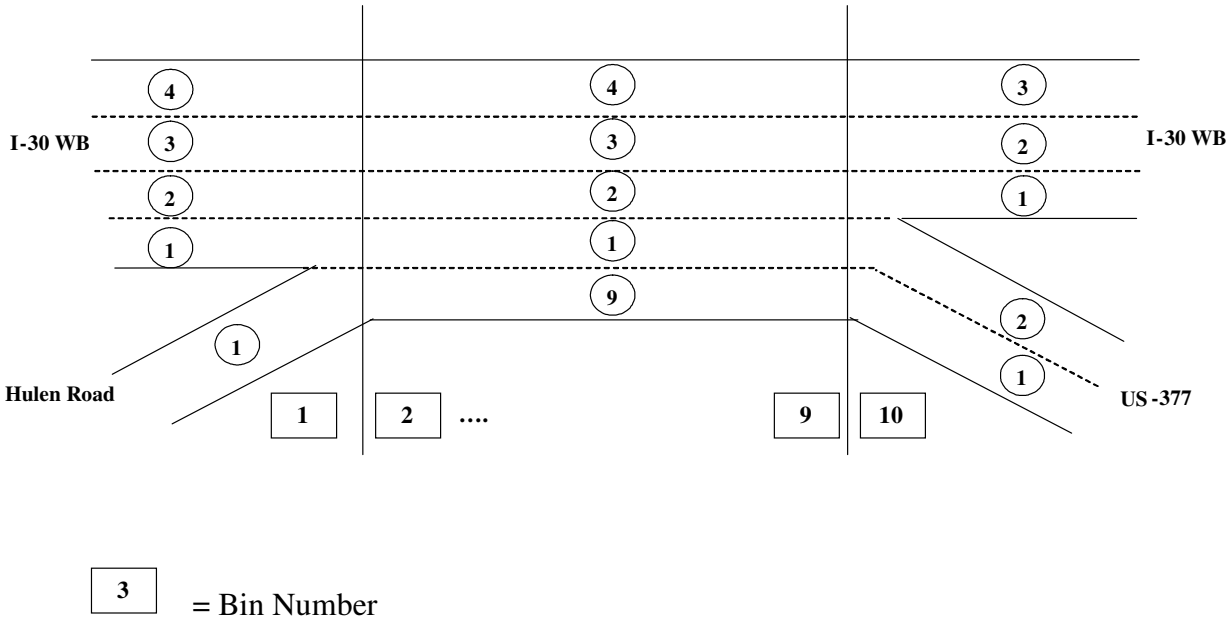

Figure 8.2. IH-30 Westbound (Texas), Type C, Two Required Lane Changes to Left

The second general configuration of Type C weaving area consists of a two-lane entrance ramp followed by a single lane exit ramp. In this case, exiting traffic from the mainlanes must change lanes twice. Three sites were selected to represent this type:

- Eastbound IH 30 between the Camp Bowie Blvd. (US 377) entrance and the exit for Hulen Street in Fort Worth, Texas, shown in Figure 8.3.
- Northbound SH 360 between the entrance from IH 20 to the exit for Mayfield Road in Arlington, Texas, shown in Figure 8.4.
- Northbound IH-35W between IH-20 entrance and the exit for Seminary Road, shown in Figure 8.5.

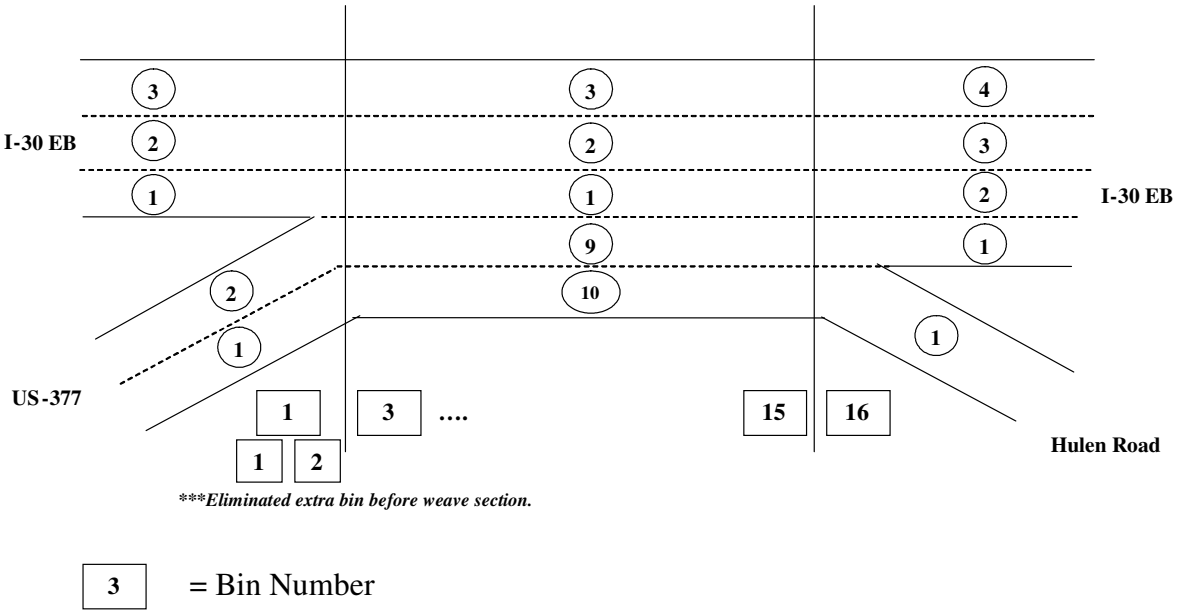

Figure 8.3. IH-30 Eastbound, Type C, Two Required Lane Changes to Right

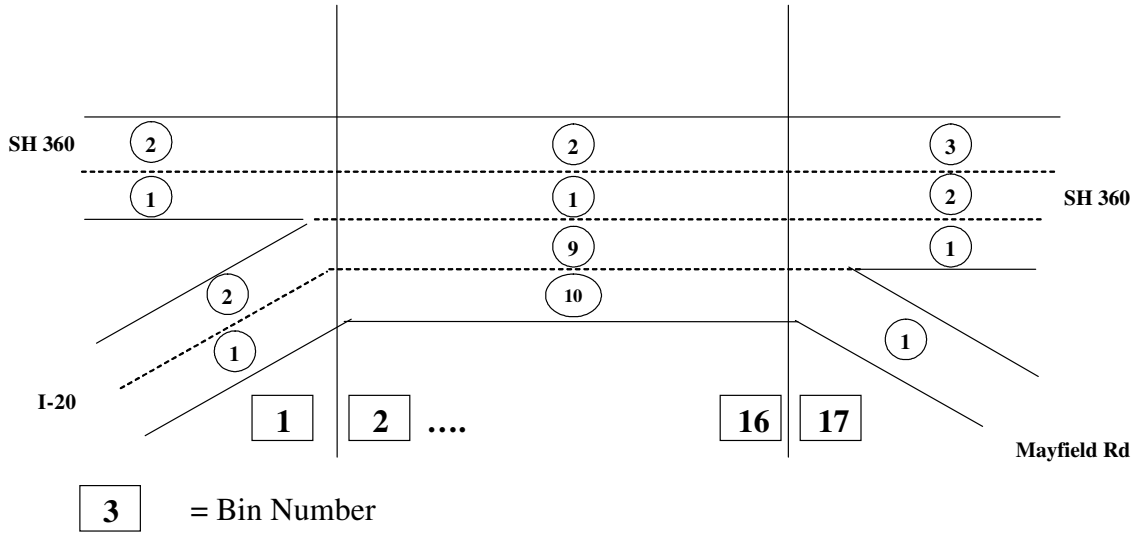

Figure 8.4. State Highway 360 Northbound, Type C, Two Required Lane Changes to Right

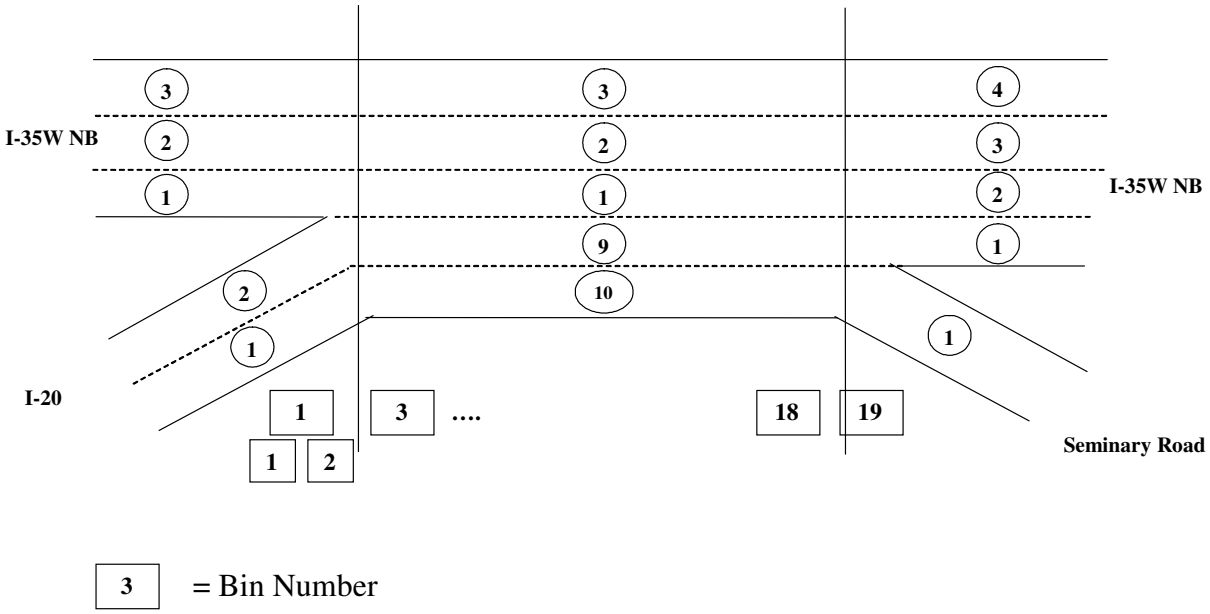

Figure 8.5. I-35W Northbound, Type C, Two Required Lane Changes to Right

The third general configuration of Type C weaving areas is the two-sided weave. It is characterized by an entrance ramp on the right followed by an exit ramp on the left, or vice versa. Entering traffic that wishes to exit on the following ramp must change lanes to cross to the other side of the mainlanes. The site selected for this project is southbound IH 35/410 between the Rittiman Road entrance on the right and the southbound IH 410 exit on the left. The weaving area is located in San Antonio, Texas, and illustrated in Figure 8.6.

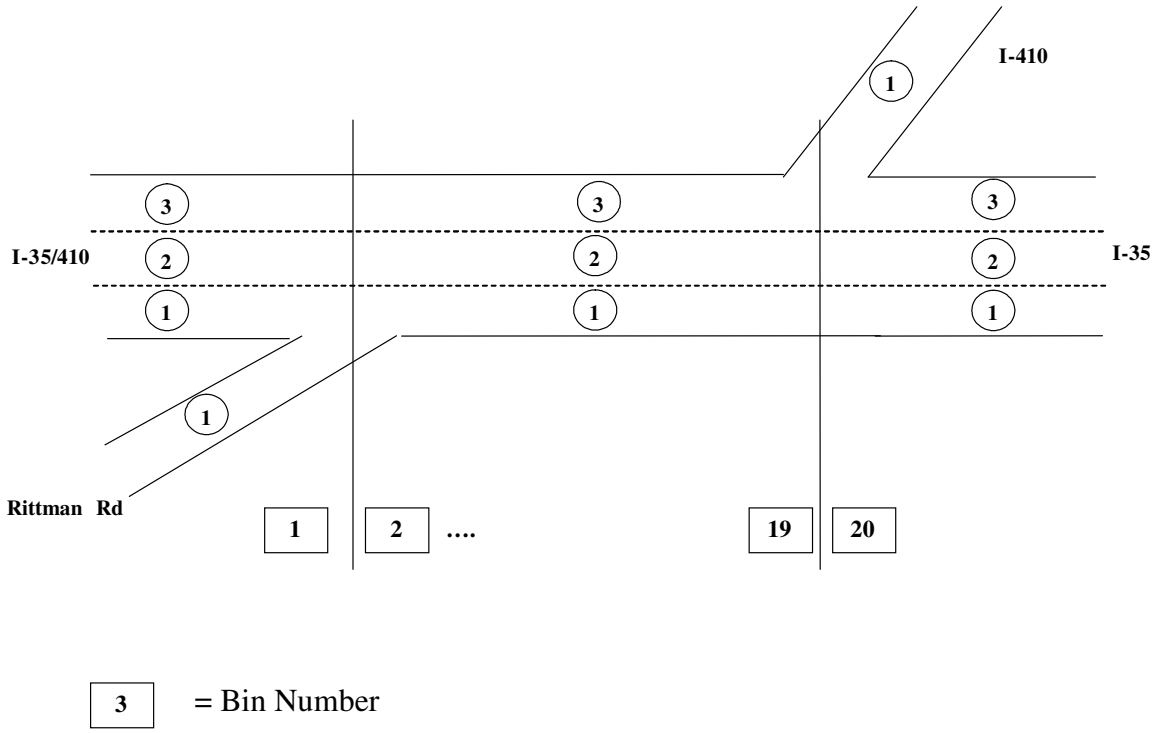

Figure 8.6. IH-35/410 Southbound, Two-Sided Weave

Data Collection

Aerial photos were used to track vehicle paths through these weaving areas and the data was reduced using the process described in Chapter 5. Initial observations indicated that congested flow would be observable at all locations, however none of the sites experienced congestion that could clearly be attributed to capacity restraints of the weaving area during the times of data collection. Nonetheless, these sites were used as the basis for the simulation studies, which are discussed in the next chapter.

Discussion

Resources for the research were depleted before much analysis could be performed on the field studies outlined above. For each of the sites, however, the researchers reduced data to include the following:

- Origin-destination flows
- Density by lane
- Space-mean speed by lane
- Location of lane change maneuvers by origin-destination pair

The first three of these do not reveal immediately useful relationships, and more detailed evaluation was not performed. The locations of lane changes were plotted and show a useful pattern. In all cases, nearly all lane changes occurred in the first 700 or 800 feet of the weaving zone, even when the weaving zone itself was much longer. This finding reinforces the proposition that the performance of the weaving zone is not determined by its length for lengths longer than a relatively short minimum. Thus, weaving zone lengths designed in accordance with free-flow speeds, using generally accepted design methods, once again do not appear to impose any constraint on operation. Figure 8.7 shows the distribution of mandatory lane changes for State Highway 121, which was the only Type B weaving zone in the study. The only vehicles which must change lanes are those which enter the freeway and must make one lane change in order to stay on the freeway mainlanes. The locations of these lane changes are the only ones shown.

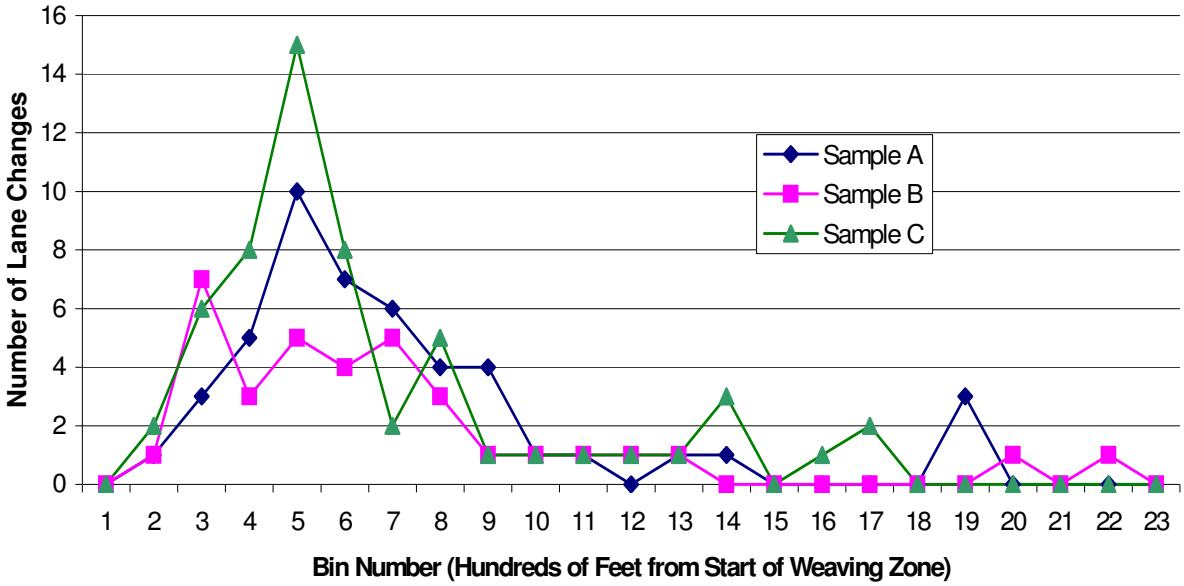

Figure 8.7. Longitudinal Distribution of Lane Changes, Type B Weave (SH-121)

Note that bins are 100 feet long, and the beginning of the weaving zone occurs at the boundary between Bin 1 and Bin 2. All the charts show the three five-minute samples that were collected and reduced for each site.

For the Type C weaves, the charts show the average number of lane changes in each bin, with each sample being normalized to a total of 100%. In cases where the lane change numbers were very small, the percentages appear to be high but noisy. Unlike Type A and Type B weaves, Type C weaves require two lane changes in one direction. Only the mandatory lanes changes are plotted—those lanes changes that are required for a weaving car to complete its weaving maneuver. For those movements that require two lane changes, the first lane change and the second lane change are plotted separately.

Figure 8.8 shows the two mandatory lane changes for westbound IH-30. Each driver appears to make lane changes about 300 or 400 feet apart, but the 900-foot length of the weaving area limits those who made their first lane change late.

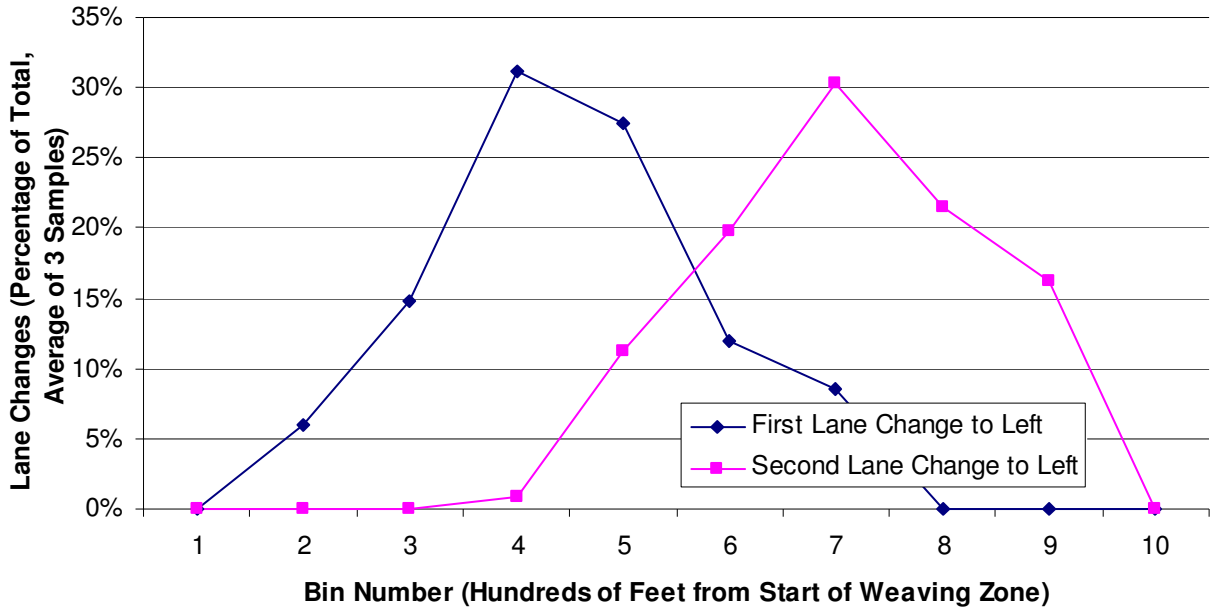

Figure 8.8. Longitudinal Distribution of Lane Changes—Type C Weave (I-30 WB)

Figure 8.9 shows the same information for eastbound IH-30. While the longer weaving zone allowed a small number of cars to make their maneuvers later, the bulk of the lane changes still occurred about the same distance into the weaving area as they did in the westbound IH-30 section that was much shorter.

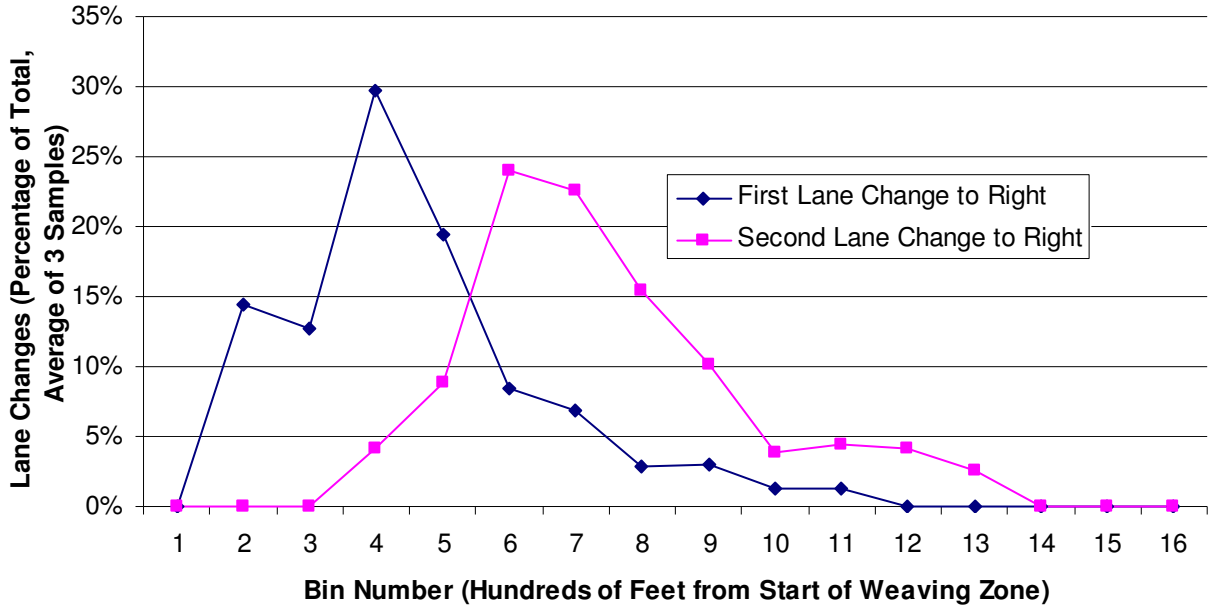

Figure 8.9. Longitudinal Distribution of Lane Changes—Type C Weave (I-30 EB)

Figure 8.10 shows the same data for IH-35W. This is the longest of the Type C weaves at 1800 feet, yet there were no lane change movements more than 1300 feet from the start of the weaving section, and the bulk of lane changes had been completed after 900 or 1000 feet into the weaving zone.

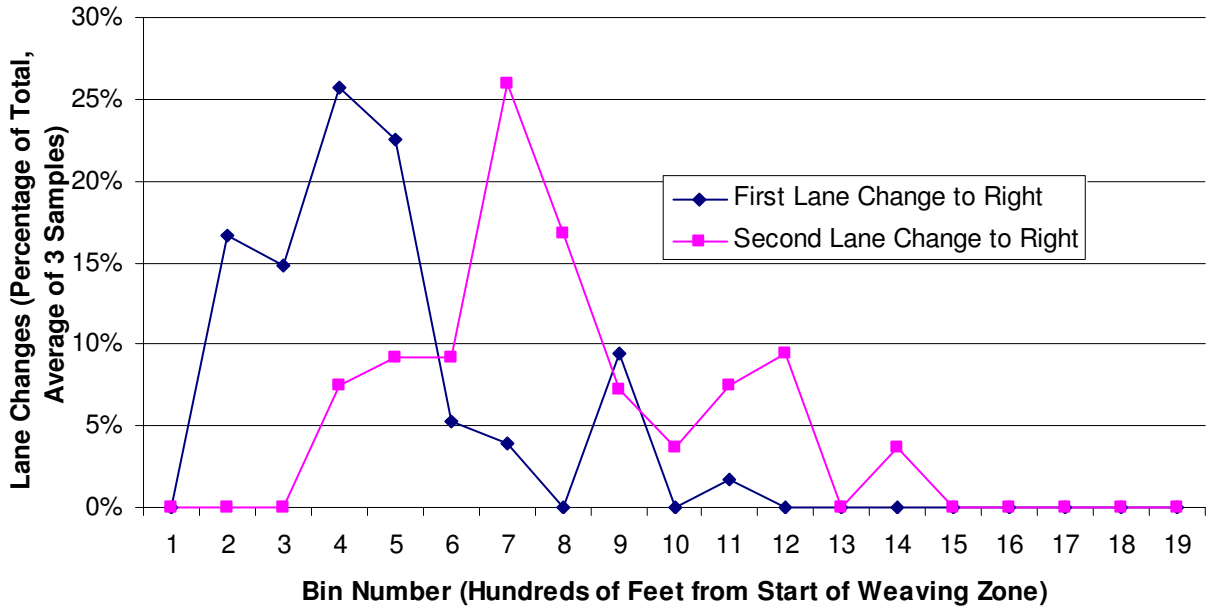

Figure 8.10. Longitudinal Distribution of Lane Changes—Type C Weave (I-35W)

The remaining Type C weave at SH-360 is shown in Figure 8.11.

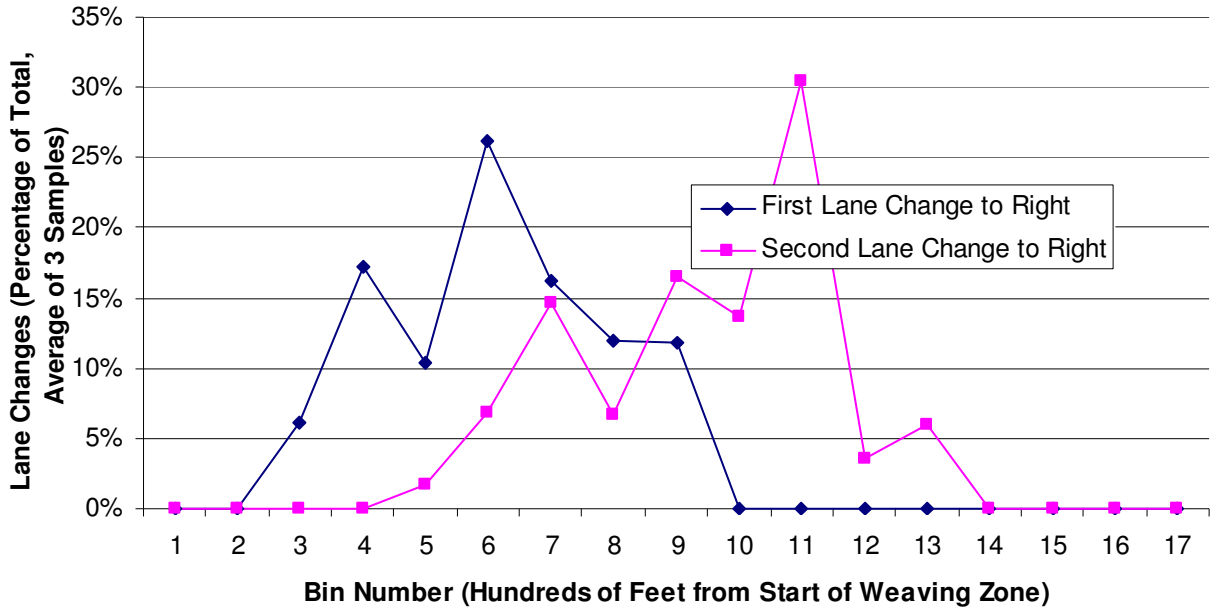

Figure 8.11. Longitudinal Distribution of Lane Changes—Type C Weave (SH 360)

Figure 8.12 shows the location of lane changes for the lane changes to the right at IH-30 westbound. This lane change is not mandatory to complete the weave. This was the only weaving zone to have a single unnecessary lane change across the mandatory two lane changes of a Type C weave. These are the lane changes from changes from Lane 1 of the mainlanes in bin 1 to Lane 2 of the exit ramp in bin 10 (Figure 8.2). The distribution is roughly centered on the two mandatory lane changes that this movement crosses.

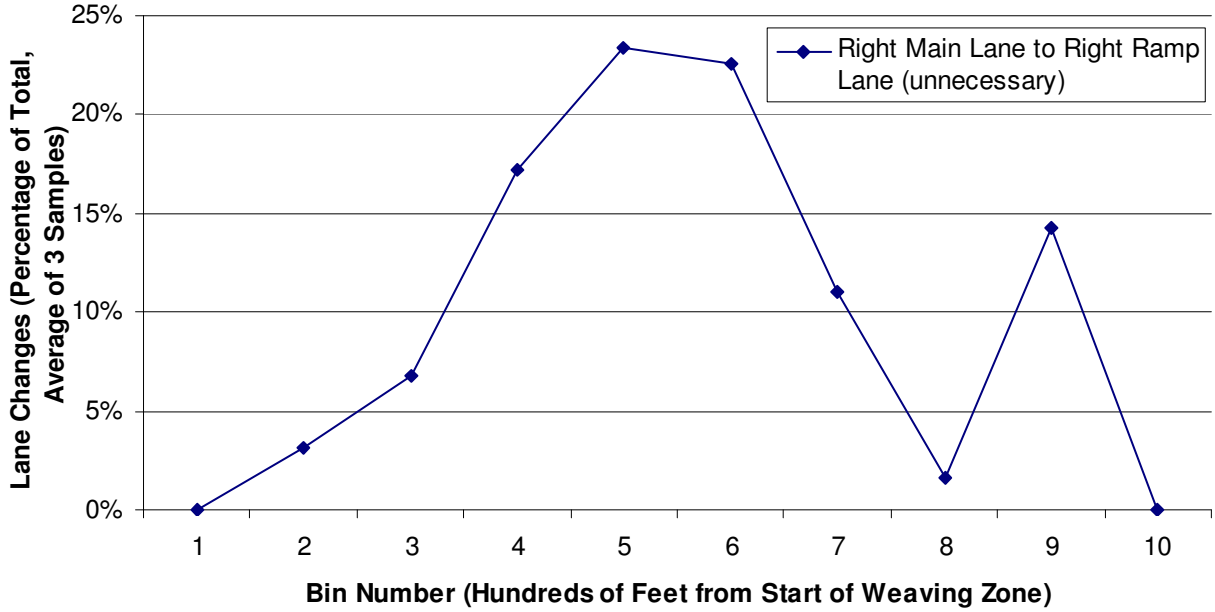

Figure 8.12. Longitudinal Distribution of Lane Changes—Type C Weave (I-30WB)

The next three Type C weaves, illustrated in Figures 8.3, 8.4, and 8.5, each have two lane entrance ramps. In these cases, traffic entering in Lane 2 of the ramp is not required to weave to stay on the mainlanes, as that lane becomes Lane 1 of the mainlanes after the weaving area. However, traffic entering in Lane 1 of

the entrance ramp must make at least one lane change to the left in order to stay on the mainlanes. The positions of these two lane changes are shown in Figures 8.13, 8.14, and 8.15 for EH IH 30, NB IH 35W, and NB SH 360, respectively.

At EB IH 30 (Figure 8.13), the number of lane changes is quite small and the data is noisy. At the other two sites, the number of lane changes were much larger, ranging from the teens to as many as 48 lane changes per five-minute period.

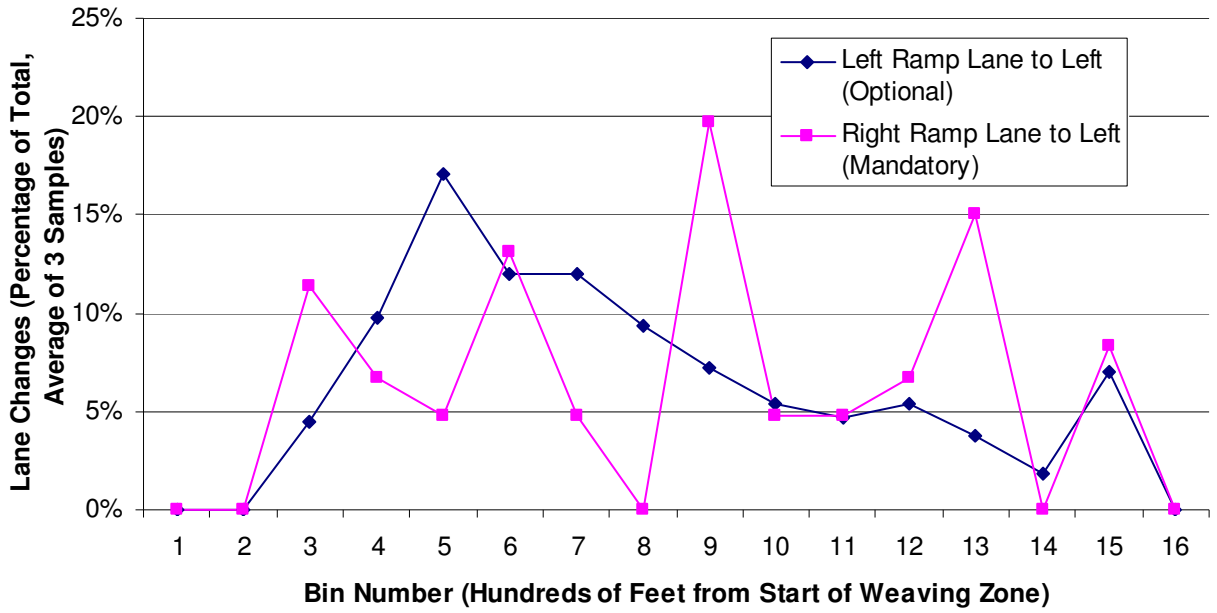

Figure 8.13. Longitudinal Distribution of Lane Changes—Type C Weave (I-30 EB)

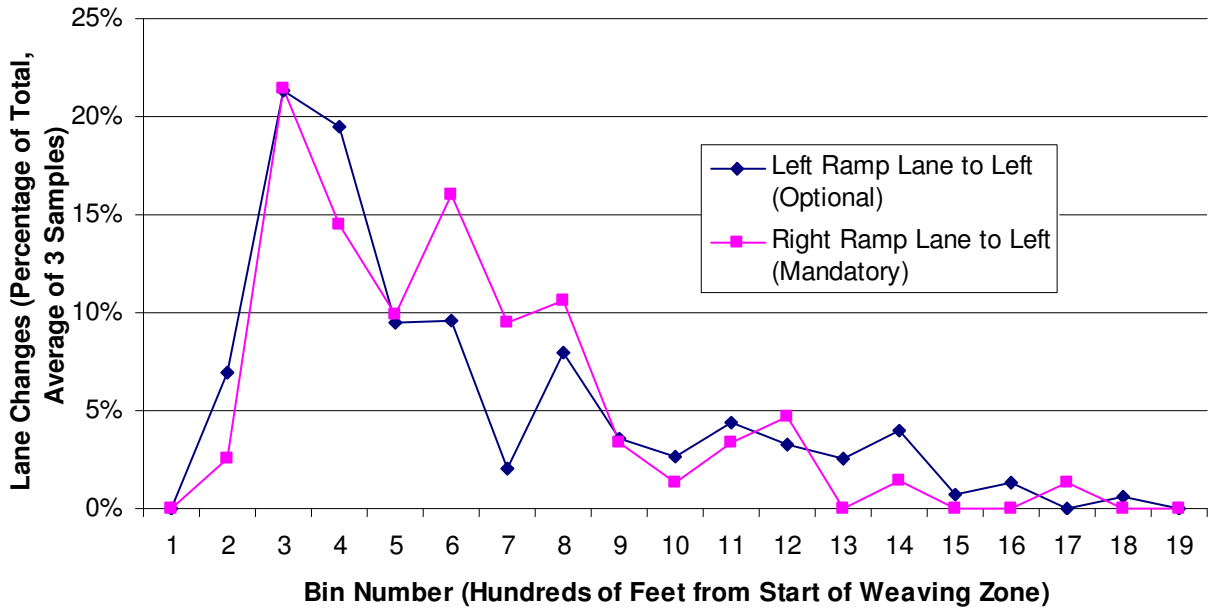

Figure 8.14. Longitudinal Distribution of Lane Changes—Type C Weave (I-35W)

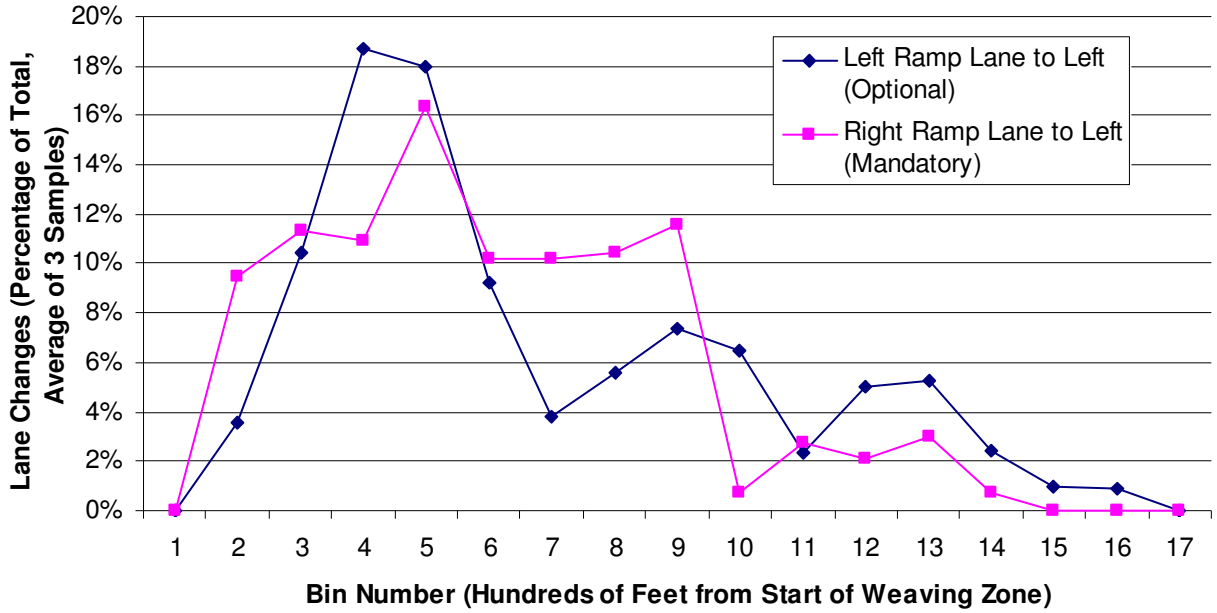

Figure 8.15. Longitudinal Distribution of Lane Changes—Type C Weave (SH-360)

Finally, Figure 8.16 shows the lane change distributions for the three required lane changes (considering the entering ramp movement as a required lane change) for the two-sided Type C weave on IH-35/410 in San Antonio. Unlike the other field studies in this section, only a single five-minute period of data was reduced. As expected, all the first lane changes occur in the first 100-foot section (remembering that the weaving zone begins at the boundary between Bins 1 and 2). Most drivers had completed the second lane change in the first 500 feet. No bin after Bin 9 (800 feet) held more than two lane changes, and only one held two.

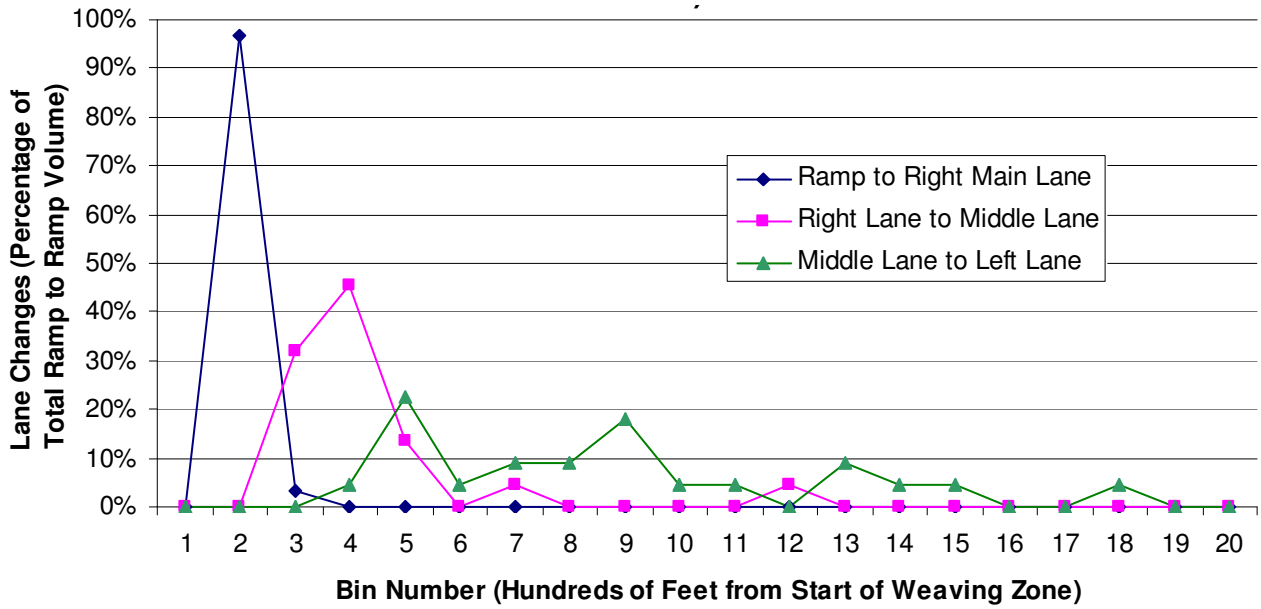

Figure 8.16. Longitudinal Distribution of Lane Changes—Two-Sided Weave (I-35/410)

Summary

Data was collected at one site for Type B weaves and five sites for Type C weaves. All six sites are in Texas. The three principal varieties of Type C weaves are represented among the sites: two lane entrance ramp with a single lane exit ramp, a single lane entrance ramp followed by a two lane exit ramp, and a two-sided weave.

The longitudinal distribution of lane changes for each of the sites is shown. Lane changes in the Type C weaves were distributed somewhat further downstream from the merge point than was found for Type A weaves, however, it should be remembered that two lane changes were required for the Type C weaves. In any case, the bulk of the lane changes were made long before the diverge point. The observations suggest that drivers make lane changes every 400 feet or so, so when two lane changes must be strung together, most lanes changes have occurred in the first 800 feet. These results suggest that weaving zones designed to provide effective free-flow operation will be sufficiently long such that length has little effect on driver behavior, and, by extension, measures of driver behavior.

Simulation results for the Types B and C weaves are described in the next chapter.

CHAPTER 9. SIMULATION RESULTS

Each of the sites described in Chapter 8 was subjected to series of simulation runs for a range of volume and fraction of weaving traffic conditions, with one exception. The I-35W site (Figure 8.5) was not simulated. Note that the proportion of weaving traffic is derived from the origin-destination information (mainlanes to mainlanes, mainlanes to ramp, etc.), and that for any one run, the sum of the proportion of mainlanes to mainlanes traffic and proportion of ramp to ramp traffic had to add to 100%. Similarly, the ramp to mainlanes and ramp-to-ramp traffic had to add to 100%.

The identification of traffic involved in the weaving maneuvers for most of these weaves was done in the same fashion as for Type A weaves. That is, the weaving lanes were identified as the lanes on each side of the entrance ramp gore, and the weaving traffic was that whose origin-destination was mainlanes-ramp or ramp-mainlanes.

Lane densities were found by taking the number of vehicles in each lane (averaged over the five-minute simulation period) and dividing by the length (which was the length of the weaving area). Densities greater than 40 vehicles/lane-mile were assumed to represent capacity conditions, and the critical lane was the lane with weaving traffic with the highest density.

Results of the simulation runs are shown in Figures 9.1 through 9.5. Total input volume in weaving lanes vs. the weaving volume is shown in each figure. Points below and at capacity are distinguished in the figure, where capacity conditions were assumed when any one lane with weaving traffic had a density greater than 40 vehicles/lane-mile.

The results for the Type B weave (southbound SH 121) are shown in Figure 9.1. The plotted points fall above the diagonal, as the weaving volume can be no greater than the total volume in the weaving lanes. Note that capacity conditions are scattered throughout the volume levels rather than just at the high volumes. The value of capacity will depend on the fraction of weaving traffic, since higher weaving volumes indicate a greater number of lane changes.

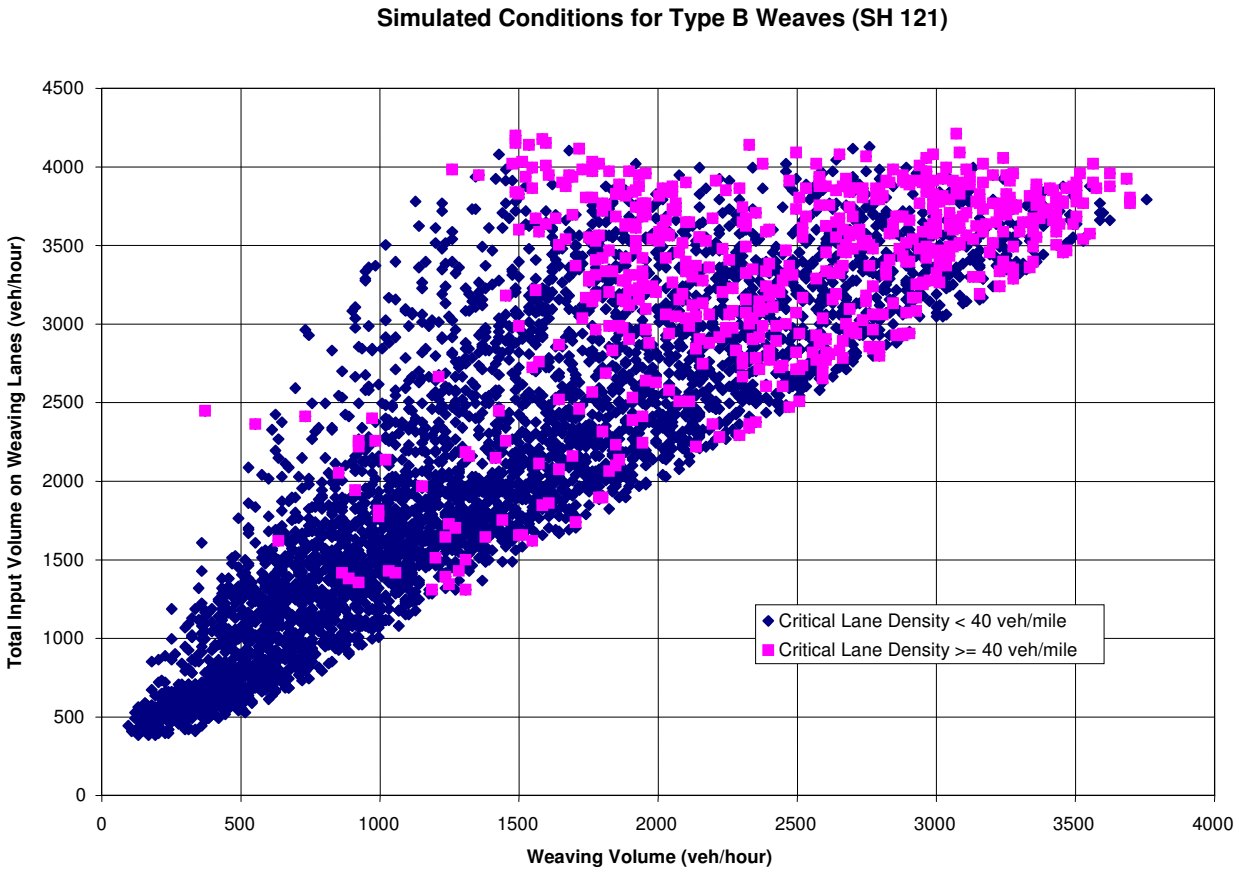

Figure 9.1. Simulated Conditions for Type B Weave (SH 121)

The results for the Type C weave that requires two lane changes for the left weave (westbound IH 30) are shown in Figure 9.2. Since virtually all of the traffic in the right lane of the mainlanes (at the merge point) is weaving traffic (since that lane exits), the observations fall along a fairly narrow strip. That is, virtually all of the traffic included in the total input on the weaving lanes is also included in the weaving flow. Only as traffic volumes increase will there be a substantial number of vehicles in the right lane that then move to the left to avoid the exit.

The two sites for Type C weaves that require two lane changes for the right weave are, as expected, fairly similar (eastbound IH 30 and northbound SH 360). The results, shown in Figures 9.3 and 9.4, indicate an apparent anomaly where the weaving volume is larger than the total input volume at higher volume levels, especially when weaving capacity was achieved (critical lane density greater than 40 vehicles/lane-mile). Only the two lanes on either side of the merge are considered to be weaving lanes (right lane of the mainlanes and left lane of the two-lane entrance ramp). At lower flows, the ramp to ramp traffic can largely sort into the right lane of the entrance ramp, and the ramp to mainlane traffic can sort into the left lane of the entrance ramp. However, as volume increases, especially in cases with a high proportion of ramp to mainlane traffic, many of the weaving vehicles will enter in the right lane, and not be included in the total input volume. As such, the total input volume in the weaving lanes is likely undercounted, especially at higher volumes.

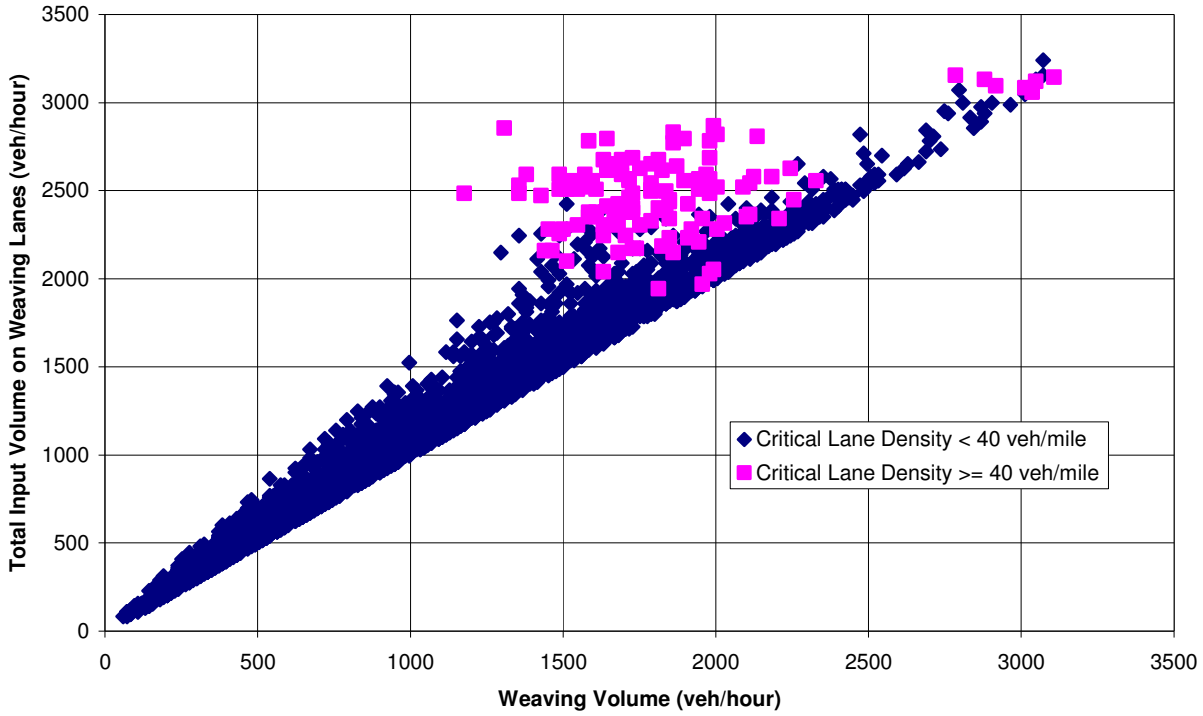

Figure 9.2. Simulated Conditions for Type C Weave (IH-30 Westbound)

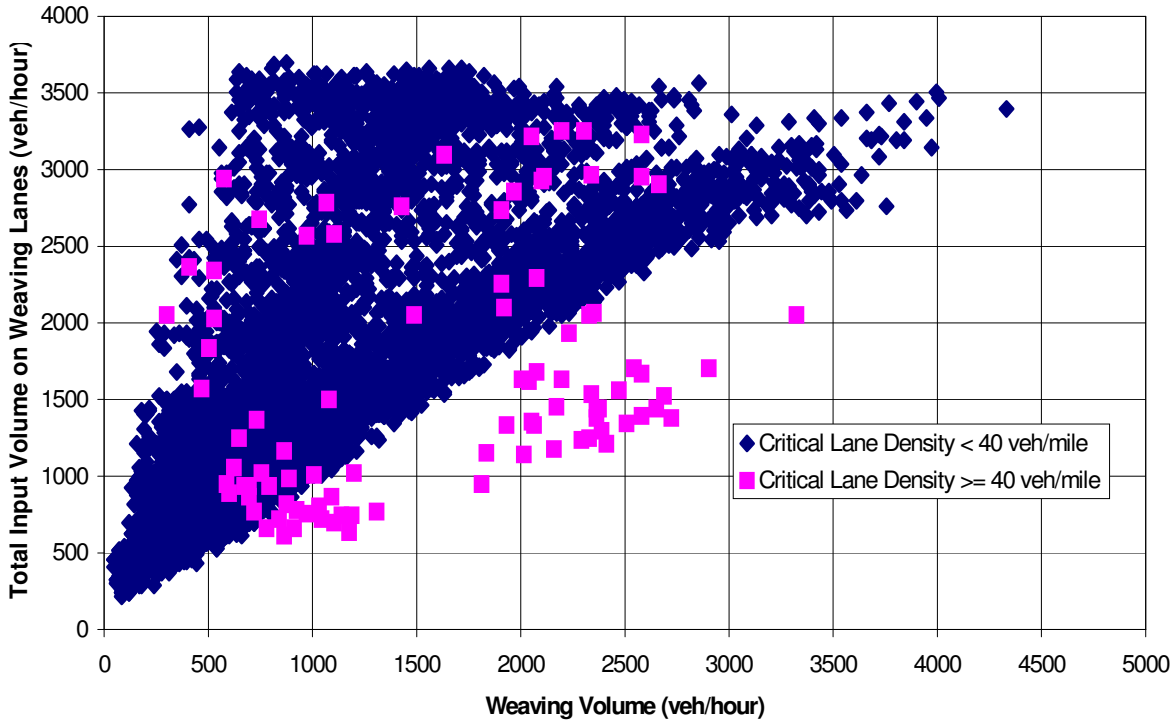

Figure 9.3. Simulated Conditions for Type C Weave (IH-30 Eastbound)

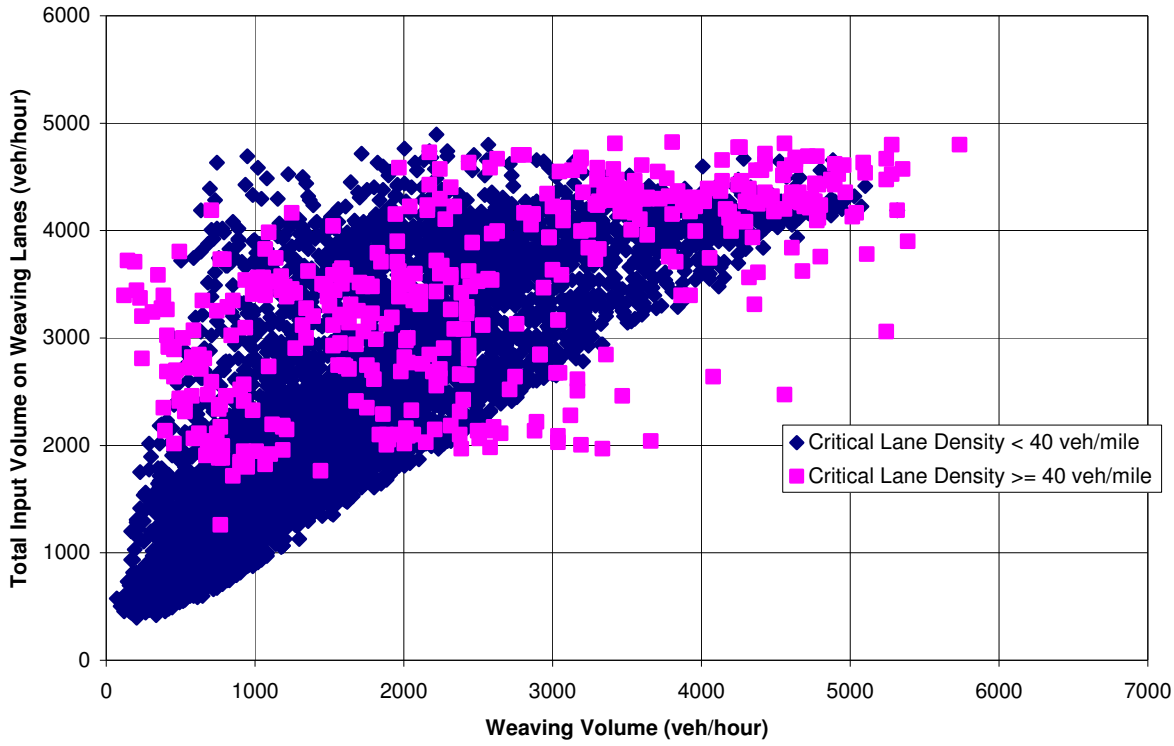

Figure 9.4. Simulated Conditions for Type C Weave (State Highway 360)

The final Type C configuration under consideration is the two-sided weave (southbound IH 35/410). Since the ramp-to-ramp movement must be made across all the lanes, all lanes are considered to be weaving lanes. Also, the weaving traffic is now considered to be the mainlane to mainlane and the ramp-to-ramp traffic (rather than the mainlane to ramp and ramp to mainlane traffic in the other weaving cases). Thus, in Figure 9.5, the total input volume in the weaving lanes is the total traffic entering the entire weaving area. Since there are three mainlanes, maximum flows between 6000 and 7000 vehicles per hour are not unexpected.

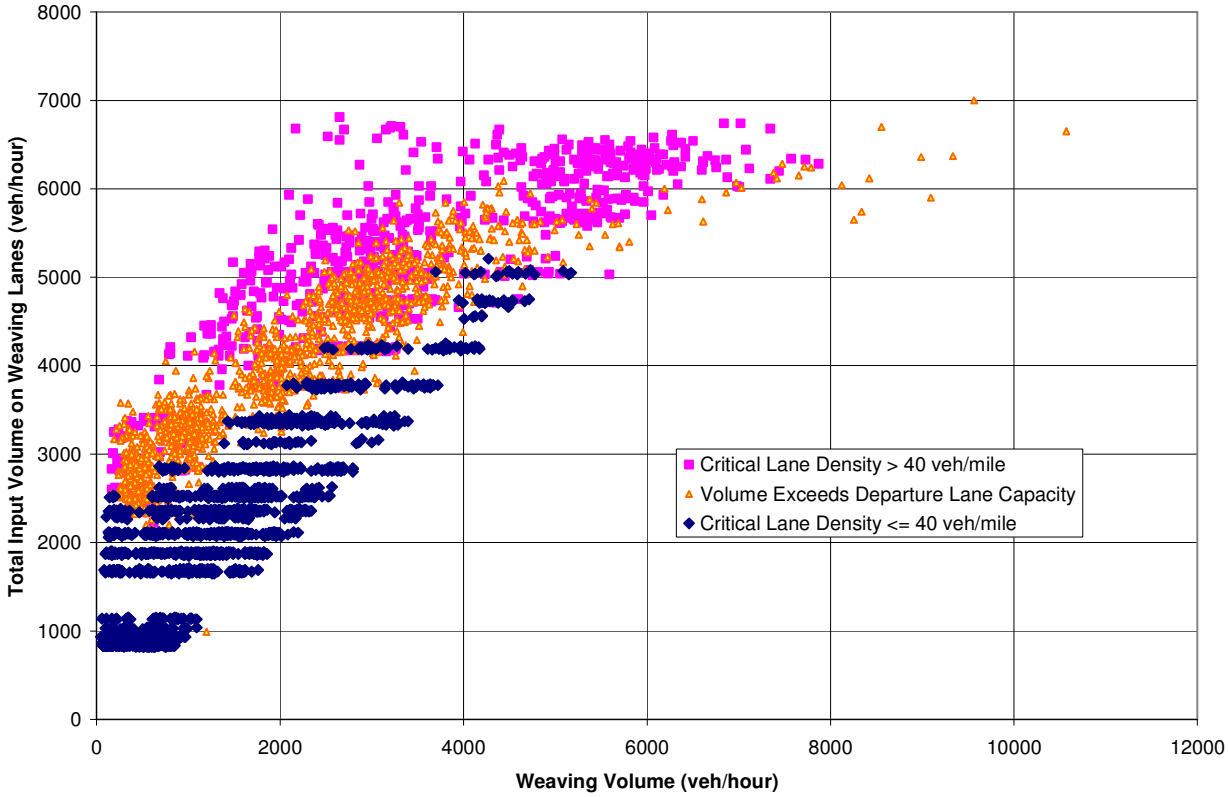

Figure 9.5. Simulated Conditions for Two-Sided Weave (IH-35/410)

The data for the two-sided weave is stratified into three classes: those with a critical lane density less than 40 vehicles/lane-mile, those with a critical lane density greater than 40 vehicles/lane-mile, and those where the volume exceeded the capacity of the exit ramp to southbound IH 410. In the latter case, traffic was queueing in the left lane of the weaving area.

Points below the diagonal in Figure 9.5 represent cases where the total weaving volume is greater than the total volume in the weaving lanes. Since the total volume in the weaving lanes is the total volume within the weaving area, there should be no points below the diagonal. These represent cases where the simulation model was unable to process the specified volumes, i.e., the demand was greater than the capacity of the weaving area, and queues were developing on the approaches to the weaving area.

General Observations

The procedure used to examine the Types B and C weaves was based on the tools developed to examine the Type A weaves. In this process, both weaving movements (weave to the left and weave to the right) are treated in the same fashion, i.e., they are added to produce the total volume that is weaving. While this is probably a good assumption for Type A weaves since both weaving movements require the vehicles to change lanes, the two weaving movements in Types B and C weaves are not equivalent. One of the weaving movements requires that the vehicles change one or two lanes, while the other requires no lane changes, at least at low and moderate volume levels.

CHAPTER 10. SUMMARY AND FURTHER WORK

The goal of this work was to develop models to define capacity and levels of service for weaving areas on freeways. Weaving areas on arterials were also in the original scope, but were not addressed except in the literature survey. Resources proved inadequate to address all of the issues, though both a capacity model and a density model for the weaving lanes in Type A weaves has been provided. Field studies were also performed for Types B and C weaves and preliminary simulations were made as well.

The research team recognized from the beginning that simulation would play a vital role in this project, as the number of field studies were necessarily very limited. The research team selected CORSIM for two primary reasons. At least at the time of the work, it was the most widely recognized and accepted microscopic simulation model that deals with freeways. As such, the researchers did not justify the use of this model, but only to calibrate it to the field conditions under study. The second reason is that one of the research team members is intimately familiar with the model, as he participated in its original creation (as INTRAS, and, later, FRESIM). This experience and knowledge was vital to the success of the simulations, as some of the calibration was done by modifying the source code, as these particular parameters are not normally accessible to users.

The researchers were fortunate in being given access to data that had been collected by others. This included data collected by JHK for the FHWA and, especially, data collected by CalTrans and the University of California at Berkeley. The JHK data was already digitized and ready for use. The California data was provided on video tape. The data which had been reduced by CalTrans and UC-Berkeley was not in a format usable in this work, and the necessary data was pulled directly from the tapes. This included the O-D flows and the longitudinal distribution of lane changes.

The data provided to the team consisted entirely of Type A ramp weaves. The field data collected by the project team included one Type A ramp weave (the preliminary site in Houston), one Type A major weave (near Baltimore, Maryland), one Type B weave (near Fort Worth, Texas), and five Type C weaves (in Fort Worth, Arlington, and San Antonio, Texas).

Key findings from the data were:

- Weaving vehicles made their lane changes very early in the weaving area, especially under capacity conditions. For Type A weaves, the vast majority of the lane changes occurred within the first 500 feet of the weaving area. No relationship was found between weaving zone length and capacity or true level of service for Type A weaves longer than 400 feet. Lane changes in Type C weaves were distributed a bit further downstream, but two lane changes were required. This reflects observations made by some of the references noted in the literature survey (in Chapter 2). This implies that, beyond a certain minimum length, the capacity and level of service of a weaving area is unrelated to the length. Drivers appear to want to get into an appropriate lane as soon as possible under heavy traffic conditions. This does not mean that the length of a weaving area is unimportant. Under light traffic conditions, vehicles should be able to make safe lane changes at design speed. But it does mean that increasing the length of a weaving zone beyond the length needed for free-flow speeds is unlikely to improve its capacity or level of service, and it also means that the capacity of a weaving zone is mostly defined by its merge point.

- The second key finding is that, under capacity conditions, drivers are willing to accept much shorter headways as they change lanes. This allows an effective lane capacity of over 3000 vehicles/hour.

With these findings, and many simulation runs, the study team developed two capacity models, one for Type A ramp weaves, the other for Type A major weaves. These models reflect the headway reduction at high weaving flows. It should be noted that there has been no capacity model for weaving areas in the Highway Capacity Manual. Until the release of the 2000 HCM, users could not estimate weaving area capacity, just level of service. The 2000 HCM has a multiple-page table to allow users to estimate capacity for a range of volume conditions.

The capacity model developed in this work for Type A ramp weaves is:

For total weaving volumes, V_w, less than 700 veh/hour:

$$C_w = 2300 + V_w$$

For $V_w \geq 700$ veh/hour **and** total entering volume on the weaving lanes, $V_t \leq 3000$ veh/hour:

$$C_w = 3000$$

For $V_t > 3000$ veh/hour:

$$C_w = (2 - VR_w)\left(1 + \frac{V_w - 2142}{2370}\right)(2300)$$

Capacity is not defined for weaving volumes greater than 3700 veh/hour

The capacity model developed in this work for Type A Major weaves is:

For total weaving volumes, V_w, less than 1200 veh/hour:

$$C_w = 2300 + V_w$$

For $V_w \geq 1200$ veh/hour **and** total entering volumes on the weaving lanes, $V_t \leq 3500$ veh/hour:

$$C_w = 3500$$

For $V_t > 3500$ veh/hour:

$$C_w = (2 - VR_w)\left(1 + \frac{V_w - 2142}{2370}\right)(2300)$$

Capacity is not defined for weaving volumes greater than 3700 veh/hour

Density models were also developed for both Type A ramp and major weaves. Levels of service in the in the freeway components of the HCM are defined in terms of density. The models provided here allow the density to be estimated for any value of V/C which is less than one. (V/C can be found by using the capacity model.) The researchers have not defined specific cutoffs for each level of service because they are determined by the Highway Capacity and Quality of Service Committee of TRB.

The density model for Type A ramp weaves is:

$$D_w = 13.2(V/C)^2 + 29(V/C)$$

And the final model of density for Type A Major weaves is

$$D_w = 0.2(V/C)^2 + 37(V/C)$$

The work for Types B and C weaves is more preliminary in nature. The longitudinal distribution of lane changes is shown for each of the field study sites, and a number of simulation runs were made for a wide range of total flows in the weaving lanes and fraction of weaving traffic, from low volumes up to capacity.

Further Work

No one research project can answer all questions on a single topic. And, while there were significant findings and some singular developments, much more work is required in this area.

The Type A analysis included only the two lanes involved in the weave, i.e., the lanes on each side of the crown line that connects the merge and diverge gores. Based on the field data, the researchers believe that they have accurately captured the capacity and density in these two lanes. However, for a full evaluation of the weaving area, the lanes not involved in weaving must be considered as well. This would include the mainlanes other than the right main lane and the right lane(s) of the ramps in the case of major weaves. It might be possible for a basic freeway analysis to be performed for these lanes, though this requires the assumption that the presence of weaving does not impact the flow in these lanes. This was not investigated.

The same two lanes were considered to be the weaving lanes for Types B and C weaves, i.e., the lane on each side of the entrance merge gore. (The exception here is the two-sided weave, where all lanes were considered to be weaving lanes.) The simulation results seem to indicate that the adjacent lanes, especially the right lane of two-lane entrance ramps, also have an impact on the weaving capacity. A more thorough analysis of Types B and C weaves is needed to produce capacity and density models. As for Type A weaves, these models need to encompass the entire weaving area, not just the lanes involved in the weaving.

Once satisfactory density and level-of-service models are developed, the usual HCM adjustment factors must be tested. This would include factors to account for heavy vehicles, grades, free-flow speeds, and so forth. This amounts to fine-tuning the models, but is necessary for eventual incorporation in the HCM.

Lastly, beyond inclusion in the literature survey, arterial weaving was not investigated in this study. Arterial weaving presents additional complications. One typical example is where an exit ramp merges into a frontage road, and some of the drivers wish to turn right at the downstream cross road. While this may appear to be an application of a two-sided weave, where the length is measured from the merge of the ramp with the frontage road to the downstream intersection, the length is more properly measured to the back of the queue created by the intersection control, often a traffic signal. The increased side friction on arterials (driveways, minor side streets) will also have an impact on the weave's capacity and quality of service.

APPENDIX I. ADDITIONAL DATA SOURCES

Existing Data

University of California Data

All of the University of California data sets are for major weaves where either there are two lanes on the entry ramp and one on the exit ramp, one lane on the entry ramp and two lanes on the exit ramp, or two lanes on both. The data was collected using video and was reported at five-minute intervals. The amount of collected data varies from two to five hours, depending on the site. The volume data is by origin/destination pair. The spatial distribution of the number of vehicle origin/destination pairs is given at intervals over the length of the weaving area and the average weaving and non-weaving speeds for each one-hour period is given.

Interstate Highway 10 WB between Garvey Street and Interstate Highway 605, in the Los Angeles, California area. A schematic of this section is shown in Figure I.1. Congestion levels appear to be about B or C based upon the average speeds reported.

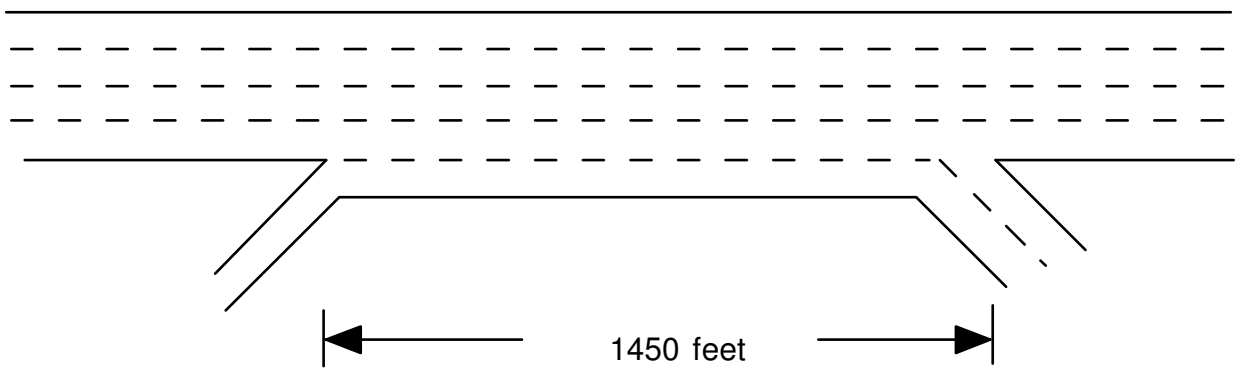

Figure I.1. IH-10 Westbound between Garvey and IH-605

Interstate Highway 10 WB between Etiwandia Avenue and Interstate Highway 15, in the Los Angeles, California area. A schematic of this section is shown in Figure I.2. Congestion levels appear to be about A or B, based upon the average speeds reported.

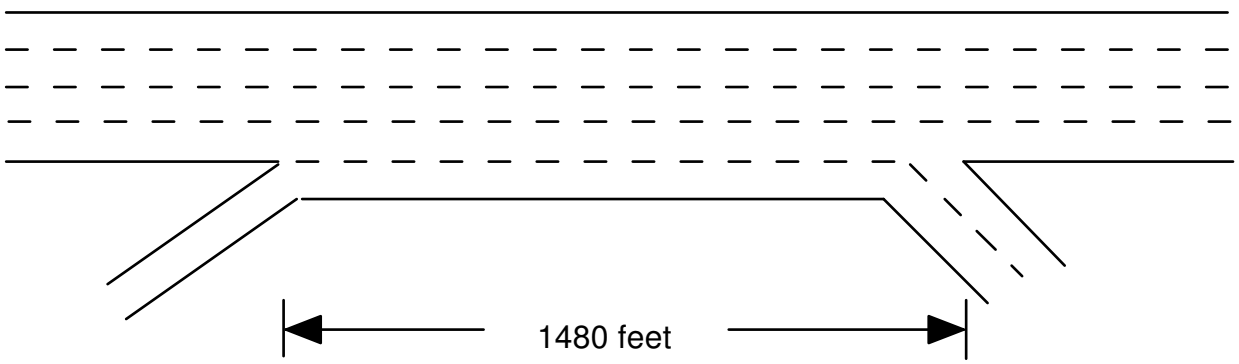

Figure I.2. IH-10 Westbound between Etiwqandia Avenue and IH-15

Interstate Highway 805 NB between University Avenue and El Cajon, in the San Bernardino, California area. A schematic of this section is shown in Figure I.3. Congestion levels appear to be about B to D, based upon the average speeds reported.

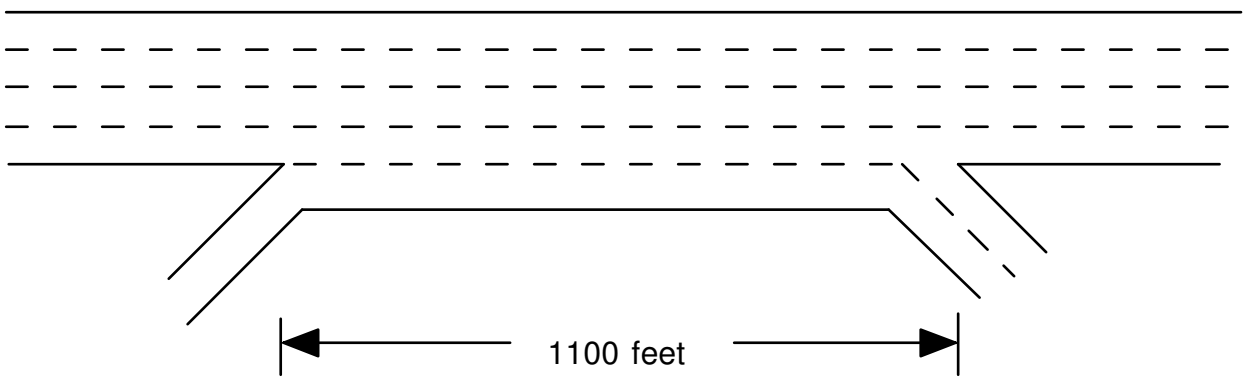

Figure I.3. IH-805 between University and El Cajon.

US Highway 101 SB between Interstate Highway 110 and Broadway, in the Los Angeles, California area. A schematic of this section is shown in Figure I.4. Congestion levels appear to be about C or D based upon the average speeds reported.

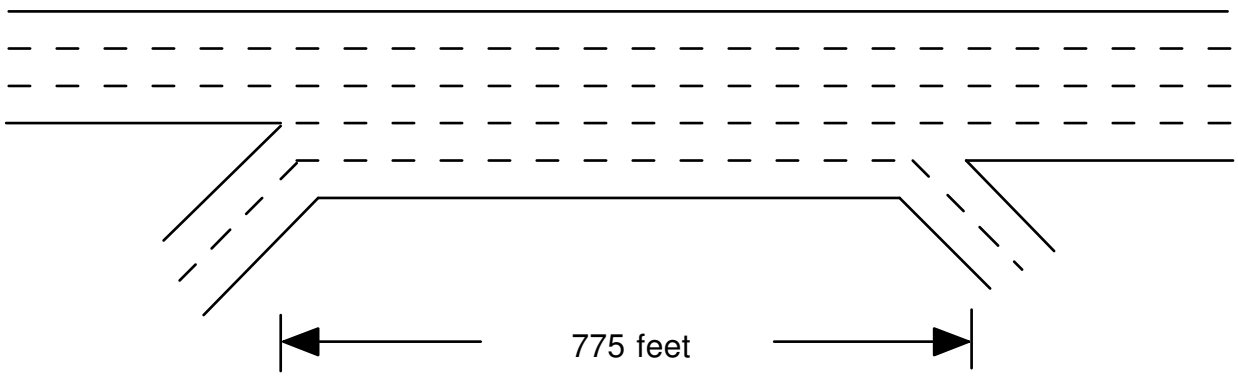

Figure I.4. US-101 Southbound between IH-110 and Broadway

US Highway 101 NB between Broadway and Interstate Highway 110, in the Los Angeles, California area. A schematic of this section is shown in Figure I.5. Congestion levels appear to range between B and D, based upon average speeds reported.

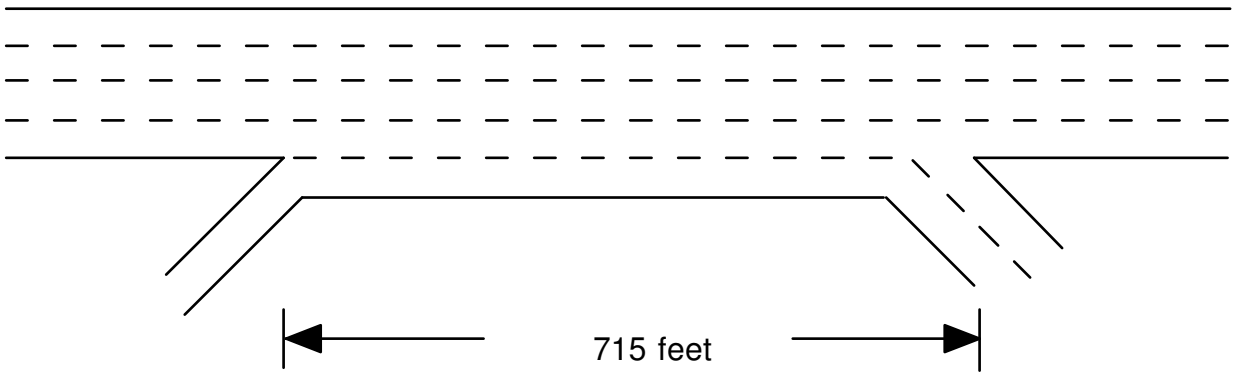

Figure I.5. US-101 Northbound between Broadway and IH-110

Interstate Highway 10 EB between Interstate Highway 605 and Frazier Street in the Los Angeles, California area. A schematic of this section is shown in Figure I.6. Congestion levels appear to range between B and C, based upon the average speeds reported.

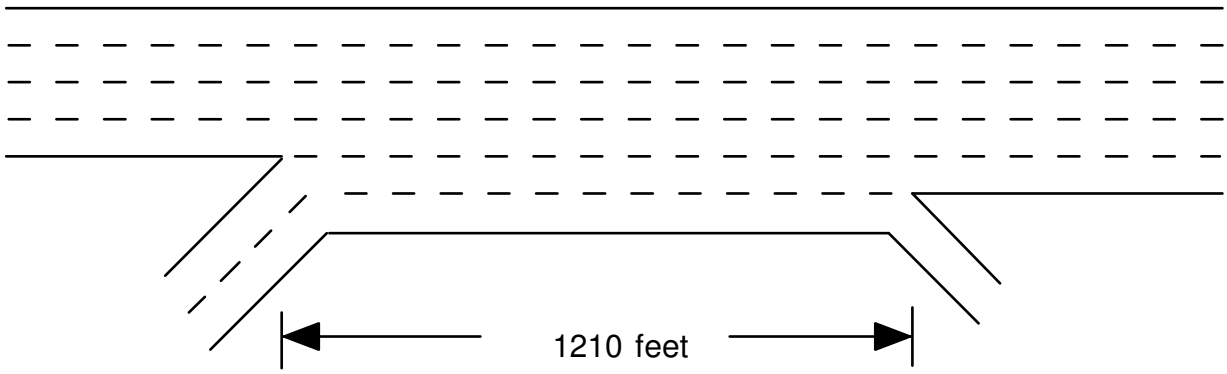

Figure I.6. IH-10 Eastbound between IH-605 and Frazier

Interstate Highway 280 SB between Interstate Highway 17 and Bascom Avenue, in the San Francisco, California bay area. A schematic of this section is shown in Figure I.7. Congestion levels appear to range between A and B, based upon the average speeds reported.

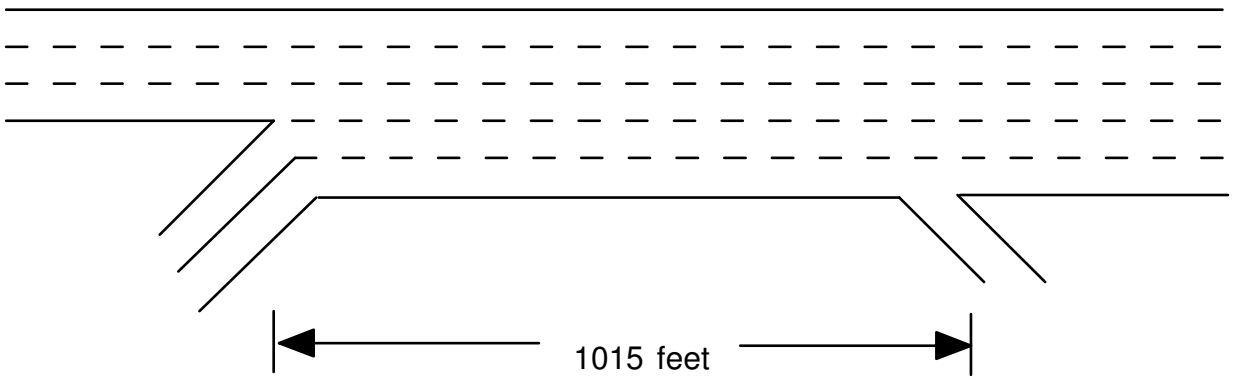

Figure I.7. IH-280 between IH-17 and Bascom Avenue

In addition to these sites, there are four other sites where data were collected. The extent of the data collection efforts for these sites is not clear from the cited report.

Freeway Data Collected by JHK [Ref. 1]

The JHK data consists of vehicle trajectory points at one-second intervals for a period of one hour. The data was collected using time lapse aerial photography and consists of data records for each photographic frame which provide the longitudinal location, the lateral location, the vehicle type, the vehicle identification number and an estimated lane for each vehicle which was digitized. Speeds of each vehicle are obtained from the distance traveled between frames. The data collection was designed so that there was no congestion at the start. There are six weaving data sets among a total of twelve collected data sets. Because of the detail of the data, all demand data can be obtained and any and all measures of effectiveness can be computed.

Interstate Highway 295 southbound (SB) between 11th Street and Howard Road in Washington, D. C. A schematic of this section is shown in Figure I.8. It should be noted that this weaving section is on a slight curve and free flow speeds are low, around 50 mph. Congestion levels start at B and end at D/E.

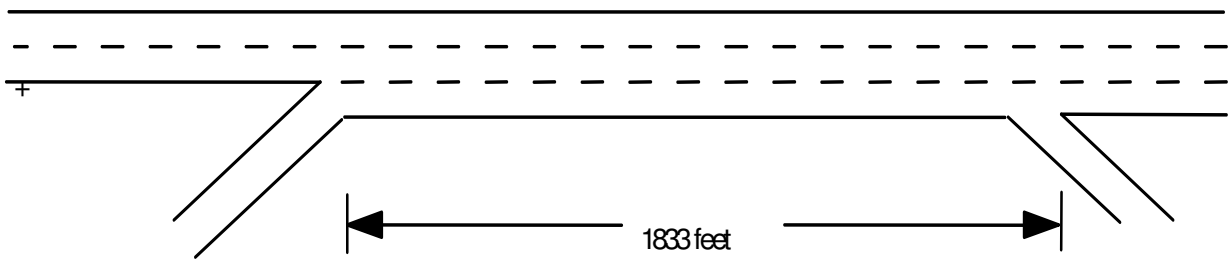

Figure I.8. IH 295 Westbound, 11th to Howard

Harbor Freeway northbound (NB) between Interstate Highway 10 and 6th Street in Los Angeles, California. A schematic of this section is shown in Figure I.9. This is an A Major weave with two ramp lanes in and two ramp lanes out. Congestion level starts at D and ends at F (there is queuing on both the on-ramp and the mainline).

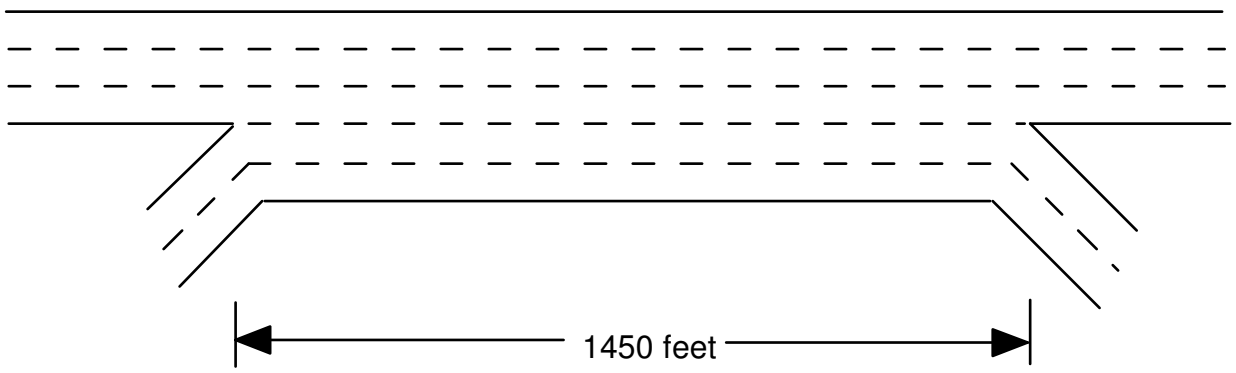

Figure I.9. Harbor Freeway, Northbound from IH-10 to 6th St.

Interstate Highway 295 NB between Howard Road and 11th Street in Washington, D. C. A schematic of this section is shown in Figure I.10. This is a complex weave which involves a ramp merge followed by a diverge in which on-ramp vehicles must cross two lanes to stay on the freeway mainline. It should be noted that this section is slightly curved and free flow speeds are low, around 50 mph. Congestion level was estimated to be about C.

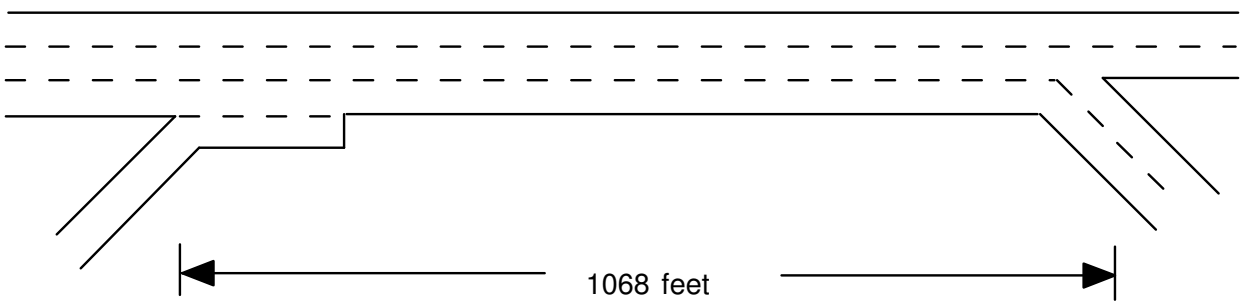

Figure I.10. IH-295 Northbound from Howard Rd. to 11th St.

14th Street Bridge WB between the merge of Interstate Highway 295 and 14th Street and the Exit to the George Washington Parkway NB, in Washington D.C. A schematic of this section is shown in Figure I.11. This section is a major weave to the right. Congestion levels are from D to E. It should be noted that there is an interchange with the George Washington Parkway SB located about 350 feet downstream of the off-ramp gore area which will effect the volume in the right lane and that free flow speeds are low, ranging between 50 and 55 mph.

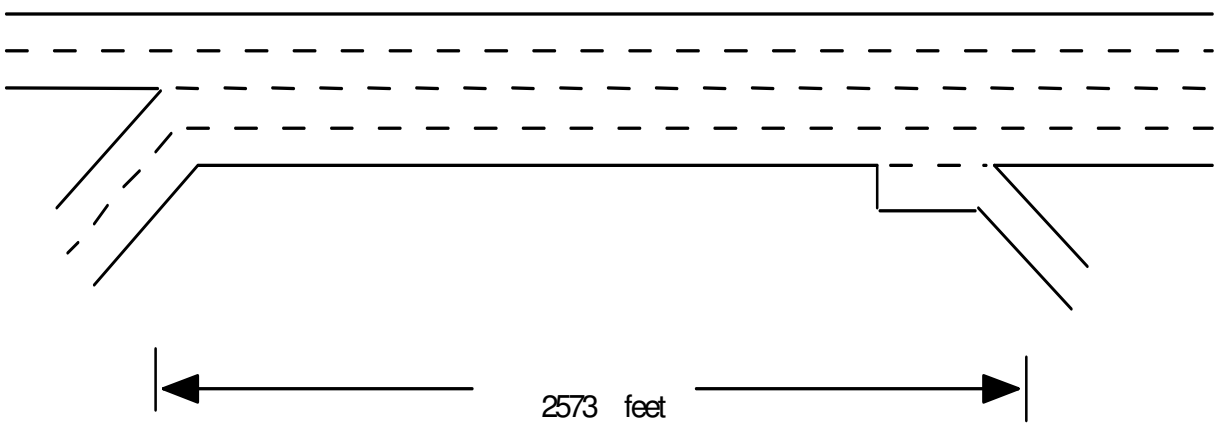

Figure I.11. 14th St. Bridge Westbound from IH-295 to George Washington Pkwy.

California Department of Transportation Data [Ref. 2]

See Chapter 5 for a description of the Caltrans data and the site that was used in the study. The following are those sites for which data were reduced from video, but that were not used in the development of the capacity or level-of-service models.

California Route 91 eastbound (EB) from Wilmington Avenue to Acacia Avenue, in the Los Angeles, California area. A schematic of this section is shown in Figure I.12. Congestion levels appear to be about C, based on the observed densities in the right lane. It should be noted that there is an off-

ramp an unknown distance, but probably less than one mile, downstream of the section that may have an effect on volume in the right lane.

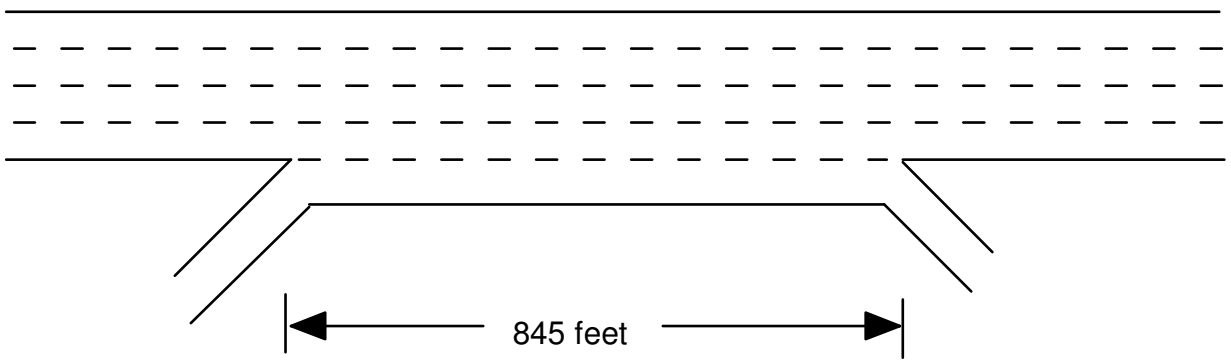

Figure I.12. Rt. 91 Eastbound from Wilmington to Acacia

Interstate Highway 10 EB from Ganesha Street to Dudley Street, in the Los Angeles, California area. A schematic of this section is shown in Figure I.13. Congestion levels appear to be about B, based on the observed densities in the right lane.

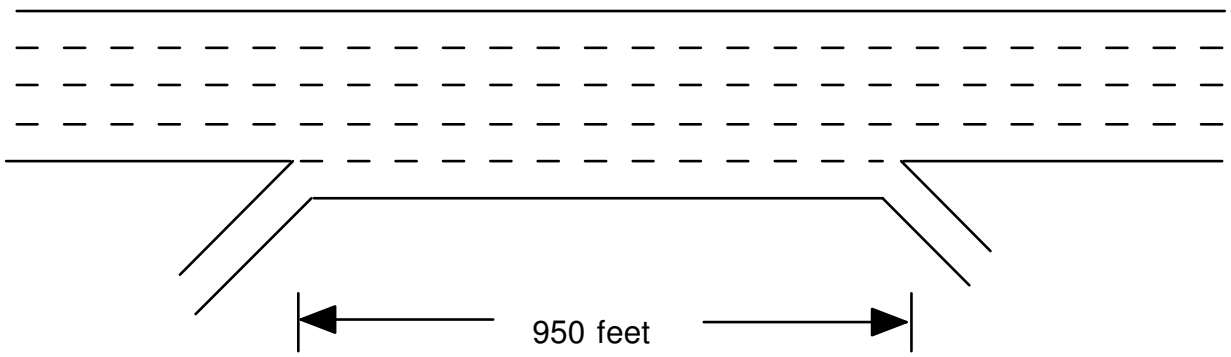

Figure I.13. IH-10 Eastbound from Ganesha to Dudley

California Route 91 from 183rd Street to Artesia Boulevard, in the Los Angeles, California area. A schematic of this section is shown in Figure I.14. Congestion levels appear to be about A, based on the observed densities in the right lane. Data points at the five and ten intervals are missing from the data set.

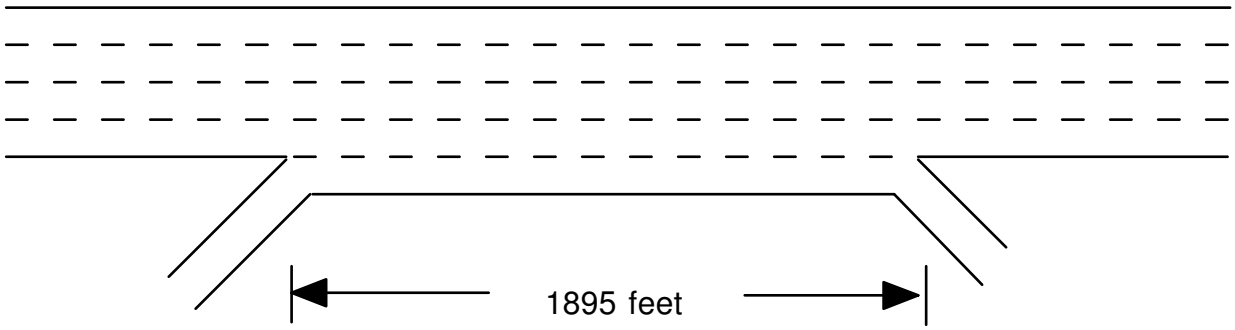

Figure I.14. Rt. 91 Westbound from 183rd St. and Artesia

Interstate Highway 580 EB from Oakland Avenue to Grand Avenue, in the San Francisco, California bay area. A schematic of this section is shown in Figure I.15. Congestion levels appear to be about A, based on the observed densities in the right lane. There is a sharp curve just beyond the diverge point that may affect speeds in the section.

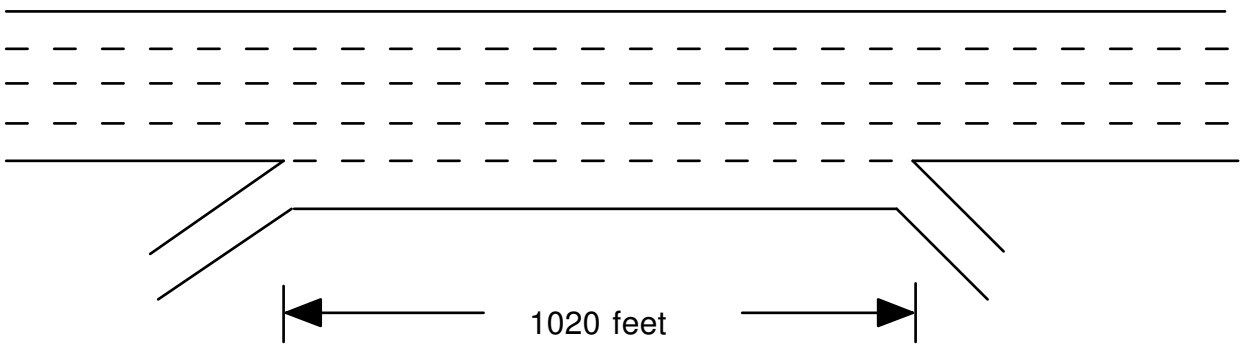

Figure I.15. IH-580 Westbound from Oakland to Grand

Interstate Highway 5 SB from Palomar Street to Main Street, in the San Diego, California area. A schematic of this section is shown in Figure I.16. Congestion levels appear to be about C, based upon the observed densities in the right lane. There is a sharp curve just beyond the diverge point that may affect speeds in the section.

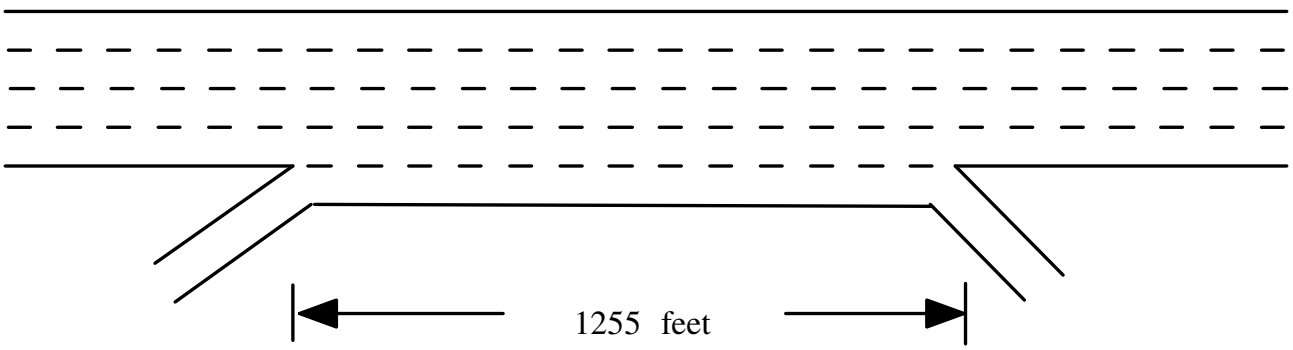

Figure I.16. IH-5 Southbound from Palomar to Main

Interstate Highway 110 SB from Vernon Avenue to 51st, in the Los Angeles, California area. A schematic of this section is shown in Figure I.17. Congestion levels appear to be about B or C, based upon the observed densities in the right lane.

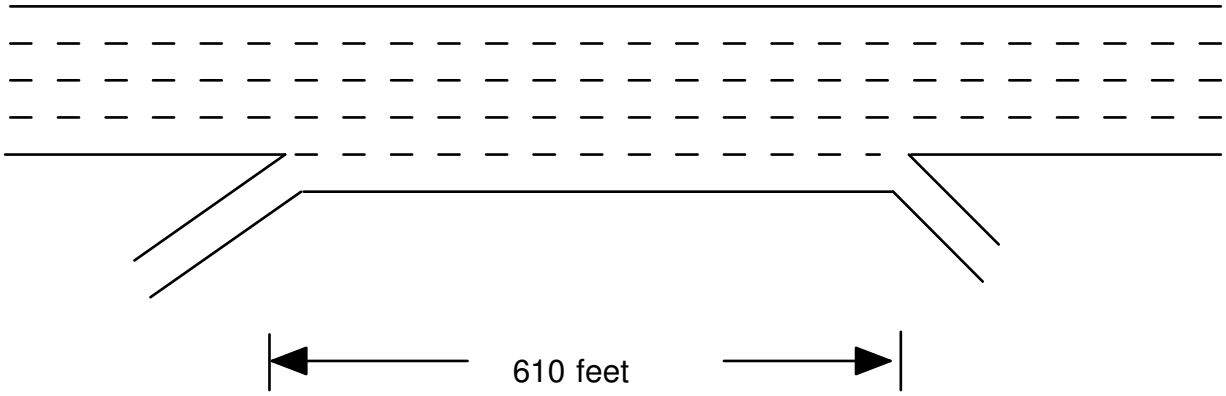

Figure I.17. IH-110 Southbound from Vernon to 51st

Interstate Highway 10 WB from Barranca Street to Citrus Street, in the Los Angeles, California area. A schematic of this section is shown in Figure I.18. Congestion levels appear to be about B based upon the densities in the right lane.

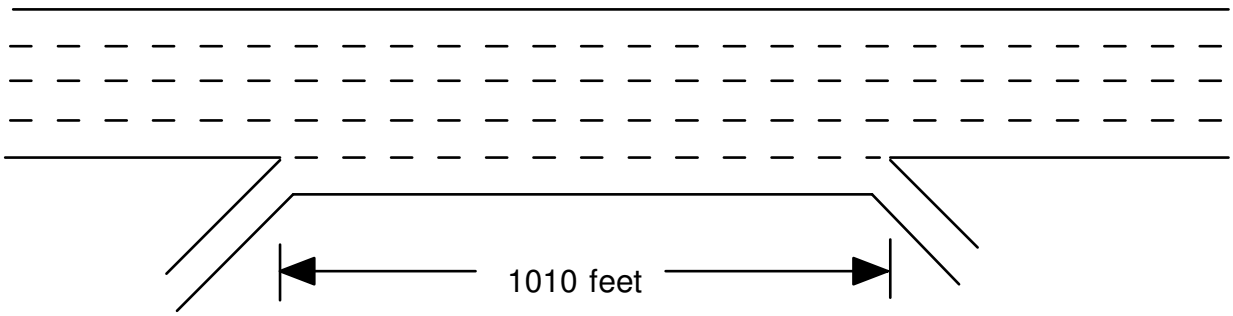

Figure I.18. IH-10 Westbound from Barranca to Citrus

References

1. "Freeway Data Collection for Studying Vehicle Interactions - Technical Report," May, 1985. Federal Highway Administration, Washington, D.C.

2. "Weaving Data, 1987," California Department of Transportation, Sacramento, California.